Mag. rer. nat. Mareike Monschein, Bakk. rer. nat.

Enhancing the efficiency of lignocellulose saccharification by modifying enzyme- and substrate associated determinants: Evidence from kinetic analysis.

DOCTORAL THESIS

to achieve the university degree of

Doktorin der Naturwissenschaften

submitted to

Graz University of Technology

Supervisor

Univ.-Prof. Dipl.-Ing. Dr. techn. Bernd Nidetzky

Institute of Biotechnology and Biochemical Engineering
Faculty of Technical Chemistry, Chemical and Process Engineering and Biotechnology

Graz, November 2015

AFFIDAVIT

I declare that I have authored this thesis independently, that I have not used other than the declared sources/resources, and that I have explicitly indicated all material which has been quoted either literally or by content from the sources used. The text document uploaded to TUGRAZonline is identical to the present doctoral thesis.

Date

Signature

“Science is not only a disciple of reason but, also, one of romance and passion.”
― Stephen Hawking

Dedicated to my parents, Anita and Helfried Monschein.
Thank you for everything.

Acknowledgements

Undertaking this PhD has been truly a life-changing experience for me and it would not have been possible without the support and guidance I received from many people.

First and foremost, I would like to express my sincere gratitude to my supervisor Univ.-Prof. Dipl.-Ing. Dr. techn. Bernd Nidetzky for giving me the opportunity to perform my thesis at the Institute of Biotechnology and Biochemical Engineering. His guidance helped me in all the time of research and writing of this thesis and his encouragement of critical thinking allowed me to grow as an independent thinker and research scientist.

I would also like to express my gratitude to CLARIANT Produkte for financial support. Contributions of Dr. Christoph Reisinger and Dr. Georg Schirrmacher are thankfully acknowledged

I thank my colleagues at the Institute of Biotechnology and Biochemical Engineering, whose helpfulness and team spirit created a pleasant and enriching working environment. Dip.-Ing. Dr. techn. Alexandra Schwarz and Ing. Dr. techn. Tibor Czabany supported me during different periods of the project and I have greatly benefited from their knowledge and guidance. I am particularly grateful for the assistance given by Ing. Margaretha Schiller and Karin Longus. My deepest appreciation goes to Ass.-Prof. Dipl.-Ing. Dr. techn. Regina Kratzer for her constructive comments, warm encouragement and friendship.

I would also like to say a heartfelt ‘thank you’ to the people who made graduate school a memorable experience: Manuel Reisinger- you will always be the best project student I ever had. Thanks for your origami presents, our coffee breaks and talks. Natascha Loppitsch- both for technical assistance and all the fun we had in the lab. Bernhard Lauß- your sunny charisma made each day at university something to look forward to. For sure, fate had a hand in guiding you to our office. Sabine Schelch- BFF, office wife, dead end- there are not enough words to describe what you mean to me. No matter what struggles I had to face- you stood by my side. Your advice, both in scientific questions or private issues was, is and will always be appreciated. This thesis would have never been finished without your support and encouragement.

There is a saying that friends are the family we choose for ourselves. I’m feeling blessed for all the wonderful people making up my ‘extended family’: Isabella Fleischhacker, Susanne Fleischhacker, Viktoria Fruhwirth, Stefan Holy, Barbara Kapfer, Victoria Langeder, Katharina Mackinger, Elisa

Manninger, Florian Pock, Sarah Steiner, Helmut Vrabec and Christina Zöhrer. Without you, I would not be where I am today- thank you for being at my side in good times and bad, for your support, your confidence and your friendship. I cherish the memories we made and look forward to many more to come. A special 'thank you' goes out to my fellow teammates at Ausufern for their enthusiasm, the rewarding experience of volunteering in a committed team and for sharing the vision of make society more accepting

My parents Anita and Helfried Monschein receive my deepest gratitude. Thank you for giving me the opportunity to pursue a higher education, for your support, your encouragement and for giving me a home- in more than one way. I can almost hear your sigh of relief- yep, I finally made it ;).

This study was performed within the COMET K-Project Macro-Fun and the COMET-K2-centre ACIB. Financial support from the Province of Styria is gratefully acknowledged. This work received support from the Federal Ministry of Economy, Family and Youth (BMWFJ); the Federal Ministry of Traffic, Innovation and Technology (bmvit); the Styrian Business Promotion Agency SFG; the Standortagentur Tirol; and ZIT-Technology Agency of the City of Vienna. Funding was through the COMET-Funding Program managed by the Austrian Research Promotion Agency FFG.

Abstract

Lignocellulose is the most abundant renewable biomass resource, having great potential for the sustainable production of chemicals and biofuels. Enzymatic hydrolysis of plant polysaccharides emerged as the most prominent technology for the production of fermentable sugars. However, large-scale process commercialization has been impeded by several technical and economical bottlenecks. Both enzyme- and substrate associated determinants impede efficient saccharification, most notably the highly recalcitrant structure of lignocellulose, a rapid slow-down of hydrolysis rate and a need for high enzyme loadings. Addressing these issues and gaining a better understanding of the interactions between enzymes and lignocellulose are of major importance for the development of more cost efficient conversion technologies.

In this study, a simple set of kinetic descriptors of hydrolysis process efficiency was established, enabling the association of reducing sugar release with enzyme adsorption and an evaluation of hydrolysis efficiency. Application of these descriptors on hydrolysis of pure microcrystalline cellulose and pretreated wheat straw hydrolysis by *Trichoderma reesei* cellulase allowed the identification of important conversion-limiting factors. To increase the hydrolytic efficiency of a model system compromised of thermo-acidically pretreated wheat straw and *T. reesei* cellulase, enzyme- and substrate associated bottlenecks were systematically removed in process optimization: The effects of non-ionic or cationic surfactants, polyether polymers or chaotropic agents on hydrolytic efficiency were compared on a kinetic level, allowing insights into the diverse mechanisms of action of these chemical additives. While retaining a high level of lignocellulose conversion, this approach allowed a reduction of enzyme loading or a shortening of hydrolysis process time.

The influence of pretreatment severity on enzymatic hydrolysis of wheat straw was investigated based on kinetic evaluation of the saccharification of six differently pretreated substrates. The focus was on continuous steam explosion with different acid loadings accounting for a variation in pretreatment severity. Thereby a beneficial effect of mild-acidic pretreatment conditions on wheat straw digestibility was revealed.

A novel non-hydrolytic protein, *Pc*Lrbp was identified by screening the secretome of *Phanerochaete chrysosporium*. *Pichia pastoris*-expressed *rPc*Lrbp was characterized in adsorption- and hydrolysis studies, revealing its ability for specific binding to lignacious hydrolysis residue. *rPc*Lrbp showed synergism with the cellulolytic system of *T. reesei* and boosted reducing sugar release in the initial phase of hydrolysis, presumably by interacting with the lignin component of substrates.

Zusammenfassung

Lignocellulose ist die häufigste erneuerbare BiomasseResource und besitzt großes Potential für die nachhaltige Produktion von Chemikalien und Biotreibstoffen. Die enzymatische Hydrolyse von Pflanzenpolysacchariden entwickelte sich hierbei zur leistungsfähigsten Technologie für die Produktion von fermentierbaren Zuckern. Die groß angelegte Kommerzialisierung wird jedoch durch mehrere technische und wirtschaftliche Engpässe erschwert. Sowohl Enzym- als auch Substrat-assoziierte Determinanten erschweren eine effiziente Verzuckerung, vor allem die schwer abbaubare Struktur von Lignocellulose, eine rasche Verlangsamung der Hydrolyserate und die Notwendigkeit hoher Enzymbeladungen. Eine Auseinandersetzung mit diesen Problemen und ein besseres Verständnis der Interaktionen zwischen Enzymen und Lignocellulose Substraten sind von großer Bedeutung für die Entwicklung von kosteneffizienteren Konversionstechnologien.

In dieser Studie wurde ein einfaches Set von kinetischen Deskriptoren der Hydrolyseprozess Effizienz etabliert, das die Assoziierung der Zuckerfreisetzung mit der Enzymadsorption und die Beurteilung der Hydrolyse Effizienz ermöglichte. Die Anwendung dieser Deskriptoren auf die Hydrolyse von reiner mikrokristalliner Cellulose und vorbehandeltem Weizenstroh durch *Trichoderma reesei*-Cellulasen erlaubte die Identifizierung wichtiger konversionslimitierender Faktoren. Um die hydrolytische Effizienz eines Modellsystems zu erhöhen, das thermisch-sauer vorbehandeltes Weizenstroh und *T. reesei* Cellulasen beinhaltete, wurden Enzym- und Substrat-assoziierte Engpässe in einer Prozessoptimierung systematisch entfernt:

Die Effekte von nicht-ionischen oder kationischen Tensiden, Polyether Polymeren oder chaotrotpen Verbindungen auf die Hydrolyse Effizienz wurden auf kinetischer Ebene verglichen, was Einsicht in die vielfältigen Wirkungsmechanismen dieser chemischen Additiva erlaubte. Bei Beibehaltung einer hochgradigen Lignocellulose Konversion ermöglichte diese Strategie eine Reduktion der Enzymbeladung oder eine Verkürzung der Reaktionszeit.

Basierend auf der der kinetischen Evaluierung der Verzuckerung von 6 unterschiedlich vorbehandelten Substraten wurde der Einfluss des Schweregrades der Vorbehandlung auf die enzymatische Hydrolyse von Weizenstroh untersucht. Das Hauptaugenmerk lag dabei auf kontinuierliche Dampfexplosion, wobei unterschiedliche Säurebeladungen eine Variation des Vorbehandlungsschweregrades ergaben. Dadurch wurde ein günstiger Effekt von schwach-sauren Vorbehandlungsbedingungen auf die Verdaulichkeit von Weizenstroh offenbart.

Ein neuartiges nicht-hydrolytisches Protein, *Pc*Lrbp, wurde durch ein Screening des Sekretoms von *Phanerochaete chrysosporium* identifiziert. *Pichia pastoris*-exprimiertes *rPc*Lrbp wurde in Adsorptions- und Hydrolysestudien charakterisiert, wodurch seine Fähigkeit zur spezifischen Bindung an ligninhaltigen Hydrolyserückstand nachgewiesen wurde. *rPc*Lrbp zeigt Synergismus

mit dem cellulolytischen System von *T. reesei* und verstärkt die Freisetzung reduzierender Zucker in der initialen Hydrolysephase, vermutlich über Interaktion mit dem Ligninanteil der Substrate.

Table of contents

Enzymatic hydrolysis of microcrystalline cellulose and pretreated wheat straw: A detailed comparison using convenient kinetic analysis.

Bioresource Technology 128 (2013) 679–687

Contents lists available at SciVerse ScienceDirect

Bioresource Technology

journal homepage: www.elsevier.com/locate/biortech

Enzymatic hydrolysis of microcrystalline cellulose and pretreated wheat straw: A detailed comparison using convenient kinetic analysis

Mareike Monschein [a], Christoph Reisinger [b], Bernd Nidetzky [a,c,*]

[a] Austrian Center of Industrial Biotechnology (ACIB) GmbH, Petersgasse 14, 8010 Graz, Austria
[b] Clariant AG, Staffelseestraße 6, 81477 Munich, Germany
[c] Institute of Biotechnology and Biochemical Engineering, Graz University of Technology, Petersgasse 12/I, 8010 Graz, Austria

HIGHLIGHTS

- Purpose-built kinetic descriptors for hydrolysis of lignocellulosic substrates.
- Slow hydrolysis rate is identical for pure cellulose and pretreated wheat straw.
- Fast initial hydrolysis rate depends on substrate and enzyme loading.
- Transition from fast to slow hydrolysis rate reflects enzyme–substrate interactions.

ARTICLE INFO

Article history:
Received 16 May 2012
Received in revised form 23 October 2012
Accepted 25 October 2012
Available online 3 November 2012

Keywords:
Enzymatic hydrolysis
Adsorption
Hydrolysis rate
Lignocellulose
Microcrystalline cellulose

ABSTRACT

Marked slow-down of soluble sugar production at low degree of substrate conversion limits the space–time yield of enzymatic hydrolysis of ligno-cellulosic materials. A simple set of kinetic descriptors was developed to compare reducing sugar release from pure crystalline cellulose (Avicel) and pretreated wheat straw by *Trichoderma reesei* cellulase at 50 °C. The focus was on the rate-retarding effect of maximum hydrolysis rate at reaction start (r_{max}), limiting hydrolysis rate (r_{lim}) at extended reaction time (24 h), and substrate conversion, marking the transition between the r_{max} and r_{lim} kinetic regimes (C_{trans}). At apparent saturation of substrate (12.2 g cellulose/L) with enzyme, r_{max} for pretreated wheat straw (~9.6 g/L/h) surpassed that for Avicel by about 1.7-fold whereas their r_{lim} were almost identical (~0.15 g/L/h). C_{trans} roughly doubled as enzyme/substrate loading was increased from 3.8 to 75 FPU/g, suggesting C_{trans} to be a complex manifestation of cellulase–cellulose interaction, not an intrinsic substrate property. A low-temperature adsorption step preceding hydrolysis at 50 °C resulted in enhanced cellulase binding at reaction start without increasing r_{max}. C_{trans} was higher for pretreated wheat straw (~30%) than for Avicel (~20%) under these conditions.

1. Introduction

Lignocellulosic biomass is a potential source of fermentable sugars for production of biofuels and other biochemicals; however, full-scale process commercialization has been plagued by technical and economical obstacles concerning the release of the sugars from lignocellulosic feedstock (Himmel et al., 2007). Identification of key system properties and quantification of their contribution to overall process efficiency would be important in the development of more cost-competitive technologies (Bansal et al., 2009). Lignocellulose bioconversion is usually achieved through a suitable combination of substrate pretreatment and enzymatic saccharification. Both steps constitute mechanistically and technologically complex unit operations where each accounts for about one-third of the total process costs (Wyman, 2007). Despite pretreatment, soluble sugar formation still occurs at relatively low space-time yields, often requiring high enzyme loadings in the saccharification step. Enhancement in saccharification efficiency is therefore key in an integrated approach to process optimization. Recalcitrance of lignocellulosic biomass and efficacy of the cellulose-degrading enzymes (cellulases) are highly interdependent system parameters that crucially impinge on process performance and hence costs. The critical relationship of the two parameters is not well understood at the molecular level and therefore, process development must rely on semi-empirical descriptors that are of practical use for optimization purposes.

Among the multitude of known lignocellulose pretreatment procedures (Agbor et al., 2011; Alvira et al., 2010; Hendriks and Zeeman, 2009), thermo-chemical acid-based processes were

* Corresponding author. Tel.: +43 316 873 8400; fax: +43 316 873 8434.
E-mail address: bernd.nidetzky@tugraz.at (B. Nidetzky).

0960-8524/$ - see front matter © 2012 Elsevier Ltd. All rights reserved.
http://dx.doi.org/10.1016/j.biortech.2012.10.129

shown to be effective on a wide range of lignocellulose substrates, resulting in high sugar yields upon enzymatic conversion. Acidic pretreatment alters the lignin structure, causing rearrangement of lignin on cellulose fiber surfaces (Hendriks and Zeeman, 2009; Jorgensen et al., 2007) and results in partial hydrolysis of the hemicellulose which yields fermentable sugars, but also increases the cellulose surface area available for cellulase attack (Alvira et al., 2010; Hendriks and Zeeman, 2009).

Enzymatic hydrolysis of lignocellulose requires cellulase adsorption to the insoluble substrate (Jorgensen et al., 2007; Lynd et al., 2002; Zhang and Lynd, 2004). In contrast to hydrolysis which usually takes place over several tens of hours, adsorption is comparably fast, even at the optimum temperature for the enzymatic reaction, reaching an apparent dynamic equilibrium within only a few minutes (Steiner et al., 1988; Nidetzky and Steiner, 1993; Varnai et al., 2010). The volumetric hydrolysis rate usually increases with the amount of adsorbed cellulase in a linear or hyperbola-like relationship depending on substrate and reaction conditions. In addition to cellulase adsorption, the hydrolysis rate is affected by a variety of strongly interrelated factors, including substrate type and structure (e.g. surface area and crystallinity), intrinsic cellulase activity, and reaction conditions (Kumar and Wyman, 2009; Zhang and Lynd, 2004).

A characteristic feature of cellulose hydrolysis is that the initially established hydrolysis rate decreases fast as the reaction progresses, resulting in long process times or a requirement for high enzyme loadings (Himmel et al., 2007; Zhang and Lynd, 2004). The decrease in the hydrolysis rate is somewhat enigmatic and enzyme-associated factors such as enzyme denaturation or deactivation, enzyme product inhibition, decrease in synergism, and jamming due to overcrowding of enzymes on cellulose surface as well as substrate-associated factors such as decreasing substrate reactivity and accessibility, multiphasic composition of the cellulose, changes in degree of polymerization, crystallinity, and other physical substrate properties have been proposed to account for the decrease (Bansal et al., 2009; Hall et al., 2010; Yu et al., 2012). For lignocellulosic substrates, additional factors such as the presence of the non-hydrolyzable lignin may contribute to rate limitation development during the course of the reaction (Bansal et al., 2009; Zhang and Lynd, 2004). Lignin is known to reduce cellulose accessibility and to result in adsorption of cellulases in a non-productive way, probably concurrent with enzyme inactivation (Berlin et al., 2006; Jorgensen et al., 2007).

Strong efforts were made to apply mathematical modeling to obtain useful descriptors of hydrolysis process efficiency. Using detailed analysis of enzyme and substrate variables, modeling may allow for kinetic isolation of important rate-limiting factor(s) and therefore contribute to the systematic removal of bottlenecks as part of process optimization (Bansal et al., 2009). Models differ widely with respect to mechanistic backgrounds applied. Highly advanced structured models of enzymatic cellulose hydrolysis have been proposed (Bansal et al., 2009; Griggs et al., 2011; Levine et al., 2010; Nidetzky et al., 1994), but they are not yet applicable to lignocellulosic substrate conversion. Therefore, simple, yet practical approaches of kinetic analysis need to be developed.

In the present study, a simple set of kinetic descriptors was established, providing the basis for evaluation and association of hydrolytic efficiency with enzyme adsorption. By comparing conversion of pure crystalline cellulose and acid-pretreated wheat straw, it could be shown that the transition of the maximum hydrolysis rate at reaction start to the slow, limiting hydrolysis rate at extended reaction time is not an intrinsic substrate property. Transition depends on enzyme–substrate loading and therefore constitutes a kinetically complex manifestation of cellulase–cellulose interactions.

2. Methods

2.1. Substrates and chemicals

Thermo-acidically pretreated wheat straw with a total dry matter content of 20.7% was supplied by Süd-Chemie AG (Munich, Germany). The lignin and sugar content of the dry matter was 25.6% and 48.6%, respectively. Cellulose accounted for 63.8% of the total sugar content. Pure crystalline cellulose, Avicel PH-101 (~50 μm particle size), was purchased from Sigma–Aldrich (St. Louis, MO, USA). It contained more than 97% cellulose and less than 0.16% water-soluble materials (Yang et al., 2006). Roti-Nanoquant and Roti-Quant reagents were obtained from Carl Roth (Karlsruhe, Germany). Glucose (HK) assay reagent, D-(+)-gluconic acid δ-lactone and nitrophenyl glycosides were purchased from Sigma–Aldrich. All other chemicals were reagent grade.

2.2. Enzymes

ENZ-SC01 cellulase-mixture was kindly provided by Süd-Chemie AG with 18 FPU/mL and 13 β-glucosidase U/mL activities and a protein concentration of 10 g/L. Novozyme 188 contained 81 g protein/L and 237 β-glucosidase U/mL.

2.3. Cellulase adsorption and enzymatic hydrolysis

Adsorption and hydrolysis experiments were performed in duplicates and replicated a second time. A suspension of the substrate (12.2 g/L Avicel; 21.4 g/L pretreated wheat straw) was prepared in a total reaction volume of 1.8 mL of 50 mM Na-acetate buffer (pH 5.0). The concentrations of Avicel and pretreated wheat straw were chosen to give an identical concentration of polymeric glucose of 12.2 g/L. Experiments were performed using an optional pre-adsorption step in which cellulases were adsorbed to the substrate at 4 °C to minimize hydrolysis during adsorption. Different concentrations of ENZ-SC01 (from 3.8 to 75 FPU/g glycan) were added to the substrate suspension, and reaction tubes were incubated for 20 min at 4 °C and 1000 rpm using an Eppendorf Thermomixer comfort (Eppendorf AG, Hamburg, Germany). After a brief centrifugation (30 s at 9300×g) the supernatant was collected for analysis (protein concentration, enzymatic activities) and the pellet was suspended in 50 mM preheated Na-acetate buffer (pH 5.0), supplemented with Novozyme 188 to reach a total β-glucosidase activity of 0.63 U/mL in the reaction. The hydrolysis reaction was performed at 50 °C in a thermal shaker at 1000 rpm for 48 h. At certain time points, samples were taken and inactivated at 95 °C for 7 min. To separate the solid fraction, samples were again centrifuged and the supernatant was used for further analyses (glucose, reducing sugars).

For hydrolysis experiments without a pre-adsorption step, the substrate suspension was supplemented with ENZ-SC01 and Novozyme 188 to a total β-glucosidase activity of 0.63 U/mL. Hydrolysis was started immediately by incubation at 50 °C in a thermal shaker at 1000 rpm and reaction was continued for 48 h. Sampling was performed as stated above with the exception that part of the supernatant was retained for protein measurements, whereas the rest was inactivated prior to sugar analysis.

2.4. Measurement of enzyme activities

FPU activities were measured in duplicates according to the standard procedure (Ghose, 1987). For measurement of arabinosidase, galactosidase, glucosidase, mannosidase, cellobiohydrolase and xylosidase activity, the nitrophenol assay was used. Assays were performed in 96-well flat-bottom microtiter plates (Greiner

Bio-One International AG, Frickenhausen, Germany). Fifty μL of the corresponding substrate (4-nitrophenyl-α-L-arabinofuranoside, 4-nitrophenyl-β-D-xylopyranoside, 2-nitrophenyl-β-D-galactopyranoside, 4-nitrophenyl-β-D-glucopyranoside, 4-nitrophenyl-β-D-mannopyranoside or 4-nitrophenyl-β-D-cellobioside) were mixed with 50 μL of sample diluted in 50 mM Na-acetate buffer, pH 5.0. In 4-nitrophenyl-β-D-cellobioside assays, 5 mM D-(+)-gluconic acid δ-lactone was added to inhibit β-glucosidase activity. Incubation was performed for 10 min at 50 °C and 300 rpm in an Eppendorf Thermomixer comfort. After 5 min on ice, reactions were stopped by addition of 100 μL of 1 M Na_2CO_3 and the amount of liberated nitrophenol was measured at 405 nm against a blank of substrate incubated with Na-acetate buffer. A Fluostar Omega Platereader (BMG Labtech GmbH, Ortenberg, Germany) was used (Table A.1; Supporting Information).

2.5. Sugar analysis

Reducing sugar concentration was measured in duplicates according to standard procedure using the DNS method (Miller, 1959). Forty μL of 50 mM Na-acetate buffer (pH 4.8), 20 μL of sample and 120 μL of DNS reagent were pipetted into 96-well PCR-plates (VWR International, Vienna, Austria). After 5 min at 95 °C in a PCR-cycler, the samples were diluted in H_2O and adsorption was measured at 540 nm. Glucose concentration was determined using a commercial hexokinase-glucose 6-phosphate dehydrogenase assay (Sigma–Aldrich). Measurements were done in duplicates at 340 nm against a substrate blank incubated with H_2O instead of reagent solution. For both assays, the sugar concentration at the start of hydrolysis was considered as background resulting from substrate impurities. The blank was subtracted from the measured values.

2.6. Analysis of protein adsorption

Protein concentration in the supernatant, which corresponded to unbound protein, was measured using either the Roti-Quant or Roti-Nanoquant assay according to the manufacturers' instructions. Measurements were performed in duplicates at 595 nm (Roti-Quant assay) or at 590 nm and 450 nm (Roti-Nanoquant assay) against blanks of H_2O and H_2O incubated with reagent.

2.7. Curve fitting and calculations

Nonlinear curve fitting was performed with the SigmaPlot Version 11.0 program (Systat Software Inc., San Jose, CA, USA). Experimental hydrolysis time courses were fitted with Eq. (1)

$$y = \frac{ax}{b+x} + \frac{cx}{d+x} \quad (1)$$

where x is time [h] and y is the reducing sugar concentration [g/L]. Using the resulting parameter estimates, Eq. (1) was applied to calculate y for every 10 min within the first 3 h of hydrolysis, later for every 30 min. The volumetric hydrolysis rate r [g/L/h] was calculated using Eq. (2) from the y change within the 10 or 30-min time span.

$$r = \frac{\Delta y}{\Delta x} \quad (2)$$

Values of y were converted into substrate conversion values (C) based on the initial cellulose concentration (12.2 g/L). Plots of r versus C were usually biphasic with high r values at low C and low r values at high C. These dependencies were fitted with a thirdorder polynomial. Tangents were calculated for the resulting curve, and their point of intersection marks the transition between phases of high and low hydrolysis rates (C_{trans}).

The amount of protein and enzyme activity adsorbed to insoluble substrate was determined as the difference between total added protein and activity (see Table A.1) and measured protein and activity in the supernatant after incubation. Protein and activity measurements are described in Sections 2.4 and 2.6, respectively.

The specific initial hydrolysis rate ($r_{in\_specific}$) was obtained by dividing the maximum volumetric hydrolysis rate r_{max} by the concentration of adsorbed protein at the reaction start (P_{ads_in}). Note that the value of P_{ads_in} was obtained after about 20 min when adsorption was assumed to have reached apparent equilibrium.

3. Results and discussion

3.1. Development of an empiric model for analysis of hydrolysis efficiency

Experimental time courses of reducing sugar release from Avicel and pretreated wheat straw were described well by the double-rectangular hyperbola in Eq. (1), as shown by superimposition of the model fit on the measured data in Fig. 1A. Considering prior work, a single hyperbola (Nidetzky et al., 1993) and a double exponential function (Nidetzky and Steiner, 1993) were also tested. Criteria for selecting a mathematical model for curve fitting were the sum of least squares, mean square error, and normal distribution of residuals. The double hyperbola in Eq. (1) surpassed the other models in terms of quality of fit; however, the suitability of the mathematical model strongly depends on the used data set in which sampling procedures (number of samples, sampling time) have a decisive role.

The reaction rate r was calculated using the model fit, and Fig. 1B shows an example of the typical dependence of r on conversion C. The r–C dependence was biphasic and a rapid decline of r from an initially high value to a limiting low value was evident. The low rate was maintained until conversion was completed (Fig. 1B). Even though this pattern is similar for different cellulosic substrates and has been known for many years, the resulting curves often lack more detailed analyses and thus the role of different factors in retarding r at relatively low C is still under debate (Bansal et al., 2009; Hall et al., 2010; Yu et al., 2012). The high rate at reaction start was designated as maximum hydrolysis rate (r_{max}), and the hydrolysis rate at extended reaction times was considered to be limiting for hydrolysis efficiency. The 24-h time point was chosen as a reference for extended reaction time, and the corresponding hydrolysis rate was designated as limiting hydrolysis rate (r_{lim}). The value of C marking the transition between r_{max} and r_{lim} was designated C_{trans}, and Fig. 1B shows that C_{trans} was obtained from the intersection point of tangents placed onto the r–C curve. The C value after exhaustive hydrolysis time (48 h) was recorded for each experiment (C_{max}). Protein adsorption measurements were performed along the course of the reaction. At each time, the adsorbed protein concentration was related to the remaining polysaccharide concentration, which was calculated as the difference between initially added and already degraded polymeric reducing sugar. Fig. 1B depicts specific protein adsorption ($P_{ads\_specific}$) with respect to C. Note that contrary to the volumetric concentration of adsorbed protein such as P_{ads_in}, the physical dimension of $P_{ads\_specific}$ does not contain volume. $P_{ads\_specific}$ was fairly constant for most of the reaction and only after C had increased to 60% or higher, it started to rise sharply. The observation that r–C and $P_{ads\_specific}$–C dependencies showed break points at completely different values of C (Fig. 1B) immediately led to the conclusion that a decline in r at C of around 20% could not be due to cellulase adsorption in inadequate amounts. The possibility that unspecific and non-productive cellulase adsorption plays a

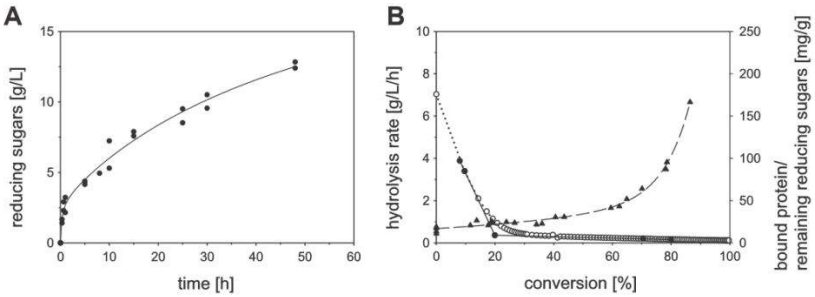

Fig. 1. Development of an empirical model for kinetic analysis of enzymatic hydrolysis of (ligno)cellulosic substrates. (A) Time course of hydrolysis. Pretreated wheat straw (12.2 g/L glucan; 2.5% dry matter) was hydrolyzed for 48 h at 50 °C using 75 FPU/g glucan ENZ-SC01. Black circles (●) represent reducing sugar concentration, the solid line curve fitting according to Eq. (1). (B) Decrease of r with C in comparison to protein binding per remaining reducing sugars. White circles (○) represent r and were fitted with a third-order polynomial, shown in dotted lines. Black circles (●) represent data points used for construction of tangents to r, shown in solid lines. The intersection of the tangents was used to determine C_{trans}. Black triangles (▲) represent bound protein per remaining reducing sugars. Dashed lines correspond to a bi-exponential fit.

role in the hydrolysis will be discussed later. An additional parameter obtained from each experiment was $r_{in\_specific}$ calculated as the ratio of r_{max} and P_{ads_in}.

3.2. Comparison of hydrolysis of pure crystalline cellulose and lignocellulosic substrate

The time courses for the analyses of Avicel and pretreated wheat straw hydrolysis were analyzed systematically, as shown in Fig. 1, to obtain r–C and $P_{ads\_specific}$–C dependencies. The results for hydrolysis of pretreated wheat straw and Avicel at 75 FPU/g glucan are presented in Fig. 2. As shown in Fig. 2A, pretreated wheat straw hydrolysis differed from that of Avicel in that both r_{max} and r_{lim} (Fig. 2A, inset) were increased, and C_{trans} was also shifted to a higher value under the conditions used. Therefore, this result supported detailed comparison of the two substrates during enzymatic conversion at different enzyme loadings. The $P_{ads\_specific}$–C dependencies in Fig. 2B revealed a sharper increase in $P_{ads\_specific}$ at high C for pretreated wheat straw as compared to Avicel. Possibly, lignin in pretreated wheat straw might be responsible for adsorbing additional protein. As the increased protein binding per remaining glycan at high C in pretreated wheat straw as compared to Avicel had only a minor effect on enhancing r_{lim} (Fig. 2A, inset), the notion of a non-productive adsorption of the cellulases, presumably to lignin, seemed to be therefore more reasonable. It is interesting that Bansal et al. (2012), who performed adsorption experiments on partially hydrolyzed Avicel, observed that $P_{ads\_specific}$ decreased with increasing C up to a value of 66%. These differences are worth noting, even though their causes are not understood at this time.

Kinetic descriptors of enzymatic hydrolysis of Avicel and pretreated wheat straw were obtained at different cellulase-to-cellulose ratios, and the results are shown in Fig. 3. P_{ads_in} was generally higher for pretreated wheat straw than Avicel (Fig. 3A). With both substrates, P_{ads_in} increased initially upon raising the enzyme loading to around 30 FPU/g and remained approximately constant at higher loadings. The protein adsorption measurement at low loadings (⩽15 FPU/g) were complicated by the presence of a relatively large amount of non-cellulolytic and non-adsorbing protein present, resulting from the addition of a constant β-glucosidase activity to avoid product inhibition. P_{ads_in} values at low FPU loading are therefore afflicted with a higher relative error. Findings in Fig. 3A are in good accordance with those in the literature that showed that pretreated lignocellulosic substrates had a higher adsorption capacity than Avicel (Kumar and Wyman, 2009; Kumar et al., 2012).

Comparison of panels B and C in Fig. 3 reveals that with Avicel and pretreated wheat straw, r_{max} displayed a stronger dependence on enzyme loading than r_{lim}. In fact, r_{lim} was almost constant across the different enzyme loadings while r_{max} increased approximately 2.6-fold (Avicel) and 5.6-fold (pretreated wheat straw) across the same enzyme loading range. In terms of r_{max}, the

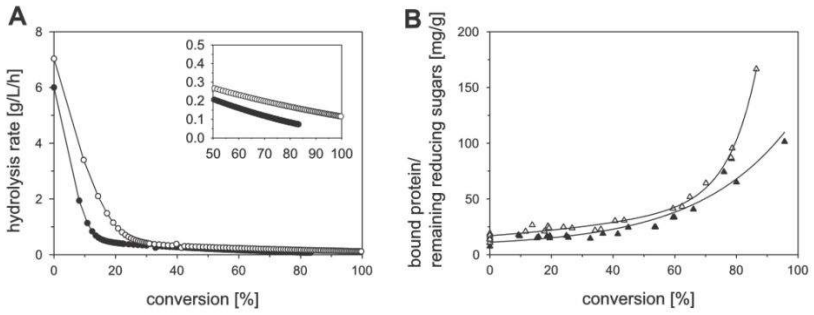

Fig. 2. Comparison of protein adsorption and hydrolysis of pretreated wheat straw and Avicel. (A) Progress of r with C. Substrates (12.2 g/L glucan) were hydrolyzed for 48 h at 50 °C using 75 FPU/g glucan. Figure detail displays r_{lim} in the second phase of hydrolysis. Black circles (●) represent hydrolysis of Avicel, white circles (○) hydrolysis of pretreated wheat straw. (B) Protein binding per remaining reducing sugars. Substrates (12.2 g/L glucan) were hydrolyzed for 48 h at 50 °C using 75 FPU/g glucan ENZ-SC01. White triangles (△) represent pretreated wheat straw, black triangles (▲) Avicel. Solid lines correspond to a bi-exponential fit.

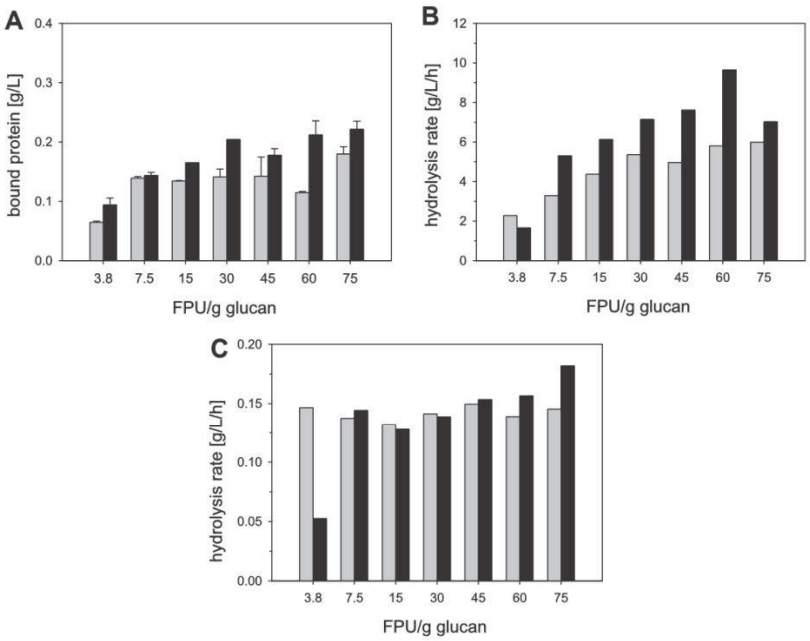

Fig. 3. Comparison of hydrolysis parameters for pretreated wheat straw and Avicel. Substrates were hydrolyzed for 48 h at 50 °C using the indicated activities. Black bars represent pretreated wheat straw, gray bars Avicel. (A) P_{ads_in}. (B) r_{max}. (C) r_{lim}.

optimum enzyme loading was 60 FPU/g. In pretreated wheat straw, r_{max} decreased upon a further increase in enzyme loading. At apparent saturation with enzyme ($\geqslant$30 FPU/g), r_{max} for pretreated wheat straw (~9.6 g/L/h) surpassed the r_{max} for Avicel about 1.7-fold. Only minor differences between the two substrates were detected for r_{lim}, with similar values at enzyme saturation (~0.15 g/L/h) (Fig. 3C). r_{lim} of pretreated wheat straw tended to increase slightly with enzyme loading, whereas that of Avicel exhibited no correlation. Overall, r_{lim} was up to 60-fold lower than r_{max}.

Fig. A.1 (Supporting Information) shows a comparison of r_{max} and r_{lim} obtained from r_(glucose) data with the corresponding descriptors derived from r_(reducing sugar) data. Using Avicel as substrate, there were only small differences in r_{max} and r_{lim} derived from glucose and reducing sugar data sets, as shown in panels B and D of Fig. A.1. Assuming that the added β-glucosidase had converted cellobiose and higher cello-oligosaccharides into glucose, the result was independent of the applied analytical procedure, as expected for a pure cellulosic substrate; however, when using pretreated wheat straw the comparison of r_{max} and r_{lim} from the r_(glucose)–C dependence with the corresponding parameters from the r_(reducing sugar)–C dependence was important to discriminate between cellulose and hemicellulose degradation in the lignocellulosic substrate. Panel A of Fig. A.1 shows that $r_{max\_}$(reducing sugar) was up to approximately 2-fold higher than $r_{max\_}$(glucose). On the contrary, $r_{lim\_}$(reducing sugar) was hardly different from the corresponding $r_{lim\_}$(glucose). These results suggest that r_{max} for pretreated wheat straw represented hydrolysis of both cellulose and hemicellulose components, while cellulose degradation solely accounted for r_{lim}. This pointed to a restriction in hemicellulose hydrolysis in the first phase of substrate conversion, a finding differing somewhat from that of Billard et al. (in press), who proposed an increased importance of xylan-hydrolyzing activity in later stages of the hydrolysis.

Time course data for reducing sugar release from pretreated wheat straw and Avicel were used to determine C_{trans} and C_{max} at each of the different enzyme loadings applied. Results are summarized in Table 1. C_{trans} was usually higher for pretreated wheat straw than Avicel, suggesting that the parameter was substrate-dependent. Provided that comparison is made on the basis of similar r_{max} and r_{lim} values as is the case for Avicel and pretreated wheat straw, a higher C_{trans} implies that transition to the slow r_{lim} kinetic regime can be deferred somewhat during the enzymatic reaction, with consequent positive effects on space–time yield. However, C_{trans} was also dependent on the enzyme loading. With both substrates, C_{trans} increased as the enzyme loading was raised (not considering the data at 75 FPU/g). Kinetically, the effect may be largely caused by the relatively greater influence of enzyme loading on r_{max} than on r_{lim} (Fig. 3). Using pretreated wheat straw at low enzyme loadings, the C_{trans} concept was not applicable due to an almost single-phasic decrease in r with C. These results indicate that C_{trans} is not just an intrinsic property of the chosen substrate, but also reflects interactions between cellulases and their substrate. Values of C_{max} were generally higher for pretreated wheat straw than for Avicel and increased with increasing enzyme loading (Table 1). Complete conversion of pretreated wheat straw necessitated the use of very high loadings of 60 FPU/g or more. Using Avicel, the conversion was always partial with a maximum around 80–84% at high enzyme loadings.

For most enzyme loadings, $r_{in\_specific}$ was similar for pretreated wheat straw and Avicel (Table 1). $r_{in\_specific}$ increased with increasing enzyme loading. With both substrates, it reached a maximum value of about 50 (1/h) at 60 FPU/g. These results suggested that the higher r (or r_{max}) of pretreated wheat straw as compared to that of Avicel (Fig. 3B) was at least partly due to enhanced enzyme adsorption. Moreover, optimum activity of adsorbed enzyme required a relatively high enzyme loading.

When comparing hydrolysis efficiencies for Avicel and pretreated wheat straw, a difference in cellulose crystallinity could be an important factor (Chang and Holtzapple, 2000; Zhang and

Table 1
Conversion parameters and specific hydrolysis rate for conversion of pretreated wheat straw and Avicel in dependence of enzyme loading and application of a low-temperature adsorption step.

Enzyme loading [FPU/g glucan]	Substrate	C_{trans}[a] [%]	C_{48h} [%]	$r_{in\_specific}$ [1/h]
Direct start of hydrolysis				
3.8	Avicel	5	65	35
	Wheat straw	–[b]	66	18
7.5	Avicel	10	67	24
	Wheat straw	15	72	37
30	Avicel	15	77	38
	Wheat straw	25	86	35
60	Avicel	20	83	51
	Wheat straw	25	89	46
75	Avicel	10	84	33
	Wheat straw	20	100	32
Hydrolysis after a pre-adsorption step				
3.8	Avicel	–[b]	66	41
	Wheat straw	25	63	73
7.5	Avicel	20	67	27
	Wheat straw	30	84	74
30	Avicel	15	66	15
60	Avicel	20	80	13
	Wheat straw	30	92	21
75	Avicel	20	72	9
	Wheat straw	30	100	20

[a] S.D. ⩽ 15% of the value reported.
[b] Single-phase decrease of hydrolysis rate.

Lynd, 2004; Bommarius et al., 2008); however, it must be noted that crystallinity index measurements in lignocellulosic substrate are affected by hemicellulose and lignin (Zhang and Lynd, 2004; Xu et al., 2012). For Avicel PH-101, a crystallinity index of 55.6% was reported (Bommarius et al., 2008). This value can be compared to a value of 28.4% for acid pretreated wheat straw (Gharpuray et al., 1983). Fungal cellulases hydrolyze amorphous cellulose three to 30 times faster than crystalline cellulose (Lynd et al., 2002). For Avicel, the initial enzymatic rate increases with a decreasing crystallinity index. At low degrees of crystallinity, adsorbed enzymes are more active at the same overall concentration (Hall et al., 2010). According to Chang and Holtzapple (2000), cellulose crystallinity affects the initial hydrolysis rate regardless of lignin content. This observation is in agreement with our findings that r_{max} was higher for pretreated wheat straw than Avicel. Crystallinity is also closely related to cellulose accessibility. Hall et al. (2010) suggested that the rigid structure of highly crystalline cellulose samples leaves little space for enzymes to initiate hydrolysis. This notion appears to be consistent with our observation that protein binding was lower to Avicel than pretreated wheat straw (Fig. 3A). Interestingly, $r_{in\_specific}$ values (Table 1) appear to not reflect the differences in crystallinity. Note that determination of $r_{in\_specific}$ for pretreated wheat straw does not distinguish between protein adsorption to cellulose, hemicellulose, and lignin. It can therefore only give a total apparent specific activity for this substrate.

3.3. Influence of a low-temperature adsorption step on hydrolysis efficiency

Evidence from Fig. 3 and Table 1 suggested that enhanced protein adsorption to pretreated wheat straw might constitute an important factor of the higher hydrolytic efficiency with this substrate as compared to Avicel. Further enhancement of protein binding was therefore intended by applying an adsorption step at 4 °C prior to hydrolysis at 50 °C. An incubation time of 20 min was sufficient for Avicel and pretreated wheat straw for protein adsorption to reach equilibrium under the conditions used. This finding is in good agreement with those from the literature (Nidetzky and Steiner, 1993; Varnai et al., 2010).

Results of protein adsorption measurements performed at different enzyme loadings are summarized in Fig. 4A. Avicel and pretreated wheat straw adsorbed similar amounts of protein at all enzyme loadings. Comparison of Figs. 4A and 3A reveal that adsorption at 4 °C was markedly different from that at 50 °C. P_{ads_in} at 4 °C increased strongly with increasing enzyme loading and, contrary to 50 °C, it did not level off at high enzyme loadings. Moreover, P_{ads_in} at high enzyme loadings was substantially higher at 4 than at 50 °C. For Avicel at 75 FPU/g, P_{ads_in} at 4 °C doubled that at 50 °C. Interestingly, P_{ads_in} at low to intermediate enzyme loadings (⩽30 FPU/g) was smaller at 4 than at 50 °C.

In order to identify binding of different enzymes (auxiliary to the cellulase) as part of the total protein adsorption, adsorption of selected enzyme activities onto Avicel and pretreated wheat straw were determined (Fig. A.2; Supporting Information). Xylosidase and arabinosidase were adsorbed by pretreated wheat straw, but not by Avicel. A linear relationship between adsorbed activity and protein was obtained in both cases, indicating that xylosidase and arabinosidase represented a constant fraction of the total adsorbed protein. β-Glucosidase did not bind to either substrate. This is interesting because adsorption of β-glucosidase to lignin was reported in several studies (Kadam et al., 2004; Kumar and Wyman, 2009; Yu et al., 1995). Galactosidase was bound by both pretreated wheat straw and Avicel. Its adsorption to pretreated wheat straw appeared to be weaker than that of xylosidase and arabinosidase. Mannosidase was not adsorbed. It seems plausible that binding of hemicellulolytic activities was partly responsible for protein adsorption in slightly higher amounts on pretreated wheat straw as compared to Avicel (Fig. 4A).

Hydrolysis parameters r_{max} and r_{lim} derived from time courses of reducing sugar release at 50 °C recorded after the foregoing adsorption at 4 °C are depicted in panels B and C of Fig. 4, respectively. The overall trends from the hydrolysis experiment without a low-temperature adsorption step (Fig. 3) were preserved or even reinforced, in that r_{max} but not r_{lim} was strongly dependent on enzyme loading (Fig. 4B); r_{max} was higher for pretreated wheat straw than Avicel (Fig. 4B); r_{lim} was similar for both substrates (Fig. 4C); and r_{max} was up to 60 times greater than r_{lim} (Fig. 4B and C); however, direct comparison of hydrolysis parameters between experiments with or without low-temperature adsorption steps revealed

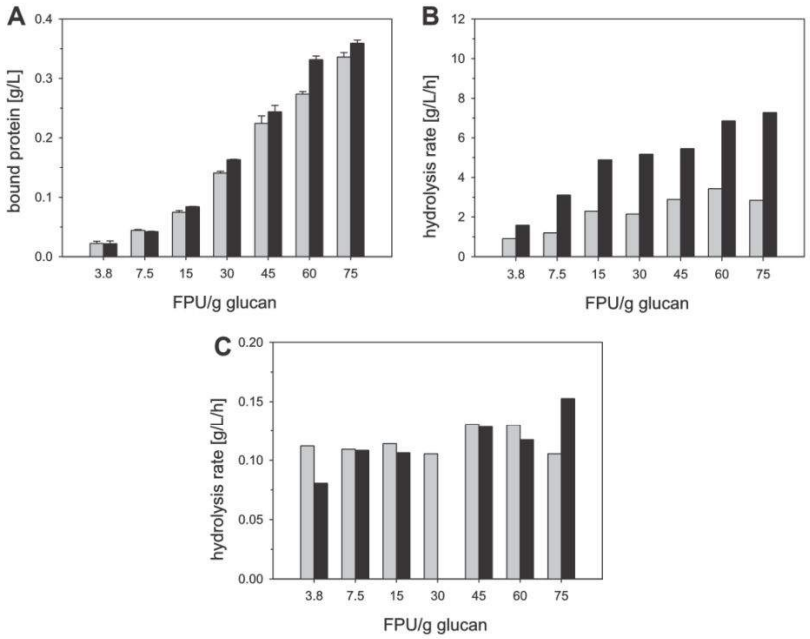

Fig. 4. Influence of a low-temperature adsorption step on parameters of enzymatic hydrolysis at 50 °C. A pre-adsorption step for 20 min at 4 °C and 300 rpm was followed by enzymatic hydrolysis (for 48 h at 50 °C) using the indicated activities. Black bars represent pretreated wheat straw, gray bars Avicel. (A) P_{ads_in}. (B) r_{max}. (C) r_{lim}.

that r_{lim} and in particular r_{max} were decreased as result of a prior adsorption at 4 °C. The effect in r_{max} was also substrate-dependent, giving a substantially larger, about 2-fold decrease for Avicel as compared to pretreated wheat straw where the decrease was relatively small (Fig. 4B). The lowering of r_{max} is even more remarkable when taking into account the increase in P_{ads_in} resulting from low-temperature adsorption at high enzyme loadings (Fig. 4A). The increase in P_{ads_in} is highlighted in Fig. 5 where reducing sugar release from Avicel (panel A) and pretreated wheat straw (panel B) after 20 min incubation at 50 °C is compared for experiments done with and without prior adsorption at 4 °C. Especially for Avicel, the hydrolysis rate was lowered at all protein loadings as result of the adsorption step.

Results for the determination of r_{max} and r_{lim} based on glucose release data are shown in Fig. A.3 (Supporting Information) where both $r_{max\_}$(glucose) and $r_{lim\_}$(glucose) are compared to the corresponding parameters based on reducing sugar data. Highly consistent values of r_{max} and r_{lim} were obtained from the different data sets. A major difference to experiments done without low-temperature adsorption is therefore revealed because under these conditions (Fig. A.1, panel A), $r_{max\_}$(reducing sugar) surpassed $r_{max\_}$(glucose) by a large amount. This result implies that adsorption at 4 °C could have negatively affected hemicellulose degradation in pretreated wheat straw. Interestingly and consistent with this notion, $r_{max\_}$(glucose) for pretreated wheat straw was not decreased by prior adsorption at 4 °C (Fig. A.3) as compared to

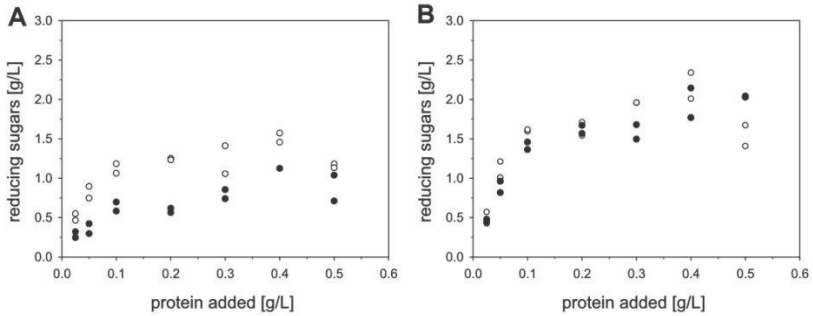

Fig. 5. Influence of a low-temperature adsorption step on initial reducing sugar release from pretreated wheat straw and Avicel in dependence on protein loading. A pre-adsorption step for 20 min at 4 °C and 300 rpm was followed by enzymatic hydrolysis for 20 min at 50 °C. Black circles (●) represent sugar release upon application of a pre-adsorption step followed by hydrolysis, white circles (○) direct start of hydrolysis without pre-adsorption. (A) Hydrolysis of Avicel. (B) Hydrolysis of pretreated wheat straw.

the direct hydrolysis experiment (Fig. A.1). However, in the case of Avicel, the lower values of $r_{max\_}$(reducing sugar) and $r_{max\_}$(glucose) resulting from the low-temperature pre-adsorption step indicate that cellulose conversion was also influenced.

Adsorption at 4 °C also affected the conversion parameters C_{trans} and C_{max} in a comparison to parameters from direct hydrolysis (Table 1); however, the effects were rather small and with Avicel, no uniform trend was recognized on C_{trans}. C_{max} for Avicel was decreased upon pre-adsorption at 4 °C, however, with pretreated wheat straw, C_{trans} and C_{max} were (slightly) increased as result of the low-temperature adsorption step. The C_{trans} increase implied that establishment of r_{lim} was shifted toward a higher substrate conversion. This result again indicated that C_{trans} was not a substrate characteristic alone, but was also dependent on cellulase interaction with the substrate. The small C_{max} increase may have been a consequence of C_{trans} up-shift.

Comparison of results obtained at low enzyme loading with the corresponding $r_{in\_specific}$ data from direct hydrolysis experiments indicated a marked increase in $r_{in\_specific}$ on pretreated wheat straw as result of adsorption at 4 °C (Table 1). For Avicel, no such increase was noted, but, as already mentioned, the P_{ads_in} determination at low enzyme loading was afflicted with a comparably large error, and error propagation in $r_{in\_specific}$ could be significant, especially for adsorption to pretreated wheat straw where at 4 °C only a small amount of protein was bound to substrate. At intermediate to high enzyme loadings, $r_{in\_specific}$ was lowered upon inclusion of the low-temperature pre-adsorption step, as compared to direct hydrolysis. Therefore, the foregoing adsorption at 4 °C appears to have resulted in non-productive protein adsorption, which could be ascribed to jamming (Bansal et al., 2009), enzyme clogging (Bubner et al., 2012) or low-affinity binding. When several cellulase molecules bind adjacent to one another on the same small surface area of cellulose, they might impede each other (Bommarius et al., 2008). This type of jamming seems to be of particular significance for the hydrolysis of crystalline cellulose (Xu and Ding, 2007; Igarashi et al., 2011), hence on Avicel. On pretreated wheat straw, other components of non-productive binding of the cellulases might come into play. Binding to lignin is certainly one of them.

4. Conclusion

Significant slow-down of sugar release at low degrees of substrate conversion is a major drawback hindering large-scale process commercialization of enzymatic hydrolysis of lignocellulosic substrates. Unfortunately, clear assignment of effect to underlying cause(s) is hampered by process complexity. In the present study, a set of kinetic descriptors was established to enable a correlation between enzyme adsorption and hydrolytic efficiency. The transition of r_{max} into r_{lim}, a crucial parameter for hydrolytic efficiency, was shown to be not only a characteristic of the substrate used, but also a complex revelation of cellulase–cellulose interaction. Therefore, in addition to the low r_{lim}, C_{trans} is a prime target to enhance hydrolytic efficiency.

Acknowledgements

The authors wish to thank Dr. Georg Schirrmacher (Süd-Chemie AG, Munich) for helpful discussions and comments. Support of Dr. Alexandra Schwarz (Institute of Biotechnology and Biochemical Engineering, Graz University of Technology) is thankfully recognized. This study was performed within the COMET K-Project Macro-Fun. Financial support from the Province of Styria is gratefully acknowledged. This work has been supported by the Federal Ministry of Economy, Family and Youth (BMWFJ), the Federal Ministry of Traffic, Innovation and Technology (bmvit), the Styrian Business Promotion Agency SFG, the Standortagentur Tirol and ZIT-Technology Agency of the City of Vienna through the COMET-Funding Program managed by the Austrian Research Promotion Agency FFG.

Appendix A. Supplementary data

Supplementary data associated with this article can be found, in the online version, at http://dx.doi.org/10.1016/j.biortech.2012.10.129.

References

Agbor, V.B., Cicek, N., Sparling, R., Berlin, A., Levin, D.B., 2011. Biomass pretreatment: fundamentals toward application. Biotechnol. Adv. 29, 675–685.
Alvira, P., Tomás-Pejó, E., Ballesteros, M., Negro, M.J., 2010. Pretreatment technologies for an efficient bioethanol production process based on enzymatic hydrolysis: a review. Bioresour. Technol. 101, 4851–4861.
Bansal, P., Hall, M., Realff, M.J., Lee, J.H., Bommarius, A.S., 2009. Modeling cellulase kinetics on lignocellulosic substrates. Biotechnol. Adv. 27, 833–848.
Bansal, P., Vowell, B.J., Hall, M.J., Realff, M.J., Lee, J.H., Bommarius, A.S., 2012. Elucidation of cellulose accessibility, hydrolysability and reactivity as the major limitations in the enzymatic hydrolysis of cellulose. Bioresour. Technol. 107, 243–250.
Berlin, A., Balakshin, M., Gilkes, N., Kadla, J., Maximenko, V., Kubo, S., Saddler, J., 2006. Inhibition of cellulase, xylanase and β-glucosidase activities by softwood lignin preparations. J. Biotechnol. 125, 198–209.
Billard, H., Faraj, A., Lopes Ferreira, N., Menir, S., Heiss-Blanquet, S., in press. Optimization of a synthetic mixture composed of major *Trichoderma reesei* enzymes for the hydrolysis of steam-exploded wheat straw. Biotechnol. Biofuels, doi:10.1186/1754-6834-5-9.
Bommarius, A.S., Katona, A., Cheben, S.E., Patel, A.S., Ragauskas, A.J., Knudson, K., Pu, Y., 2008. Cellulase kinetics as a function of cellulose pretreatment. Metab. Eng. 10, 370–381.
Bubner, P., Dohr, J., Plank, H., Mayrhofer, C., Nidetzky, B., 2012. Cellulases dig deep: in situ observation of the mesoscopic structural dynamics of enzymatic cellulose degradation. J. Biol. Chem. 287, 2759–2765.
Chang, V.S., Holtzapple, M.T., 2000. Fundamental factors affecting biomass enzymatic reactivity. Appl. Biochem. Biotechnol. 84–86, 5–37.
Gharpuray, M.M., Lee, Y.-H., Fan, L.T., 1983. Structural modification of lignocellulosics by pretreatments to enhance enzymatic hydrolysis. Biotechnol. Bioeng. 25, 157–172.
Ghose, T.K., 1987. Measurement of cellulase activities. Pure Appl. Chem. 59, 257–268.
Griggs, A.J., Stickel, J.J., Lischeske, J.J., 2011. Mechanistic Model for enzymatic saccharification of cellulose using continuous distribution kinetics I: depolymerization by EG_I and CBH_I. Biotechnol. Bioeng. 109, 665–675.
Hall, M., Bansal, P., Lee, J.H., Realff, M.J., Bommarius, A.S., 2010. Cellulose crystallinity-a key predictor of the enzymatic hydrolysis rate. FEBS J. 277, 1571–1582.
Hendriks, A.T.W.M., Zeeman, G., 2009. Pretreatments to enhance the digestibility of lignocellulosic biomass. Bioresour. Technol. 100, 10–18.
Himmel, M.E., Ding, S.Y., Johnson, D.K., Adney, W.S., Nimlos, M.R., Brady, J.W., Foust, T.D., 2007. Biomass recalcitrance. Engineering plants and enzymes for biofuels production. Science 315, 804–807.
Igarashi, K., Uchihashi, T., Koivula, A., Wada, M., Kimura, S., Okamoto, T., Penttilä, M., Ando, T., Samejima, M., 2011. Traffic jams reduce hydrolytic efficiency of cellulase on cellulose surface. Science 333, 1279–1282.
Jorgensen, H., Kristensen, J.B., Felby, C., 2007. Enzymatic conversion of lignocellulose into fermentable sugars: challenges and opportunities. Biofuels. Bioprod. Bioref. 1, 119–134.
Kadam, K.L., Rydholm, E.C., McMillan, J.D., 2004. Development and validation of a kinetic model for enzymatic saccharification of lignocellulosic biomass. Biotechnol. Prog. 20, 698–705.
Kumar, R., Wyman, C.E., 2009. Access of cellulase to cellulose and lignin for poplar solids produced by leading pretreatment technologies. Biotechnol. Prog. 25, 807–819.
Kumar, L., Arantes, V., Chandra, R., Saddler, J., 2012. The lignin present in steam pretreated softwood binds enzymes and limits cellulose accessibility. Bioresour. Technol. 103, 201–208.
Levine, S.E., Fox, J.M., Blanch, H.W., Clark, D.S., 2010. A mechanistic model of the enzymatic hydrolysis of cellulose. Biotechnol. Bioeng. 107, 37–51.
Lynd, L.R., Weimer, P.J., van Zyl, W.H., Pretorius, I.S., 2002. Microbial cellulose utilization: Fundamentals and biotechnology. Microbiol. Mol. Biol. Rev. 66, 506–577.
Miller, G.L., 1959. Use of dinitrosalicylic acid reagent for determination of reducing sugar. Anal. Chem. 31, 426–428.
Nidetzky, B., Steiner, W., 1993. A new approach for modeling cellulase-cellulose adsorption and the kinetics of the enzymatic hydrolysis of microcrystalline cellulose. Biotechnol. Bioeng. 42, 469–479.

Nidetzky, B., Steiner, W., Hayn, M., Esterbauer, H., 1993. Enzymatic hydrolysis of wheat straw after steam pretreatment: experimental data and kinetic modelling. Bioresour. Technol. 44, 25–32.

Nidetzky, B., Zachariae, W., Gercken, G., Hayn, M., Steiner, W., 1994. Hydrolysis of cellooligosaccharides by *Trichoderma reesei* cellobiohydrolases - experimental-data and kinetic modeling. Enzyme Microb. Technol. 16, 43–52.

Steiner, W., Sattler, W., Esterbauer, H., 1988. Adsorption of *Trichoderma reesei* cellulase on cellulose: Experimental data and their analysis by different equations. Biotechnol. Bioeng. 32, 853–865.

Varnai, A., Siika-Aho, M., Viikari, L., 2010. Restriction of the enzymatic hydrolysis of steam-pretreated spruce by lignin and hemicellulose. Enzyme Microb. Technol. 46, 185–193.

Wyman, C.E., 2007. What is (and is not) vital to advancing cellulosic ethanol. Trends Biotechnol. 25, 153–157.

Xu, F., Ding, H., 2007. A new kinetic model for heterogeneous (or spatially confined) enzymatic catalysis: contributions from the fractal and jamming (overcrowding) effects. Appl. Catal. A 317, 70–81.

Xu, N., Zhang, W., Ren, S., Liu, F., Zhao, C., Liao, H., Xu, Z., Huang, J., Li, Q., Tu, Y., Yu, B., Wang, Y., Jiang, J., Qin, J., Peng, L., 2012. Hemicelluloses negatively affect lignocellulose crystallinity for high biomass digestibility under NaOH and H_2SO_4 pretreatments in *Miscanthus*. Biotechnol. Biofuels 5, 58.

Yang, B., Willies, D.M., Wyman, C.E., 2006. Changes in the enzymatic hydrolysis rate of Avicel cellulose with conversion. Biotechnol. Bioeng. 94, 1122–1128.

Yu, A.H.C., Lee, D., Saddler, J.N., 1995. Adsorption and desorption of cellulase components during the hydrolysis of steam-exploded birch substrate. Appl. Biochem. Biotechnol. 21, 203–216.

Yu, Z., Jameel, H., Chang, H.-M., Philips, R., Park, S., 2012. Evaluation of the factors affecting Avicel reactivity using multi-stage enzymatic hydrolysis. Biotechnol. Bioeng. 109, 1131–1139.

Zhang, Y.H., Lynd, L.R., 2004. Toward an aggregated understanding of enzymatic hydrolysis of cellulose: noncomplexed cellulase systems. Biotechnol. Bioeng. 88, 797–824.

SUPPORTING INFORMATION

Enzymatic hydrolysis of microcrystalline cellulose and pretreated wheat straw: a detailed comparison using convenient kinetic analysis

Mareike Monschein[a], Christoph Reisinger[b] and Bernd Nidetzky [a,c,*]

[a] Austrian Center of Industrial Biotechnology (ACIB) GmbH, Petersgasse 14, 8010 Graz, Austria.
[b] Süd-Chemie AG, Staffelseestraße 6, 81477 Munich, Germany.
[c] Institute of Biotechnology and Biochemical Engineering, Graz University of Technology, Petersgasse 12/I, 8010 Graz, Austria.
*Corresponding author. phone number: +43 316 873-8400
fax: +43 316 873-8434
e-mail address: bernd.nidetzky@tugraz.at (B. Nidetzky)

Supporting Figures

Figure A.1: Comparison of *r* based on release of reducing sugars and glucose. Substrates (12.2 g/L glucan) were hydrolyzed for 48 h at 50°C using the indicated activities. Black bars represent *r* based on release of reducing sugars, grey bars *r* based on release of glucose. (A) r_{max} for pretreated wheat straw. (B) r_{max} for Avicel. (C) r_{lim} for pretreated wheat straw. (D) r_{lim} for Avicel.

Figure A.2: Binding of enzymatic activities. Substrates (12.2 g/L glucan) and enzyme (3.8 to 75 FPU/g glucan) were incubated for 20 min at 4°C and 300 rpm. Using a nitrophenol assay, enzymatic activities in the supernatant were measured and bound activities calculated. Arabinosidase activity was determined in a separate experiment. Stars (★) represent galactosidase activity, triangles (▲) mannosidase activity, X (✕) xylosidase activity and circles (●) arabinosidase activity. Black symbols represent pretreated wheat straw, white symbols Avicel.

Figure A.3: Comparison of r_{max} based on release of reducing sugars and glucose after a pre-adsorption step. A pre-adsorption step for 20 min at 4°C and 300 rpm was followed by enzymatic hydrolysis (for 48 h at 50°C) using the indicated activities. Black bars represent r_{max} based on release of reducing sugars, grey bars r_{max} based on glucose. (A) Pretreated wheat straw. (B) Avicel.

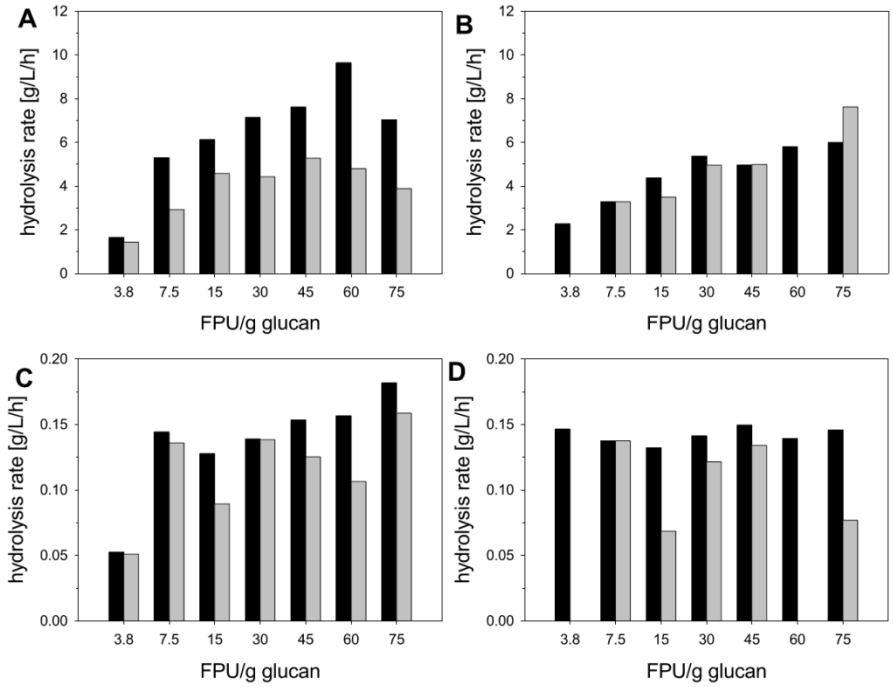
A
B
C
D
hydrolysis rate [g/L/h]
FPU/g glucan
3.8
7.5
15
30
45
60
75
0
2
4
6
8
10
12
0.00
0.05
0.10
0.15
0.20

Figure A.1

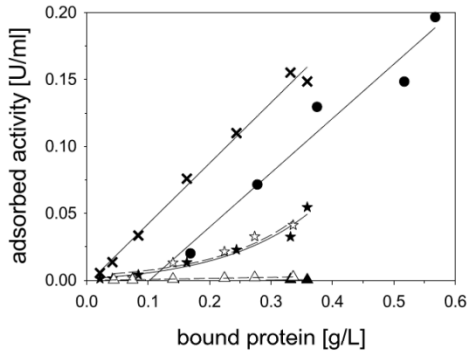
adsorbed activity [U/ml]
0.20
0.15
0.10
0.05
0.00
0.0
0.1
0.2
0.3
0.4
0.5
0.6
bound protein [g/L]

Figure A.2

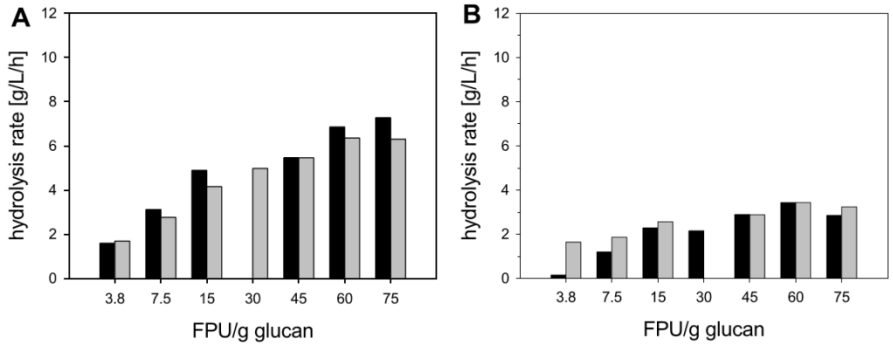
A
B
hydrolysis rate [g/L/h]
0
2
4
6
8
10
12
3.8
7.5
15
30
45
60
75
FPU/g glucan

Figure A.3

Supporting Table

Table A.1: Activity of ENZ-SC01 against nitrophenyl glycosides[a]

substrate	[U/mL]
4-nitrophenyl-α-L-arabinofuranoside	4.5
4-nitrophenyl-β-D-xylopyranoside	5.9
4-nitrophenyl-β-D-mannopyranoside	0.2
4-nitrophenyl-β-D-cellobioside	1.6
4-nitrophenyl-β-D-glucopyranoside	12.6
2-nitrophenyl-β-D-galactopyranoside	0.1

[a] measurement as described in section 2.4

Dissecting the effect of chemical additives on the enzymatic hydrolysis of pretreated wheat straw

Bioresource Technology 169 (2014) 713–722

Contents lists available at ScienceDirect

Bioresource Technology

journal homepage: www.elsevier.com/locate/biortech

Dissecting the effect of chemical additives on the enzymatic hydrolysis of pretreated wheat straw

Mareike Monschein [a], Christoph Reisinger [b], Bernd Nidetzky [a,c,*]

[a] Austrian Centre of Industrial Biotechnology (ACIB), Petersgasse 14, 8010 Graz, Austria
[b] CLARIANT Produkte (Deutschland) GmbH, Group Biotechnology, Staffelseestraße 6, 81477 Munich, Germany
[c] Institute of Biotechnology and Biochemical Engineering, Graz University of Technology, Petersgasse 12/I, 8010 Graz, Austria

HIGHLIGHTS

- Enzymatic hydrolysis of pretreated wheat straw in the presence of chemical additives.
- Final substrate conversion enhanced by urea.
- Late-stage hydrolysis rate enhanced by cetyl-trimethylammonium bromide.
- Enzyme adsorption mainly affected by PEG8000.
- Synergistic effect of combination of PEG8000 and urea.

ARTICLE INFO

Article history:
Received 17 May 2014
Received in revised form 13 July 2014
Accepted 14 July 2014
Available online 21 July 2014

Keywords:
Cellulase
Enzymatic hydrolysis
Protein adsorption
Chemical additives
Urea

ABSTRACT

Chemical additives were examined for ability to increase the enzymatic hydrolysis of thermo-acidically pretreated wheat straw by *Trichoderma reesei* cellulase at 50 °C. Semi-empirical descriptors derived from the hydrolysis time courses were applied to compare influence of these additives on lignocellulose bioconversion on a kinetic level, presenting a novel view on their mechanism of action. Focus was on rate retardation during hydrolysis, substrate conversion and enzyme adsorption. PEG 8000 enabled a reduction of enzyme loading by 50% while retaining the same conversion of 67% after 24 h. For the first time, a beneficial effect of urea is reported, increasing the final substrate conversion after 48 h by 16%. The cationic surfactant cetyl-trimethylammonium bromide (CTAB) enhanced the hydrolysis rate at extended reaction time (r_{lim}) by 34% and reduced reaction time by 28%. A combination of PEG 8000 and urea increased sugar release more than additives used individually.

1. Introduction

Lignocellulosic biomass is a potential feedstock for production of second-generation biofuels and other (bio)chemicals. However, several technical and economic factors still prevent the large-scale utilization of lignocellulose as a source for fermentable sugars, most notably a rapid decrease in hydrolysis rate and a need for high enzyme loadings (Himmel et al., 2007). Enzyme-associated factors such as product inhibition, enzyme denaturation, enzyme clogging or jamming as well as substrate-associated factors such as decreasing substrate reactivity and accessibility, multiphasic composition of cellulose, changes in degree of polymerization or crystallinity have been held responsible for sugar production at low space–time yields (Bansal et al., 2009; Bubner et al., 2012; Eibinger et al., 2014; Zhang and Lynd, 2004; Zhao et al., 2012).

To overcome these challenges and improve the economic viability of enzymatic hydrolysis, different strategies have been applied: Screening of microorganisms for new lignocellulose-degrading enzymes with better performance (Marjamaa et al., 2013), protein engineering (Thongekkaew et al., 2013), improvement of pretreatment technologies to increase cellulose accessibility (Agbor et al., 2011) or recovery and reuse of cellulases to reduce enzyme cost (Rodrigues et al., 2012). One promising approach to increase the enzymatic hydrolysis of cellulose is the supplementation of surfactants (e.g. Tween, Q-86W, Triton, Anhitole 20 BS), polymers (e.g. poly(ethylene glycol) (PEG), ricin oil ethoxylate, alcohol ethoxylate) or non-catalytic proteins (e.g. bovine serum albumin (BSA)) (Börjesson et al., 2007; Eriksson et al., 2002; Kristensen et al., 2007; Ooshima et al., 1986). It has been concluded that non-ionic

* Corresponding author at: Institute of Biotechnology and Biochemical Engineering, Graz University of Technology, Petersgasse 12/I, 8010 Graz, Austria. Tel.: +43 316 873 8400; fax: +43 316 873 8434.
E-mail address: bernd.nidetzky@tugraz.at (B. Nidetzky).

http://dx.doi.org/10.1016/j.biortech.2014.07.054
0960-8524/

surfactants are most effective in improving cellulose hydrolysis (Ooshima et al., 1986). Supplementation of poly(oxyethylene)$_{20}$ sorbitan monooleate (Tween 80) during cellulase hydrolysis of pretreated lodgepole pine resulted in a 32% increase of cellulose-to-glucose yield and reduced the hydrolysis time by 50%, while enhancing the amount of free enzyme in the hydrolysate (Tu et al., 2009). Ethylene oxide polymers like PEG showed a similar effect, increasing the conversion while enhancing the amount of free enzymes in the liquid phase and reducing process time (Ouyang et al., 2011). The main mechanism of surfactants, polymers and non-catalytic proteins might be a prevention of unspecific enzyme adsorption on lignin (Eriksson et al., 2002). Non-biospecific adsorption of proteins on lignin induces protein unfolding and enzyme inactivation, contributing to the excessive consumption of enzymes (Helle et al., 1993). Surfactants and polymers are believed to form a hydrated layer on the lignin surface, presenting a steric hindrance to unproductive cellulase binding. Thus, more enzymes are available for cellulose hydrolysis (Eriksson et al., 2002). Polymers and surfactants might also disrupt the (ligno)cellulose structure by removing lignin or amorphous cellulose, reinforce biomass swelling and increase cellulose accessibility (Helle et al., 1993; Kaar and Holtzapple, 1998; Li et al., 2012). Besides substrate-related mechanisms, a stabilizing effect on enzyme activity has also been suggested. Surfactants and polymers could protect enzymes from thermal denaturation, impede aggregation of instable cellulose components and help enzymes to desorb from the binding site after completion of saccharification (Helle et al., 1993; Kaar and Holtzapple, 1998).

Previous studies investigating the effect of additives on lignocelluloses hydrolysis focused mainly on wood materials, especially softwood lignocellulose (Börjesson et al., 2007; Seo et al., 2011; Tu et al., 2009). Wheat straw (*Triticum aestivum*) is a highly abundant, low-cost agricultural residue, which is not fully exploited today, therefore an interesting raw material for bioethanol production. Compared to wood biomass, herbaceous lignin has a different monomeric composition, containing guaiacyl, syringyl and *p*-hydroxyphenyl units in significant amounts. Lignins are acylated by *p*-coumaric acid at the γ-position of lignin sidechains, and lignin–carbohydrate complexes contain ferulic acid bridges between lignin and hemicellulose. These differences could possibly influence enzyme–substrate interactions and the effect of surfactants (Buranov and Mazza, 2008; Kristensen et al., 2007). A better understanding of the connections between chemical additives, enzyme adsorption and cellulose saccharification is crucial for making adaptive changes in the hydrolysis process. In a recent publication, we established a set of simple kinetic descriptors facilitating the correlation of enzyme adsorption and cellulose hydrolysis (Monschein et al., 2013). By applying these descriptors to the enzymatic hydrolysis of thermo-acidically pretreated wheat straw, the effects of non-ionic surfactants poly(oxyethylene)$_{20}$ sorbitan monolaurate (Tween 20), Tween 80, octyl-phenol(ethylene glycol)$_{7,5}$ ether (Triton X-100); cationic surfactant cetyltrimethylammonium bromide (CTAB); chaotropic agent urea; and the uncharged polyether polymers PEG 2000 and PEG 8000 were compared on a kinetic level, presenting a novel view on their mechanism of action.

2. Methods

2.1. Substrates and chemicals

Thermo-acidically pretreated wheat straw with a total dry matter content of 20.7% was supplied by CLARIANT (Munich, Germany). Wheat straw was pretreated in a high pressure autoclave at 145 °C for 13 min. A liquor ratio of 6.5:1 was used, and the liquid was supplemented with 0.5% H_2SO_4. The dry matter was composed of 58.1% glycan, 25.6% lignin, 4.9% inorganic substances, 2.1% water-soluble substances and 1.7% acid. Glucose accounted for 86.1% of the total sugar content, with xylose (12.1%), fructose (1%), arabinose (0.5%) and mannose (0.3%) making up the remaining portion. Roti-Quant reagent, Roti-Nanoquant reagent, CTAB, urea and Triton X-100 were from Carl Roth (Karlsruhe, Germany). PEG 2000 and PEG 8000, Tween 20, Tween 80, 4-nitrophenol and 4-nitrophenyl-β-D-glucopyranoside were from Sigma–Aldrich (St. Louis, MO, USA). All other chemicals were reagent grade.

2.2. Enzymes

ENZ-SC01 cellulase-mixture, containing the complete enzyme system of *Trichoderma reesei*, was from CLARIANT. We determined cellulase activity as 27 FPU/mL, β-glucosidase activity as 52 U/mL and protein content as 20 g/L.

2.3. Measurement of enzyme activities

Cellulase activities were measured in duplicates using the standardized FPU assay (Ghose, 1987). For measurement of β-glucosidase activity, the nitrophenol assay, calibrated against 4-nitrophenol, was used. The assay was performed in 96-well flat-bottom microtiter plates (GreinerBio-One International AG, Frickenhausen, Germany). Fifty microliters of 4-nitrophenyl-β-D-glucopyranoside were mixed with 50 µL of sample diluted in 50 mM Na-acetate buffer, pH 5.0, and incubated for 10 min at 50 °C and 300 rpm in an Eppendorf Thermomixer comfort (Eppendorf AG, Hamburg, Germany). After 5 min on ice, reactions were stopped by addition of 100 µL of 1 M Na_2CO_3. Absorbances were measured at 405 nm against a blank of substrate incubated with Na-acetate buffer in a FLUOstar Omega plate reader (BMG Labtech GmbH, Ortenberg, Germany).

2.4. Enzymatic hydrolysis with supplementation of various additives

Hydrolysis experiments were performed in duplicates and replicated twice. A suspension of pretreated wheat straw (25 g/L dry matter; 14.53 g/L glycan) was prepared in a total reaction volume of 1.8 mL of 50 mM Na-acetate buffer (pH 5.0). The substrate suspension was supplemented with one of the tested additives: PEG 2000 (0.5–2.5 g/L), PEG 8000 (0.5–2.5 g/L), CTAB (0.125–0.5 g/L), urea (0.5 g/L), Triton X-100 (0.5 g/L), Tween 20 (0.125 g/L) or Tween 80 (0.125 g/L). ENZ-SC01 was added in a concentration of 25 FPU/g glycan. Reaction tubes were incubated at 50 °C and 1000 rpm for 48 h using an Eppendorf Thermomixer comfort. At certain times, samples were taken. After a brief centrifugation (9300g, 30 s) 100 µL of the supernatant was retained for protein determination. The remaining sample was heated to 95 °C for 7 min and the cleared supernatant used for sugar analysis. Control reactions were performed without additive supplementation.

For testing the influence of enzyme loading on the effect of PEG 8000, different concentrations of ENZ-SC01 (from 6.2 to 62 FPU/g glycan) were added to the substrate suspension supplemented with 2.5 g/L PEG 8000. Hydrolysis was performed as stated above. Control reactions were performed without additive supplementation.

The combined effect of different additives was investigated by supplementing the substrate suspension with two different additives in three possible combinations: PEG 8000/CTAB, PEG 8000/urea or CTAB/urea. The additives were added in concentrations ranging from 6.3×10^{-2} to 5 g/L. ENZ-SC01 was added in a concentration of 25 FPU/g glycan. Hydrolysis was performed as stated above. Control reactions were performed with and without supplementation of the individual additives.

2.5. Protein determination

Protein content of ENZ-SC01 was determined using the Roti-Quant assay according to the manufacturer's instructions, calibrated against BSA. Absorbances were recorded with a Beckman Coulter DU800 spectrophotometer (Beckman Coulter GmbH, Krefeld, Germany). Protein adsorption was determined by measuring protein concentration in the supernatant, corresponding to unbound protein. A Roti-Nanoquant assay was used according to the manufacturer's instructions, calibrated against BSA. Absorbances were recorded with a FLUOstar Omega plate reader.

2.6. Sugar analysis

The liberated reducing sugar concentration was measured using a 3,5-dinitrosalicylic (DNS) acid based assay calibrated against glucose (Xiao et al., 2004). Forty microliters of 50 mM Na-acetate buffer (pH 4.8), 20 μL of sample and 120 μL of DNS reagent were pipetted into a 96-well PCR-plate (Bio-Rad, Hercules, CS, USA) and sealed with an aluminum seal (VWR International, Radnor, PA, USA). After 5 min at 95 °C in a thermo-cycler, samples were diluted in distilled water and absorbances were measured at 540 nm in a FLUOstar Omega plate reader.

2.7. Curve fitting and calculations

Curve fitting and calculations were performed according to Monschein et al. (2013). The SigmaPlot Version 9.0 program (Systat Software Inc., San Jose, CA, USA) was used for non-linear curve fitting. Experimental hydrolysis time courses were fitted with Eq. (1),

$$y = \frac{ax}{b+x} + \frac{cx}{d+x} \tag{1}$$

where x is time [h] and y is the reducing sugar concentration [g/L]. The resulting parameter estimates of Eq. (1) were applied for calculating y for every 10 min within the first 3 h of hydrolysis, later for every 30 min. The volumetric hydrolysis rate r [g/L/h] was calculated using Eq. (2) from the y change within the 10- or 30-min time span.

$$r = \frac{\Delta y}{\Delta x} \tag{2}$$

the high rate at reaction start was designated 'maximum hydrolysis rate' (r_{max}) [g/L/h]. The hydrolysis rate at the 24-h time point, chosen as a reference for extended reaction time, was termed 'limiting hydrolysis rate' (r_{lim}) [g/L/h]. The conversion of lignocellulosic material (C) was determined as follows:

$$C\,[\%] \equiv \frac{\text{reducing sugar produced [M]}}{\text{glycan [M]}} \times 100\% \tag{3}$$

where the glycan (cellulose plus hemicelluloses) concentration of the substrate suspension was 82.68 mM. The C values after extended hydrolysis time (24 h) and exhaustive hydrolysis time (48 h) were designated $C_{24\,h}$ [%] and C_{max} [%]. By plotting C versus t, time [h] necessary to reach a C value of 75% was determined ($t_{75\%}$). The amount of protein adsorbed to insoluble substrate was determined as the difference between total added protein and measured protein in the supernatant after incubation. The concentration of adsorbed protein at reaction start was designated P_{ads-in} [g/L]. $P_{ads\_24\,h}$ [g/L] described protein adsorption at extended reaction time (24 h), $P_{ads\_48\,h}$ [g/L] represented protein adsorption at exhaustive reaction time (48 h). By relating r_{max} to P_{ads-in} the specific initial hydrolysis rate ($r_{in\_specific}$) [h^{-1}] was obtained. The specific limiting hydrolysis rate ($r_{lim\_specific}$) [h^{-1}] was determined by relating r_{lim} to $P_{ads\_24\,h}$. The adsorbed protein concentration at each time was related to the remaining glycan concentration, calculated by subtracting y from the initial glycan concentration. This specific protein adsorption ($P_{ads\_specific}$) [mg/g] was plotted versus C and fitted with a bi-exponential curve. Note that contrary to the volumetric concentration of adsorbed protein, the physical dimension of $P_{ads\_specific}$ does not contain volume. To assess a possible synergistic effect of combined additives, the degree of synergy (DS) was determined as follows:

$$DS \equiv \frac{change_{\text{additive mixture}}[\%]}{\sum change_{\text{individual additive}}[\%]} \tag{4}$$

where $\sum change_{\text{individual additive}}$ describes the sum of the increase (or decrease) in the analyzed parameter ($P_{ads\_24\,h}$, r_{lim}, $r_{lim\_specific}$ or $C_{24\,h}$) upon application of individual additives, while $change_{\text{additive mixture}}$ describes the increase (or decrease) upon application of the additive mixture. A DS value >1.0 indicated a synergistic effect. We carefully considered how experimental error and error propagation affected the determination of the described parameters. The data shown in the figures are mean values of six independent determinations and error bares show the SD. The relative error was typically below 10%.

3. Results and discussion

3.1. Screening of chemical additives for an enhancement of enzymatic hydrolysis

3.1.1. Time course of hydrolysis

Based on recent publications (Knutsen and Liberatore, 2010; Olsen et al., 2011; Zhang et al., 2013) a representative range of additives was chosen for investigation on thermo-acidically pretreated wheat straw, including Tween 20, Tween 80, Triton X-100, CTAB, PEG 2000, PEG 8000 and urea. Untreated wheat straw consists of 38% cellulose, 25% hemicellulose and 23% lignin (Zhao et al., 2012). Thermo-acidically pretreated wheat straw used in this study contained less hemicellulose (~8%) and a higher percentage of both cellulose (50%) and lignin (25.6%). This shift might be due to a solubilization of hemicellulose, influencing the accessibility of lignin and hence unspecific adsorption (Kristensen et al., 2007). In order to quantitatively evaluate the effects of additives, a model describing the hydrolysis process is required. Some studies established models in order to analyze the influence of additives on a kinetic level (Helle et al., 1993; Kaar and Holtzapple, 1998; Seo et al., 2011; Wang et al., 2011). However, these investigations focus mostly on non-ionic surfactants, lacking an analysis of a broader range of additives on a lignocellulosic material pretreated for industrial purposes. Previously we presented a mathematical model based on a double-rectangular hyperbola (Eq. (1)) to describe the experimental time course of reducing sugar release from pretreated wheat straw (Monschein et al., 2013). Since the influence of CTAB on the time course of hydrolysis has not been described elsewhere, this additive was chosen to demonstrate the analytical approach. The superimposition of the model fit on the measured data describes accurately the release of reducing sugars (Fig. 1A). Compared to the control supplementation of 0.125 g/L CTAB resulted in a significantly higher sugar release between 12 and 48 h of incubation. The reaction rate r was calculated using the model fit, and Fig. 1B describes the dependence of r on C. The r–C dependence was biphasic and a rapid decline of r from an initially high value (r_{max}) to a limiting low value (r_{lim}) was evident. The low rate was maintained until conversion was completed (Monschein et al., 2013). Supplementation of the hydrolysis reaction with 0.125 g/L CTAB gave a similar pattern. However, the addition of the surfactant resulted in a slightly lower r_{max}, but had an increasing effect on r_{lim} once a conversion of 37% was reached (Fig. 1B inset).

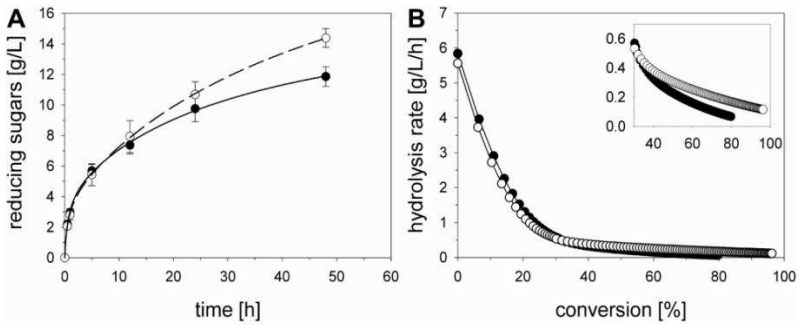

Fig. 1. Comparison of hydrolysis of pretreated wheat straw with or without supplementation of a chemical additive. Pretreated wheat straw (14.53 g/L glycan; 2.5% dry matter) was hydrolyzed for 48 h at 50 °C using 25 FPU/g glycan ENZ-SC01. (A) Time course of hydrolysis. White circles (○) represent reducing sugar concentration upon supplementation of 0.125 g/L CTAB, black circles (●) without supplementation of an additive. Solid and dashed lines represent curve fitting according to Eq. (1). (B) Decrease of r with C. The figure inset displays r_{lim} in the second phase of hydrolysis. White circles (○) represent hydrolysis of pretreated wheat straw upon addition of 0.125 g/L CTAB, black circles (●) hydrolysis without the additive. Circles were fitted with a third-order polynomial, shown in solid lines.

3.1.2. Influence of additive supplementation on protein adsorption

The volumetric hydrolysis rate usually increases with the amount of adsorbed cellulase, making it an important factor in the effectiveness of the hydrolysis reaction (Zhang and Lynd, 2004). Influence of the chosen additives on cellulase adsorption was determined based on the adsorption parameters P_{ads_in} and $P_{ads\_24\ h}$. In the control, P_{ads_in} reached a value of ~0.09 g/L, whereas supplementation of non-ionic surfactants reduced P_{ads_in} between 8% and 22% (Fig 2A). The same effect was observed when urea was present. Addition of 2.5 g/L PEG 2000 and 2.5 g/L PEG 8000 decreased the value by 21% and 18%, respectively. In contrast, the cationic surfactant CTAB enhanced P_{ads_in}, with a concentration of 0.5 g/L giving a 69% increase. The parameter $P_{ads\_24\ h}$ represents protein adsorption at extended reaction time (Fig. 2B). The only increase in $P_{ads\_24\ h}$ (~5%) was observed upon supplementation of 0.5 g/L CTAB. Addition of Triton X-100 lowered $P_{ads\_24\ h}$ by 41%, almost doubling its effect on P_{ads_in}. In the presence of PEG, $P_{ads\_24\ h}$ was inhibited by 18–60%, with 2.5 g/L PEG 8000 having the most pronounced effect of all additives tested. Tween 80, 0.125 g/L CTAB and urea reduced $P_{ads\_24\ h}$ to a smaller extent. Comparison of panels A and B of Fig. 2 shows a higher susceptibility of $P_{ads\_24\ h}$ for the influence of additives. Especially the inhibition of protein adsorption by PEG was intensified after 24 h. This indicates a certain time-span necessary for establishing the additive-related effect on protein adsorption.

3.1.3. Influence of additive supplementation on hydrolysis descriptors

The parameters r_{max}, r_{lim}, $C_{24\ h}$, C_{max} and $t_{75\%}$ were used for analyzing the saccharification reaction upon supplementation with the chosen additives. The results are shown in Fig. 3 and Table 1. Supplementation of 0.5 g/L PEG 2000 resulted in an increase of r_{max} by 13% in relation to the control. All other additives, including CTAB and urea, inhibited r_{max}. Again the most severe reduction was observed upon addition of 2.5 g/L PEG 8000, lowering r_{max} by 25%. The non-ionic surfactants tested in this study; Tween 20, Tween 80 and Triton X-100; decreased r_{max} by 14–18% (Fig. 3A). For r_{lim} the picture differed significantly. Non-ionic surfactants and 0.5 g/L PEG 2000 inhibited r_{lim} by 12–28% (Fig. 3B). On the contrary, supplementation of 2.5 g/L PEG 2000 or PEG 8000 increased r_{lim} by up to 30%. The effect of CTAB on r_{lim} changed with the concentration of the additive. Addition of 0.5 g/L CTAB inhibited r_{lim}, whereas 0.125 g/L CTAB resulted in an increase by 34%, the strongest effect of all additives tested. Urea was also very efficient in enhancing r_{lim}, increasing it by 32%.

For each of the different additives applied, cellulose conversion based on reducing sugar release was calculated after 24 or 48 h (Fig. 3C). By comparing $C_{24\ h}$ and C_{max}, we were able to assign the additive effect to the different phases of hydrolysis. Tween 80 and urea increased sugar release only in the 24–48 h time-span, enhancing C_{max} by 7% and 16%, respectively. PEG 2000, PEG 8000

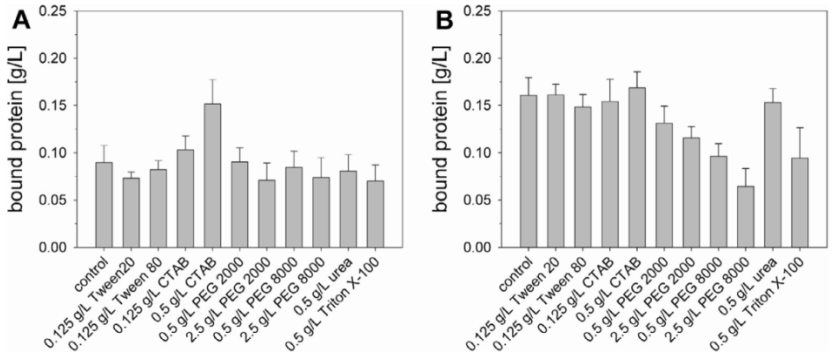

Fig. 2. Comparison of protein adsorption parameters upon supplementation of chemical additives. Pretreated wheat straw was hydrolyzed for 48 h at 50 °C using 25 FPU/g glycan ENZ-SC01 and supplemented with the indicated additives. (A) P_{ads_in}. (B) $P_{ads\_24\ h}$.

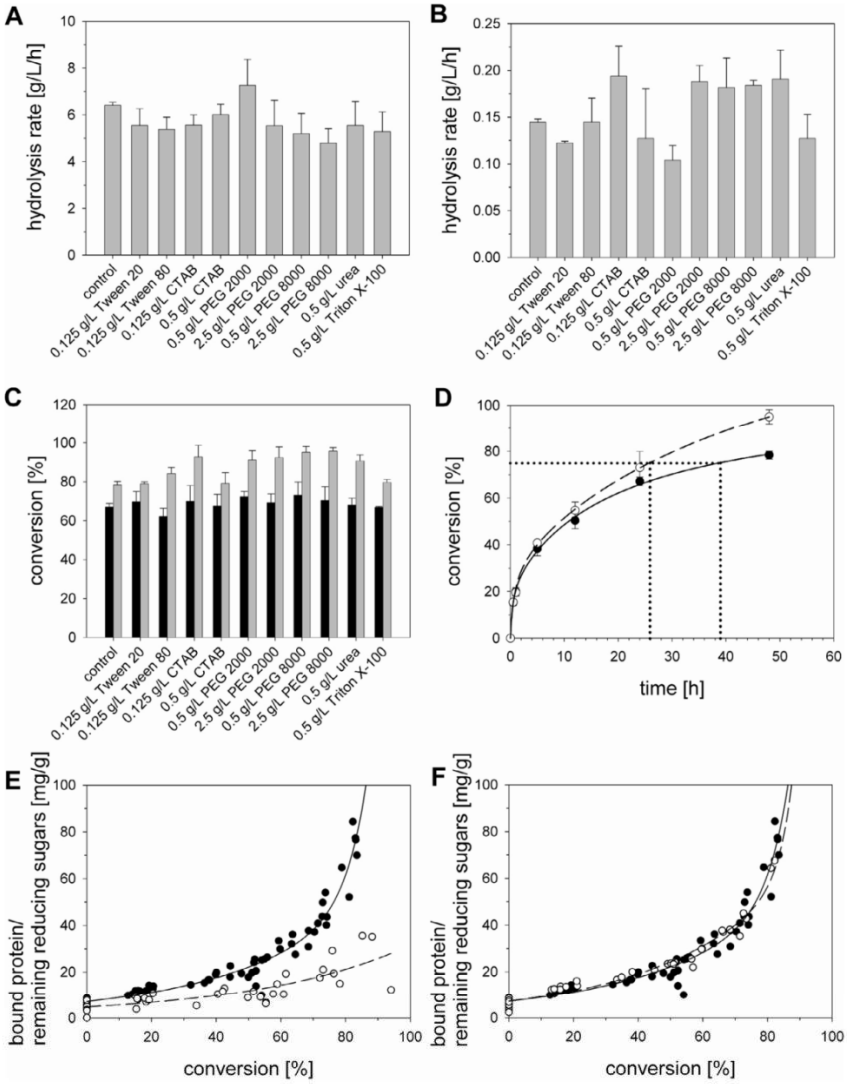

Fig. 3. Influence of chemical additives on saccharification parameters and specific protein adsorption. Pretreated wheat straw was hydrolyzed for 48 h at 50 °C using 25 FPU/g glycan ENZ-SC01 and supplemented with the indicated additives. (A) r_{max}. (B) r_{lim}. (C) Cellulose conversion. Black bars represent $C_{24\ h}$, gray bars C_{max}. (D) Cellulose conversion in relation to reaction time for determination of $t_{75\%}$. Solid lines with black dots (—●—) represent hydrolysis without supplementation of the additive, dashed lines with white dots (--○--) supplementation of 0.5 g/L PEG 8000. (E) $P_{ads\_specific}$ in relation to C upon supplementation of PEG 8000. White circles (○) represent hydrolysis of pretreated wheat straw upon addition of 2.5 g/L PEG 8000, black circles (●) hydrolysis without the additive. Solid and dashed lines correspond to a bi-exponential fit. (F) $P_{ads\_specific}$ in relation to C upon supplementation of CTAB. White circles (○) represent hydrolysis of pretreated wheat straw upon addition of 0.125 g/L CTAB, black circles (●) hydrolysis without the additive. Solid and dashed lines are bi-exponential fits to the data.

and 0.125 g/L CTAB enhanced both $C_{24\ h}$ (by 4–9%) and C_{max} (by 16–22%) with 2.5 g/L PEG 8000 showing the highest increase.

The potential to reduce process time is a benefit for applying additives in industrial-scale saccharification of lignocellulose. As demonstrated in Fig. 3D, this was evaluated by plotting C against t and determining the time at which a target conversion of 75% was reached. Graphical evaluation gave rise to the $t_{75\%}$ values presented in Table 1. In the control a C value of 75% was reached after 39 h. When urea was applied, $t_{75\%}$ was reduced to 30 h. PEG 8000 was the most efficient additive with 0.5 g/L shortening the process time to 26 h in total. PEG 2000 was a little less active, reaching $t_{75\%}$ values between 27 and 30 h. Supplementation of 0.125 g/L CTAB decreased $t_{75\%}$ to 28 h. These results illustrate the potential of additives, especially PEG, in shortening the process time of lignocelluloses conversion, thereby reducing expenses due to prolonged agitation, heating or wear and tear of the reactors.

Table 1
Reaction time parameter and specific hydrolysis rates for enzymatic hydrolysis of pretreated wheat straw in dependence of additive concentration.

Additive	Concentration [g/L]	$r_{in\_specific}$ [h^{-1}]	$r_{lim\_specific}$ [h^{-1}]	$t_{75\%}$ [h]
–	–	72	0.90	39
CTAB	0.125	54	1.3	28
	0.5	40	0.75	38
Tween 20	0.125	76	0.73	35
Tween 80	0.125	65	0.84	37
PEG 2000	0.5	80	0.79	27
	2.5	78	1.6	30
PEG 8000	0.5	61	1.9	26
	2.5	65	2.9	27
Urea	0.5	69	1.2	30
Triton X-100	0.5	75	1.3	38

S.D. ⩽ 15% of the value reported.

3.1.4. Correlation of the effects of additives on protein adsorption and hydrolysis

Connecting protein adsorption to saccharification descriptors is crucial for investigating the hydrolytic efficiency of cellulases. In accordance, $P_{ads\_specific}$, representing the adsorbed protein concentration per remaining glycan, was correlated with C. For the control, $P_{ads\_specific}$ was constant for most of the reaction. At a C value of 20%, the fitted curve showed a slope of 0.25. Once a conversion of ~70% was achieved, the curve increased sharply, with a slope of 7.9 at a C value of 85%. Addition of 2.5 g/L PEG 8000 resulted in a weaker increase of $P_{ads\_specific}$, reaching only one third of the control at final conversion, indicating a higher activity of adsorbed cellulases (Fig. 3E). At a C value of 20% the slope of the corresponding curve was 0.12. Compared to the control, the slope at 85% conversion was 17-times lower, resulting in a value of 0.47. In contrast, supplementation of 0.125 g/L CTAB did not alter $P_{ads\_specific}$–C dependencies (Fig 3F).

Protein adsorption and hydrolysis rate are reflected in the specific hydrolysis rate (Table 1). Supplementation of PEG 2000, Triton X-100 or Tween 20 caused a slight increase of $r_{in\_specific}$. An enhancement of $r_{in\_specific}$, by 11%, the highest observed, was achieved in the presence of 0.5 g/L PEG 2000. A decrease of $r_{in\_specific}$ was detected for Tween 80, urea, CTAB and PEG 8000. After 24 h, additive supplementation had a more pronounced effect on the specific hydrolysis rate. Addition of 2.5 g/L PEG 8000 to the reaction mixture resulted in a 3.2-fold higher value of $r_{lim\_specific}$. A 5-fold lower concentration of PEG 8000 still increased $r_{lim\_specific}$ by factor 2.1. Supplementation of 0.125 g/L CTAB, 2.5 g/L PEG 2000, 0.5 g/L urea or 0.5 g/L Triton X-100 had a smaller effect on $r_{lim\_specific}$, increasing it between 34% and 78%. Tween 20, Tween 80, 0.5 g/L PEG 2000 and 0.5 g/L CTAB decreased $r_{lim\_specific}$ by up to 19%, probably due to their inhibition of r_{lim}.

The results obtained by applying parameters of protein adsorption (P_{ads_in}, $P_{ads\_24\ h}$), hydrolysis parameters (r_{max}, r_{lim}, $C_{24\ h}$, C_{max}) and descriptors incorporating both factors ($P_{ads\_specific}$ versus C, $r_{in\_specific}$ $r_{lim\_specific}$) were consolidated for the individual additives, thus indicating differences in their mechanism of action:

3.1.4.1. Triton X-100. A beneficial effect of Triton X-100 on cellulose hydrolysis in the presence of lignin was attributed to a favorable association of the surfactant with the lignin surface, hence screening lignin–cellulase interactions (Olsen et al., 2011). Accordingly, we observed a decrease of P_{ads_in} and $P_{ads\_24\ h}$ (Fig. 2). One would expect an increase of hydrolysis rate upon reduction of non-specific protein adsorption. However, both r_{max} and r_{lim} were inhibited in the presence of Triton X-100 (Fig. 3). The decrease in hydrolysis rate was rather small compared to the one for protein adsorption. Thereby, specific hydrolysis rates were enhanced, but this was not reflected in conversion (Table 1). Triton X-100 did not increase $C_{24\ h}$ or C_{max} (Fig. 3). In contrast, Eriksson et al. (2002) reported an increase in $C_{24\ h}$ of steam pretreated spruce in the presence of Triton X-100. The difference might be related to the lower lignin content of pretreated wheat straw or the lower surfactant amount/g glycan used in this study.

3.1.4.2. Tween. Tween was proposed to be the most efficient surfactant in increasing cellulose conversion while lowering the necessary enzyme loading (Kaar and Holtzapple, 1998; Seo et al., 2011). In this study, Tween was rather inefficient in enhancing the saccharification of pretreated wheat straw. A reduction of P_{ads_in} and $P_{ads\_24\ h}$ was observed when Tween 80 was present. Tween 20 was only effective in decreasing P_{ads_in} (Fig. 2). Eriksson et al. (2002) proposed that non-ionic surfactants exhibit hydrophobic interaction with lignin, thereby preventing non-productive adsorption of enzymes. According to Tu et al. (2009), Tween is also able to detach already adsorbed proteins. We exclude a significant disruption of the cellulose structure proposed by Helle et al. (1993) since this would go along with an increase of protein adsorption. Similar to the findings for Triton X-100, application of Tween reduced r_{max} and r_{lim}. However, Tween 80 increased C_{max} by 7% (Fig. 3). Kaar and Holtzapple (1998) suggest a stabilizing effect of Tween on enzyme activity by reducing enzyme aggregation and thermal denaturation. It is possible, that protein inactivation due to heat and agitation affects hydrolysis beyond 24 h of reaction. Tween could counteract these effects, thus enhancing conversion at exhaustive reaction time. This hypothesis was supported by a slower decrease of r versus C later in hydrolysis when Tween 80 was present. At a C value of ~60% the slope of the corresponding curve was -7.9×10^{-3}, whereas supplementation of Tween 80 reduced this value to -4.5×10^{-3}. As a result Tween 80 increased r by ~38% after 30 h of reaction.

3.1.4.3. CTAB. So far the effect of CTAB on cellulose hydrolysis has only been investigated by Knutsen and Liberatore (2010). CTAB decreased the yield stress of pretreated corn stover slurry at high solid loading by up to 80%. Small molecule surfactants appear to lubricate the suspended particles, facilitate mixing and cause more uniform enzyme transport. An interaction of the surfactants' head groups with the substrate surface might block interparticle Columbic forces. Eriksson et al. (2002) proposed an increased binding of enzymes to lignin upon addition of positively charged surfactants like Dodecyltrimethylammonium bromide. Accordingly, 0.5 g/L CTAB increased P_{ads_in} by 69%, whereas a lower concentration had a more moderate effect on protein adsorption (Fig. 2). When CTAB was present, Knutsen and Liberatore (2010) detected the highest difference in conversion within the first 8 h of hydrolysis. An enhanced saccharification rate early in reaction suggests an advanced onset of liquefaction. In contrast, we observed a minor inhibition of r_{max} (Fig. 3). Application of 0.125 g/L CTAB significantly enhanced r_{lim} and $r_{lim\_specific}$ (Fig. 3; Table 1), which in turn

had an accelerating effect on C_{max}. Besides PEG, CTAB was the most effective additive tested in this study, increasing C_{max} by 18% and reducing $t_{75\%}$ by 28% (Table 1). However, the surfactant was only active in a concentration of 0.125 g/L, while 0.5 g/L did neither increase conversion nor reduce process time. In accordance to the observations for CTAB, the cationic surfactant Q-86W enhanced saccharification at low concentrations, but had an inhibitory effect at higher ones (Ooshima et al., 1986). Like Q-86W, CTAB might have abilities as accelerator and inhibitor of saccharification, probably due to a denaturating effect on cellulases in the liquid phase or an entrapment of cellulases in micelles at higher surfactant concentrations.

3.1.4.4. Urea. Urea is one of the important nitrogen sources used in fungi culture, but it is also a denaturant (Tao et al., 2011). NaOH/urea solutions have been used for pretreating lignocellulosic materials, disrupting its recalcitrance and improving enzymatic efficiency in the saccharification process (Li et al., 2010). For the first time, we demonstrate an improvement of hydrolytic efficiency, when urea is directly added to the reaction mixture. Compared to the control, urea enhanced C_{max} by 16% (Fig. 3). Application of urea reduced $t_{75\%}$ by 9 h, enabling a reduction in process time (Table 1). Besides CTAB, urea was the most efficient additive in enhancing r_{lim}, resulting in a 32% increase compared to the control (Fig. 3). A 33% higher $r_{lim\_specific}$ indicates an increased activity of adsorbed cellulases at extended reaction time (Table 1). In this study, urea caused a rather small inhibition of P_{ads_in} and $P_{ads\_24\ h}$ (Fig. 2). Thereby the effect of urea differs significantly from PEG (Section 3.1.4.5), which prevents unproductive cellulase adsorption. At this point we can only speculate about the mechanism of urea in enzymatic hydrolysis. An accumulation of nitrogen in lignin by nucleophilic addition reactions could impede lignin–enzyme interactions (Sewalt et al., 1997). An increased accessibility of cellulose could shift the protein adsorption equilibrium towards cellulose. Due to its considerably lower price, urea is an attractive alternative for PEG or CTAB in the hydrolysis of lignocellulosic substrates. Since urea is a nitrogen source for fermenting microorganisms, it should not interfere with subsequent fermentation of the produced sugars. Further research is needed to understand the mechanisms behind the enhancing effect of urea on hydrolytic efficiency.

3.1.4.5. PEG. Unlike Tween 20 or other non-ionic surfactants, PEG is a low cost commodity product. It has been shown to efficiently increase cellulose conversion, decrease enzyme loading and reduce process time (Ouyang et al., 2011; Sipos et al., 2010). We tested PEG 2000 and PEG 8000, differing in length of ethylene oxide chains and molecular weight. PEG is believed to block unspecific adsorption of enzyme to lignin (Kristensen et al., 2007). With exception of 0.5 g/L PEG 2000, PEG reduced both P_{ads_in} and $P_{ads\_24\ h}$ with the effect increasing over time (Fig. 2). The effect of PEG on $P_{ads\_24\ h}$ increased with the concentration of the additive and when the hydrophobic tail, the ethylene-oxide (EO) chain of the polymer, was longer. Apparently, longer EO chains are more effective in presenting a steric hindrance for cellulase adsorption to lignin (Eriksson et al., 2002). For 2.5 g/L PEG 8000 this was reflected in a reduction of $P_{ads\_24\ h}$ by 60% while increasing in $r_{lim\_specific}$ by factor 3.2, indicating a higher activity of the adsorbed

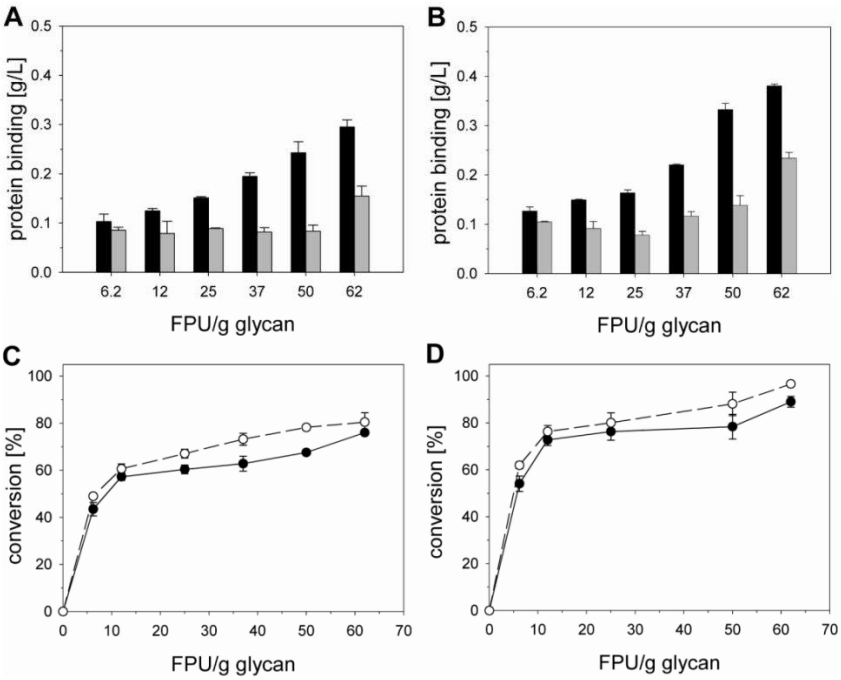

Fig. 4. Effect of PEG 8000 on the hydrolysis of pretreated wheat straw in dependence on enzyme loading. Pretreated wheat straw was hydrolyzed for 48 h at 50 °C using the indicated activities. (A) $P_{ads\_24\ h}$. Black bars represent hydrolysis without supplementation of the additive, gray bars supplementation of 2.5 g/L PEG 8000. (B) $P_{ads\_48\ h}$. Black bars represent hydrolysis without supplementation of the additive, gray bars supplementation of 2.5 g/L PEG 8000. (C) $C_{24\ h}$. Solid lines with black dots (—●—) represent hydrolysis without supplementation of the additive, dashed lines with white dots (--○--) supplementation of 2.5 g/L PEG 8000. (D) C_{max}. Solid lines with black dots (—●—) represent hydrolysis without supplementation of the additive, dashed lines with white dots (--○--) supplementation of 2.5 g/L PEG 8000.

enzymes (Fig. 2; Table 1). Corresponding to the proposed mechanism, we observed an increase in conversion accompanied by a decrease in protein adsorption, apparent in the change of $P_{ads\_specific}$–C dependencies upon supplementation of PEG 8000. Börjesson et al. (2007) observed the main difference in hydrolysis rate upon supplementation of PEG early in reaction, especially increasing hydrolysis rate at reaction start. In contrast, our results indicate a major effect of PEG later in hydrolysis by increasing r_{lim}. Of all additives tested, PEG was the most efficient one in enhancing substrate conversion, increasing C_{max} by up to 22% (Fig. 3). In accordance to its effect on protein adsorption PEG was more effective in increasing C_{max} at higher concentrations and when the polymer had a longer hydrophobic tail, a correlation also shown by Börjesson et al. (2007). The influence on C was reflected in a reduction of $t_{75\%}$ by up to 13 h while maintaining the same enzyme loading (Table 1). Therefore this additive has the highest potential to reduce process time in the saccharification of lignocellulose. Kristensen et al. (2007) found that PEG has the most pronounced effect on acid treated straw. It is possible that the acid pretreatment makes the lignin more receptive to cellulase adsorption by dissolving hemicelluloses associated with lignin or through a change of surface properties, e.g. increased hydrophobicity or hydrogen bonding capacity. Since PEG was also reported to enhance the hydrolysis of pure cellulose, it is likely that additional mechanisms besides a prevention of unproductive enzyme adsorption to lignin exist (Li et al., 2012).

3.2. Influence of enzyme dosage on the effect of PEG 8000

It is well known that the optimal ratio between enzyme and substrate is crucial for the efficient use of enzymes (Zheng et al., 2008). Thus, hydrolysis of pretreated wheat straw was performed with different concentrations of cellulase ranging from 6.2 to 62 FPU/g glycan. PEG 8000 was chosen to investigate the influence of enzyme dosage on the additive effect, since it was shown to be the most effective supplement. As expected, higher enzyme concentrations resulted in higher $P_{ads\_24\ h}$ for the control. Protein adsorption was lower when 2.5 g/L PEG 8000 was added. With exception of 62 FPU/g glycan, supplementation of PEG 8000 reduced $P_{ads\_24\ h}$ to a comparable level of 0.08 g/L (Fig. 4A). When PEG 8000 was present higher enzyme loadings did not increase $P_{ads\_24\ h}$. At 50 FPU/g glycan, supplementation of PEG 8000 decreased $P_{ads\_24\ h}$ by 65%. Between 24 and 48 h enzyme adsorption was further rising, but the increase was lower in the presence of PEG 8000 (Fig. 4B). PEG 8000 was less efficient in reducing $P_{ads\_48\ h}$, resulting in a maximum decrease by 58% at 50 FPU/g glycan. Whether PEG 8000 was present or not, substrate conversion increased rapidly until an enzyme loading of 12 FPU/g glycan. At higher enzyme loadings, the increase in $C_{24\ h}$ or C_{max} was slowed down (Fig. 4C; Fig. 4D). In the presence of PEG 8000, $C_{24\ h}$ was enhanced at all enzyme loadings, with a considerably higher effect between 37 and 50 FPU/g glycan (Fig. 4C). The strongest increase in $C_{24\ h}$ (17%) was obtained at an enzyme dosage of 37 FPU/g glycan.

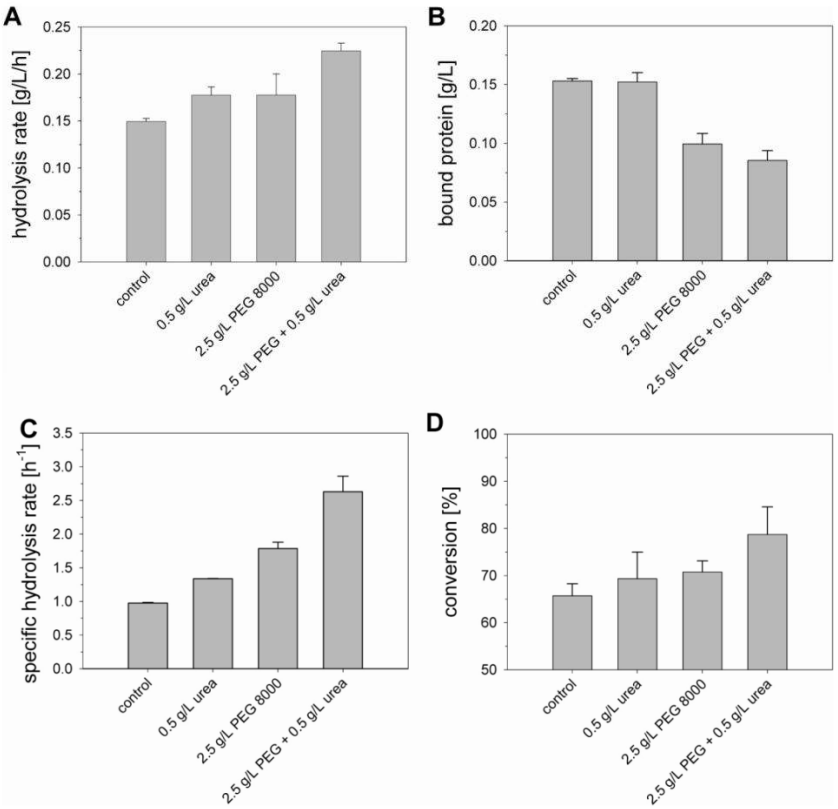

Fig. 5. Combined supplementation of PEG and urea in the hydrolysis of pretreated wheat straw. Pretreated wheat straw was hydrolyzed for 48 h at 50 °C using 25 FPU/g glycan ENZ-SC01 and supplemented with the indicated additives. (A) r_{lim}. (B) $P_{ads\_24\ h}$. (C) $r_{lim\_specific}$. (D) $C_{24\ h}$.

After 24 h of hydrolysis, the treatment with PEG 8000 at 25 FPU/g glycan gave similar results to an enzyme loading of 50 FPU/g glycan without supplementation. This indicated a possible reduction of enzyme loading by 50% upon addition of PEG 8000 while retaining a similar $C_{24\,h}$ value of 67%. As discussed, we were not able to detect an enhancement in $P_{ads\_24\,h}$ at higher enzyme loadings. Thus, the increase in $C_{24\,h}$ at higher enzyme loadings in the PEG-supplemented reaction batches could be due to a higher activity of adsorbed enzymes. A protective effect of PEG, decreasing the impact of prolonged enzyme contact to air, heat and shearing, has been suggested by Kaar and Holtzapple (1998). Li et al. (2012) proposed that PEG reduces the deactivation of cellulases upon adsorption to cellulose. Application of PEG 8000 increased C_{max} by up to 12%, observed at 50 FPU/g glycan (Fig. 4D). Due to formation of cracks in the cellulose substrate, increased conversion results in higher accessibility of the substrate and a larger surface area available for cellulase adsorption (Bubner et al., 2012). Higher $C_{24\,h}$ values might therefore explain the increase of $P_{ads\_48\,h}$ at enzyme loadings of 25–62 FPU/g glycan, which in turn enhanced C_{max}. While applying an enzyme loading of 50 FPU/g glycan, PEG 8000 reduced process time by 24 h. In accordance, 50% less enzyme was necessary for reaching a target conversion of ~80% after 48 h when PEG 8000 was present. By addition of PEG 8000, the maximum substrate conversion after exhaustive hydrolysis could be shifted from 89% to 97%, achieved at 62 FPU/g glycan. Our findings show that PEG 8000 is more effective at high enzyme loadings, a finding comparable to the results of Ouyang et al. (2011). PEG 8000 provides an opportunity for decreasing enzyme loading or process time while retaining the same degree of conversion.

3.3. Combination of additives

Kumar and Wyman (2009) observed additive effectiveness to depend on the type of sugars left in the solids, suggesting that a mixture of additives might be more beneficial to realize a high total sugar yield for a given pretreatment. PEG 8000, CTAB and urea were among the most efficient additives in enhancing hydrolysis of pretreated wheat straw, showing differences in their mechanism of action (see Section 3.1). To investigate a synergistic effect, the hydrolysis reaction was supplemented with combinations of these three additives in varying proportions. The strongest enhancement of r_{lim} and $C_{24\,h}$ was observed by addition of 2.5 g/L PEG 8000 plus 0.5 g/L urea, thus representing the most efficient additive combination. PEG 8000 reduced $P_{ads\_24\,h}$ by 35%, while urea had no influence (Fig. 5A). Addition of both components caused a further decrease in $P_{ads\_24\,h}$, reducing it by 44% in total. Accordingly, r_{lim} was increased by 50%, whereas the individual additives resulted only in an enhancement of 18% (Fig. 5B). PEG 8000/urea enhanced $r_{lim\_specific}$ by 169%, indicating an increased activity of adsorbed cellulases, while the individual additives caused an enhancement by 37–83% (Fig. 5C). Application of both additives enhanced $C_{24\,h}$ by almost 20%, surpassing the effect of urea and PEG 8000 alone (Fig. 5D). *DS* values for the change in $P_{ads\_24\,h}$ (1.2), r_{lim} (1.3), $r_{lim\_specific}$ (1.4) and $C_{24\,h}$ (1.5) confirmed a synergistic effect of urea and PEG 8000. While PEG 8000 was reported to reduce unproductive enzyme adsorption to lignin and could act as an enzyme stabilizer, urea possibly alters the structure of lignocellulose, thereby preventing lignin–enzyme interactions. This could explain the stronger reduction in protein adsorption and the higher activity of enzymes upon combination of the two additives. The effect of additives could be exploited in reducing hydrolysis time or enzyme loading, enabling a reduction in enzyme cost of the lignocellulosic ethanol process. Application of additives may be an additional financial expenditure, but it might become economically feasible, especially for high-solids loadings.

4. Conclusion

By applying semi-empirical descriptors on the enzymatic hydrolysis of pretreated wheat straw, the effect of additives was compared on a kinetic level. Supplementation of CTAB increased cellulose conversion after 48 h by 18% and for the first time, a beneficial effect was shown for urea. While retaining a similar conversion, PEG 8000 enabled either a reduction of enzyme loading by 50% or a decrease in process time by 24 h. A combination of PEG 8000 and urea enhanced sugar release more than when the additives were used individually. Supplementation of additives presents a promising approach to make large-scale saccharification economically feasible.

Acknowledgements

The authors wish to thank Dr. Georg Schirrmacher (CLARIANT, Munich) for many useful discussions and comments. Support of Dr. Alexandra Schwarz (Institute of Biotechnology and Biochemical Engineering, Graz University of Technology) is gratefully acknowledged. This study was performed within the COMET K-Project Macro-Fun and the COMET-K2-centre ACIB. Financial support from the Province of Styria is gratefully acknowledged. This work received support from: CLARIANT; the Federal Ministry of Economy, Family and Youth (BMWFJ); the Federal Ministry of Traffic, Innovation and Technology (bmvit); the Styrian Business Promotion Agency SFG; the Standortagentur Tirol; and ZIT-Technology Agency of the City of Vienna. Funding was through the COMET-Funding Program managed by the Austrian Research Promotion Agency FFG.

Appendix A. Supplementary data

Supplementary data associated with this article can be found, in the online version, at http://dx.doi.org/10.1016/j.biortech.2014.07.054.

References

Agbor, V.B., Cicek, N., Sparling, R., Berlin, A., Levin, D.B., 2011. Biomass pretreatment: fundamentals toward application. Biotechnol. Adv. 29, 675–685.
Bansal, P., Hall, M., Realff, M.J., Lee, J.H., Bommarius, A.S., 2009. Modeling cellulase kinetics on lignocellulosic substrates. Biotechnol. Adv. 27, 833–848.
Börjesson, J., Peterson, R., Tjerneld, F., 2007. Enhanced enzymatic conversion of softwood lignocellulose by poly(ethylene glycol) addition. Enzyme Microb. Technol. 40, 754–762.
Bubner, P., Dohr, J., Plank, H., Mayrhofer, C., Nidetzky, B., 2012. Cellulases dig deep: in situ observation of the mesoscopic structural dynamics of enzymatic cellulose degradation. J. Biol. Chem. 287, 2759–2765.
Buranov, A.U., Mazza, G., 2008. Lignin in straw of herbaceous crops. Ind. Crop. Prod. 28, 237–259.
Eibinger, M., Bubner, P., Ganner, T., Plank, H., Nidetzky, B., 2014. Surface structural dynamics of enzymatic cellulose degradation, revealed by combined kinetic and atomic force microscopy studies. FEBS J. 281, 275–290.
Eriksson, T., Börjesson, J., Tjerneld, F., 2002. Mechanism of surfactant effect in enzymatic hydrolysis of lignocellulose. Enzyme Microb. Technol. 31, 353–364.
Ghose, T.K., 1987. Measurement of cellulase activities. Pure Appl. Chem. 59, 257–268.
Helle, S.S., Duff, S.J., Cooper, D.G., 1993. Effect of surfactants on cellulose hydrolysis. Biotechnol. Bioeng. 42, 611–617.
Himmel, M.E., Ding, S.Y., Johnson, D.K., Adney, W.S., Nimlos, M.R., Brady, J.W., Foust, T.D., 2007. Biomass recalcitrance: engineering plants and enzymes for biofuels production. Science 315, 804–807.
Kaar, W.E., Holtzapple, M.T., 1998. Benefits from tween during enzymic hydrolysis of corn stover. Biotechnol. Bioeng. 59, 419–427.
Knutsen, J.S., Liberatore, M.W., 2010. Rheology modification and enzyme kinetics of high solids cellulosic slurries. Energy Fuels 24, 3267–3274.
Kristensen, J.B., Börjesson, J., Bruun, M.H., Tjerneld, F., Jørgensen, H., 2007. Use of surface active additives in enzymatic hydrolysis of wheat straw lignocellulose. Enzyme Microb. Technol. 40, 888–895.
Kumar, R., Wyman, C.E., 2009. Effect of additives on the digestibility of corn stover solids following pretreatment by leading technologies. Biotechnol. Bioeng. 102, 1544–1557.

Dissecting the effect of chemical additives on the enzymatic hydrolysis of pretreated wheat straw.

Li, J., Li, S., Fan, C., Yan, Z., 2012. The mechanism of poly(ethylene glycol) 4000 effect on enzymatic hydrolysis of lignocellulose. Colloids Surf. B 89, 203–210.
Li, M.F., Fan, Y.M., Xu, F., Sun, R.C., Zhang, X.L., 2010. Cold sodium hydroxide/urea based pretreatment of bamboo for bioethanol production: characterization of the cellulose rich fraction. Ind. Crop. Prod. 32, 551–559.
Marjamaa, K., Toth, K., Bromann, P.A., Szakacs, G., Kruus, K., 2013. Novel *Penicillium* cellulases for total hydrolysis of lignocellulosics. Enzyme Microb. Technol. 52, 358–369.
Monschein, M., Reisinger, C., Nidetzky, B., 2013. Enzymatic hydrolysis of microcrystalline cellulose and pretreated wheat straw: a detailed comparison using convenient kinetic analysis. Bioresour. Technol. 128, 679–687.
Olsen, S.N., Bohlin, C., Murphy, L., Borch, K., McFarland, K.C., Sweeny, M.D., Westh, P., 2011. Effects of non-ionic surfactants on the interactions between cellulases and tannic acid: a model system for cellulase–poly-phenol interactions. Enzyme Microb. Technol. 49, 353–359.
Ooshima, H., Sakata, M., Harano, Y., 1986. Enhancement of enzymatic hydrolysis of cellulose by surfactant. Biotechnol. Bioeng. 28, 1727–1734.
Ouyang, J., Ma, R., Huang, W., Li, X., Chen, M., Yong, Q., 2011. Enhanced saccharification of SO_2 catalyzed steam-exploded corn stover by polyethylene glycol addition. Biomass Bioenergy 35, 2053–2058.
Rodrigues, A.C., Leitao, A.F., Moreira, S., Felby, C., Gama, M., 2012. Recycling of cellulases in lignocellulosic hydrolysates using alkaline elution. Bioresour. Technol. 110, 526–533.
Seo, D.J., Fujita, H., Sakoda, A., 2011. Effects of a non-ionic surfactant, Tween 20, on adsorption/desorption of saccharification enzymes onto/from lignocelluloses and saccharification rate. Adsorption 17, 813–822.
Sewalt, V.J.H., Glasser, W.G., Beauchemin, K.A., 1997. Lignin impact on fiber degradation. 3. Reversal of inhibition of enzymatic hydrolysis by chemical modification of lignin and by additives. J. Agr. Food Chem. 45, 1823–1828.
Sipos, B., Dienes, D., Schleicher, A., Perazzini, R., Crestini, C., Siika-Aho, M., Reczey, K., 2010. Hydrolysis efficiency and enzyme adsorption on steam-pretreated spruce in the presence of poly(ethylene glycol). Enzyme Microb. Technol. 47, 84–90.
Tao, Y.M., Xu, X.Q., Ma, S.J., Liang, G., Wu, X.B., Long, M.N., Chen, Q.X., 2011. Cellulase hydrolysis of rice straw and inactivation of endoglucanase in urea solution. J. Agr. Food Chem. 59, 10971–10975.
Thongekkaew, J., Ikeda, H., Masaki, K., Iefuji, H., 2013. Fusion of cellulose binding domain from *Trichoderma reesei* CBHI to *Cryptococcus* sp. S-2 cellulase enhances its binding affinity and its cellulolytic activity to insoluble cellulosic substrates. Enzyme Microb. Technol. 52, 241–246.
Tu, M., Zhang, X., Paice, M., McFarlane, P., Saddler, J.N., 2009. Effect of surfactants on separate hydrolysis fermentation and simultaneous saccharification fermentation of pretreated lodgepole pine. Biotechnol. Prog. 25, 1122–1129.
Wang, Z., Xu, J.H., Feng, H., Qi, H., 2011. Fractal kinetic analysis of polymers/nonionic surfactants to eliminate lignin inhibition in enzymatic saccharification of cellulose. Bioresour. Technol. 102, 2890–2896.
Xiao, Z., Storms, R., Tsang, A., 2004. Microplate-based filter paper assay to measure total cellulase activity. Biotechnol. Bioeng. 88, 832–837.
Zhang, M., Ouyang, J., Liu, B., Yu, H., Jiang, T., Cai, C., Li, X., 2013. Comparison of hydrolysis efficiency and enzyme adsorption of three different cellulosic materials in the presence of poly(ethylene glycol). Bioenergy Res. 6, 1252–1259.
Zhang, Y.H., Lynd, L.R., 2004. Toward an aggregated understanding of enzymatic hydrolysis of cellulose: noncomplexed cellulase systems. Biotechnol. Bioeng. 88, 797–824.
Zhao, X.B., Zhang, L.H., Liu, D.H., 2012. Biomass recalcitrance. Part I: the chemical compositions and physical structures affecting the enzymatic hydrolysis of lignocellulose. Biofuel Bioprod. Bior. 6, 465–482.
Zheng, Y., Pan, Z., Zhang, R., Wang, D., Jenkins, B., 2008. Non-ionic surfactants and non-catalytic protein treatment on enzymatic hydrolysis of pretreated creeping wild ryegrass. Appl. Biochem. Biotechnol. 146, 231–248.

SUPPORTING INFORMATION

Dissecting the effect of chemical additives on the enzymatic hydrolysis of pretreated wheat straw using convenient kinetic analysis

Mareike Monschein[a], Christoph Reisinger[b] and Bernd Nidetzky [c,*]

[a] Austrian Center of Industrial Biotechnology (ACIB) GmbH, Petersgasse 14, 8010 Graz, Austria.
[b] CLARIANT Produkte (Deutschland) GmbH, Group Biotechnology, Staffelseestraße 6, 81477 Munich, Germany.
[c] Institute of Biotechnology and Biochemical Engineering, Graz University of Technology, Petersgasse 12/I, 8010 Graz, Austria.
*Corresponding author. phone: +43 316 873-8400
fax: +43 316 873-8434
e-mail address: bernd.nidetzky@tugraz.at (B. Nidetzky)

Supporting Figure

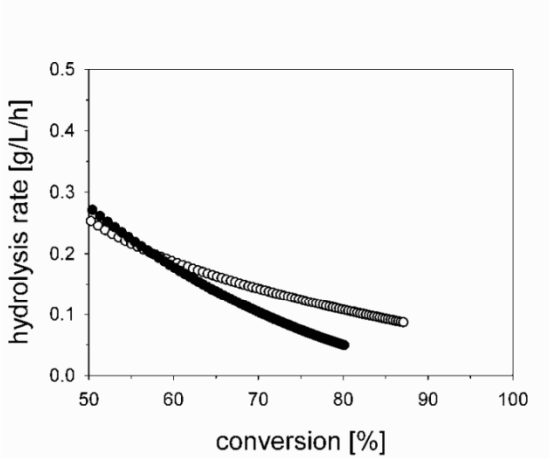

Figure A.1

Figure A.1: Influence of Tween 80 on hydrolysis rate at advanced conversion

Pretreated wheat straw (14.53 g/L glycan; 2.5% dry matter) was hydrolyzed for 48 h at 50 °C using 25 FPU/g glycan ENZ-SC01. Decrease of r with C is shown. White circles (○) show the hydrolysis of pretreated wheat straw upon addition of 0.125 g/L Tween 80, black circles (●) show hydrolysis without the additive. Circles were fitted with a third-order polynomial, shown in solid lines.

Supporting Table

Table A.1: Additive concentrations combined in the enzymatic hydrolysis of pretreated wheat straw

	additive		
reaction batch	urea [g/L]	PEG 8000 [g/L]	CTAB [g/L]
1	2.5×10^{-1}	5.0	–
2	2.5×10^{-1}	1.3	–
3	2.5×10^{-1}	5.0×10^{-1}	–
4	2.5×10^{-1}	2.5×10^{-1}	–
5	2.5×10^{-1}	1.3×10^{-1}	–
6	1.0	2.5	–
7	5.0×10^{-1}	2.5	–
8	2.5×10^{-1}	2.5	–
9	1.3×10^{-1}	2.5	–
10	6.4×10^{-2}	2.5	–
11	–	2.5	1.3×10^{-1}
12	5.0×10^{-1}	1.3	–
13	–	2.5	6.3×10^{-2}
14	–	1.3	1.3×10^{-1}
15	5.0×10^{-1}	–	1.3×10^{-1}

Effect of pretreatment severity in continuous steam explosion on enzymatic conversion of wheat straw: Evidence from kinetic analysis of hydrolysis time courses.

Effect of pretreatment severity in continuous steam explosion on enzymatic conversion of wheat straw: Evidence from kinetic analysis of hydrolysis time courses.

Bioresource Technology 200 (2016) 287–296

Contents lists available at ScienceDirect

Bioresource Technology

journal homepage: www.elsevier.com/locate/biortech

Effect of pretreatment severity in continuous steam explosion on enzymatic conversion of wheat straw: Evidence from kinetic analysis of hydrolysis time courses

Mareike Monschein [a], Bernd Nidetzky [a,b,*]

[a] Austrian Centre of Industrial Biotechnology (ACIB) GmbH, Petersgasse 14, 8010 Graz, Austria
[b] Institute of Biotechnology and Biochemical Engineering, Graz University of Technology, Petersgasse 12/I, 8010 Graz, Austria

HIGHLIGHTS

- Effect of pretreatment severity on hydrolysis of wheat straw kinetically analyzed.
- Continuous steam explosion more favorable for hydrolysis than batch pretreatment.
- Highest sugar yield from substrates pretreated at mild acidic conditions.
- Increased cellulase affinity of substrates not beneficial for saccharification.
- Transition of high to slow hydrolysis rate crucial for the achieved sugar yield.

ARTICLE INFO

Article history:
Received 17 August 2015
Received in revised form 8 October 2015
Accepted 10 October 2015

Keywords:
Cellulase
Enzymatic hydrolysis
Ligno-cellulosics
Continuous steam explosion
Kinetic analysis

ABSTRACT

Focusing on continuous steam explosion, the influence of pretreatment severity due to varied acid loading on hydrolysis of wheat straw by *Trichoderma reesei* cellulases was investigated based on kinetic evaluation of the saccharification of each pretreated substrate. Using semi-empirical descriptors of the hydrolysis time course, key characteristics of saccharification efficiency were captured in a quantifiable fashion. Not only hydrolysis rates *per se*, but also the transition point of their bi-phasic decline was crucial for high saccharification degree. After 48 h the highest saccharification was achieved for substrate pretreated at relatively low severity (1.2% acid). Higher severity increased enzyme binding to wheat straw, but reduced the specific hydrolysis rates. Higher affinity of the lignocellulosic material for cellulases does not necessarily result in increased saccharification, probably because of lignin modifications occurring at high pretreatment severities. At comparable severity, continuous pretreatment produced a substrate more susceptible to enzymatic hydrolysis than the batch process.

1. Introduction

Among agricultural residues, wheat straw (*Triticum aestivum*) is the largest biomass feedstock in Europe, representing an up to now untapped source of fermentable sugars. Since wheat straw possesses a low commercial value, its utilization for the production of bioethanol is an attractive alternative to sugar and starch based materials, compassing the food versus fuel conflict (Talebnia et al., 2010). However, bioconversion is significantly hindered by innate biomass recalcitrance, referring to the highly crystalline, complex structure of cellulose protected by lignin (Himmel et al., 2007). To overcome substrate recalcitrance, a pretreatment step is necessary, altering the chemical composition or loosening the physical structure of biomass (Meng and Ragauskas, 2014). For wheat straw, several different methods have been applied: physical (milling, chipping, etc.), physico-chemical (liquid hot water, ammonia fiber explosion, etc.), chemical (dilute or concentrated acid, alkali, etc.) and biological (degradation by microorganisms) processes (Talebnia et al., 2010).

Hydrothermal pretreatment methods, either auto- or acid-catalyzed, have attracted considerable research and development effort (Hansen et al., 2011; Ibbett et al., 2011; Nitsos et al., 2013). Among hydrothermal pretreatments steam explosion (SE) is one of the most widely employed technologies for pretreating lignocellulose for bioethanol production. Biomass is subjected to

* Corresponding author at: Institute of Biotechnology and Biochemical Engineering, Graz University of Technology, Petersgasse 12/I, 8010 Graz, Austria. Tel.: +43 316 873 8400; fax: +43 316 873 8434.
E-mail address: bernd.nidetzky@tugraz.at (B. Nidetzky).

http://dx.doi.org/10.1016/j.biortech.2015.10.020
0960-8524/

Effect of pretreatment severity in continuous steam explosion on enzymatic conversion of wheat straw: Evidence from kinetic analysis of hydrolysis time courses.

pressurized steam for a period of time and then suddenly depressurized with the explosive decompression causing fiber separation (Tomás-Pejó et al., 2011; Zhao et al., 2012a). It is a physicochemical method, where water acts as a weak acid, initiating the depolymerization and solubilization of hemicellulose. The hydrolysis of acetyl groups present in hemicellulose induces an acidic environment leading to partial cleavage of other glycosidic bonds and β-aryl ether bonds in lignin (Hansen et al., 2011; Li et al., 2007). Due to the removal of hemicellulose, surface area, porosity and thus cellulose accessibility are increased (Nitsos et al., 2013). Lignin is removed to a limited extent, but redistributed on the fiber surfaces because of melting and depolymerisation/ repolymerization reactions (Behera et al., 2014; Zhao et al., 2012a). Addition of acids like H_2SO_4 in steam explosion decreases time and temperature of reaction, improves hydrolysis rate, decreases the production of inhibitory compounds and leads to a more complete removal of hemicellulose (Behera et al., 2014). Most data available on steam explosion has been obtained using lab-scale batch reactors, while continuous reactors are of major interest for industrial applications (Chen et al., 2013; Fang et al., 2011; Zimbardi et al., 1999).

Sugar production at low space–time yields and a need for high enzyme loadings are bottlenecks preventing large-scale utilization of lignocellulose (Himmel et al., 2007). Among others, product inhibition, enzyme denaturation, clogging and jamming have been held responsible for the rapid decrease of hydrolysis rate with increasing substrate conversion. Besides enzyme-associated factors, substrate characteristics (accessibility, multiphasic composition of cellulose, degree of polymerization, crystallinity, etc.) have been linked to the slowing down of saccharification (Bansal et al., 2009; Bubner et al., 2012; Zhang and Lynd, 2004). These factors are altered by pretreatment of lignocellulosic substrates. The relationship between pretreatment, structural features of lignocellulose and hydrolytic efficiency has been the subject of extensive study and several reviews, but is still incompletely understood (Behera et al., 2014; Meng and Ragauskas, 2014; Zhao et al., 2012b; Zhu et al., 2008).

Unravelling how chemical compositions and physical structures affect the enzymatic hydrolysis of lignocellulose would greatly help to improve current pretreatment technologies (Zhao et al., 2012b). Previously we established a set of simple kinetic descriptors of both enzyme adsorption and sugar release (Monschein et al., 2013). By applying these descriptors on the enzymatic hydrolysis of 6 wheat straw substrates, the effect of severity change in steam explosion pretreatment due to varied acid loading on lignocellulose digestibility was investigated at a kinetic level. Regression analysis enabled a correlation between pretreatment conditions, substrate characteristics, protein adsorption and hydrolysis descriptors, providing further insights how pretreatment affects wheat straw digestibility.

2. Methods

2.1. Pretreated wheat straw substrates

Composition of both raw material and pretreated substrates was determined following the protocols of the National Renewable Energy Laboratory (Sluiter et al., 2010). The feedstock used was of typical composition where with reference to the dry matter (DM), about 65% was glycan and 14–16% was acid insoluble lignin. About 55% of the glycan was glucose, with xylose (38–41%), arabinose (4–5%) and galactose (0–1%) making up the remaining portion. Neither mannose nor fructose was detected. Wheat straw was ground to particles with a minimum size of 6 mm. The pretreatment was performed mainly by continuous steam explosion. Ground wheat straw was mixed with water and different concentrations of H_2SO_4, ranging from 0–3.5% relative to mass feedstock. The slurry was transferred from a storage bin into a steam gun reactor (Autoclave Engineers, Erie, PA, USA) by a screw type conveyor mechanism. The reactor consisted of a steam-jacketed reactor with Hastelloy pipe closed by two ball valves. Electrical heaters placed on all exposed, non-jacketed areas controlled the pretreatment set point temperature of 165 °C. Steam from a high-voltage steam generator was injected through nozzles with a pressure of 7 bar. Biomass was conveyed along the reactor towards the end using an auger. After a retention time of 10 min, the pressure was suddenly released by time-controlled opening of the valve. Pretreated material exited through a replaceable die at the bottom of the reactor into a cooled flash tank, where the material was withdrawn. Steam explosion in batch mode and a simple high-pressure autoclaving of the feedstock were used for reference. For steam explosion in batch mode, ground wheat straw was mixed with water and 3.2% H_2SO_4 relative to mass feedstock. Presoaked wheat straw was placed into a reactor, pressurized and heated with steam (7 bar) to 165 °C. After a retention time of 10 min, steam was quickly released through a vent. For high-pressure autoclaving, ground wheat straw was transferred into a steel container, mixed with water and 3.3% H_2SO_4 relative to mass feedstock and soaked for 4 h at room temperature. After removal of excess liquid, the sealed container was transferred into a conventional high-pressure autoclave system and sterilized at 145 °C, 4 bar for 13 min. In total, 6 differently pretreated wheat straw substrates (S1–S6) were obtained and are further described under Section 3. Corresponding pretreatment parameters and composition of the individual substrates are summarized in Table 1. Particle sizes of the obtained substrates were determined using the ImageJ 1.47v program (http://imagej.net). Reported values represent the average of six independent measurements.

2.2. Enzymes and chemicals

ENZ-SC01 cellulase-mixture, containing the complete enzyme system of *Trichoderma reesei*, was described in Monschein et al. (2013). Roti-Quant reagent and Roti-Nanoquant reagent were from Carl Roth (Karlsruhe, Germany). All other chemicals were reagent grade.

2.3. Enzymatic hydrolysis of pretreated wheat straw

Pretreated wheat straw (25 g/L DM) was suspended in 50 mM sodium acetate buffer (pH 5.0), resulting in a total reaction volume of 1.8 mL. ENZ-SC01 was added to the substrate suspension in a concentration of 14.4 FPU/g DM. Samples were incubated at 50 °C and 1000 rpm for 48 h in a Thermomixer comfort shaker (Eppendorf AG, Hamburg, Germany). At certain times, samples were taken and briefly centrifuged (9300*g*, 30 s). A 100 µL aliquot of the supernatant was retained for protein determination, while the remaining sample was heated to 95 °C for 7 min. The cleared supernatant was used for sugar analysis. Hydrolysis experiments were performed in triplicates and replicated once.

2.4. Protein determination

Protein content of ENZ-SC01 and protein adsorption to the lignocellulosic material was measured according to Monschein et al. (2014).

2.5. Sugar analysis

The liberated reducing sugar concentration was measured using a 3,5-dinitrosalicylic (DNS) acid based assay calibrated against glucose (Monschein et al., 2013). Forty microliters of 50 mM

Effect of pretreatment severity in continuous steam explosion on enzymatic conversion of wheat straw: Evidence from kinetic analysis of hydrolysis time courses.

Table 1
Pretreatment parameters, and composition and appearance of the pretreated substrates used. SE: steam explosion; AA: high-pressure autoclaving; operation mode: c, continuous; b, batch.

Pretreatment	Wheat straw substrates					
	S1	S2	S3	S4	S5	S6
Method	SE_b	SE_c	SE_c	SE_c	SE_c	AA_b
H_2SO_4 loading [% of DM]	3.2	3.5	2.3	1.2	0	3.3
Temperature [°C]	165	165	165	165	165	145
Retention time [min]	10	10	10	10	10	13
Substrate composition						
Glucose [%] (cellulose, glucan)	32.7	38.7	35.4	35.8	37.4	34.2
Xylose [%] (xylan)	20.1	15.2	19.5	22.3	24.1	2.2
Arabinose [%] (arabinan)	3.3	2.1	2.0	2.1	2.3	0.3
Galactose [%] (galactan)	1.0	0.0	0.5	0.8	0.3	0.0
Acid insoluble lignin [%]	15.1	20.9	16.3	16.0	16.9	36.0
Acid [%] (acetic acid, formic acid)	5.3	1.9	3.6	4.2	4.3	16.6
Dry matter [%]	21.6	37.9	37.9	37.8	37.8	20.9
Substrate appearance						
Average particle size [mm]	2	<1	1	4	6	<1
Morphology	Fibrous chunks	Granulate	Granulate	Fibers	Fibers	Powder
Color	Medium	Dark	Medium	Light	Light	Dark

Na-acetate buffer (pH 4.8), 20 µL of sample and 120 µL of DNS reagent were pipetted into a 96-well PCR-plate (Bio-Rad, Hercules, CS, USA) and sealed with an aluminium seal (VWR International, Radnor, PA, USA). After 5 min at 95 °C in a thermo-cycler, samples were transferred into 96-well flat-bottom microtiter plates (GreinerBio-One International AG, Frickenhausen, Germany) and diluted in distilled water. Measurements were done in duplicates at 540 nm in a FLUOstar Omega plate reader (BMG Labtech GmbH, Ortenberg, Germany).

Glucose concentration was determined using a hexokinase–glucose 6-phosphate dehydrogenase assay by Sigma–Aldrich (St. Louis, MO, USA). Measurements were done in duplicates at 340 nm in a FLUOstar Omega plate reader.

2.6. Confocal laser scanning microscopy (CLSM)

Pretreated wheat straw was analyzed in water with a Leica TCS SPE confocal laser microscope (Leica Microsystems, Wetzlar, Germany). Briefly, samples were excited with a 488-nm laser beam, and emitted light was detected in the range 500–700 nm. Offset and photomultiplier gain were optimized to provide the best signal/noise ratio possible. Images were acquired with a Leica HCX APO L U-V-I 20×/0.50 Water UV objective (NA: 0.5). Image analysis was performed using ImageJ 1.47v.

2.7. Curve fitting and calculations

Non-linear curve fitting using the SigmaPlot Version 10.0 program (Systat Software Inc., San Jose, CA, USA) and calculations were performed according to Monschein et al. (2013). Experimental hydrolysis time courses were fitted with Eq. (1).

$$y = \frac{ax}{b+x} + \frac{cx}{d+x} \quad (1)$$

x is time [h] and y is the reducing sugar concentration [g/L]. Based on parameter estimates of Eq. (1), y was calculated for every 10 min within the first 3 h of hydrolysis, later for every 30 min. The volumetric hydrolysis rate r [g/L/h] was calculated using Eq. (2) from the y change within the 10- or 30-min time span

$$r = \frac{\Delta y}{\Delta x} \quad (2)$$

The reducing sugar concentration at each time defined the saccharification (S) [mM]. S values after short (5 h), intermediate (12 h), long (24 h) and extended hydrolysis time (48 h) were designated $S_{5\ h}$ [mM], $S_{12\ h}$ [mM], $S_{24\ h}$ [mM] and S_{max} [mM]. The parameter C [%] described the conversion of the glycan portion in the lignocellulosic substrates

$$C\ [\%] \equiv \frac{S\ [\mathrm{M}]}{glycan\ [\mathrm{M}] \times 100\%} \quad (3)$$

The glycan concentration was the sum of anhydrohexoses (mainly glucose) and anhydropentoses (mainly xylose) present. The glycan conversion after short (5 h), intermediate (12 h), long (24 h) and extended hydrolysis time (48 h) was described by the parameters $C_{5\ h}$ [%], $C_{12\ h}$ [%], $C_{24\ h}$ [%] and C_{max} [%].

Plots of C versus r were usually biphasic with high r-values at low C and low r-values at high C. These dependencies were fitted with a third-order polynomial. Tangents were constructed to the resulting curve and their point of intersection marks C_{trans} [%], the transition between phases of high and low hydrolysis rate. Based on Eq. (1), these conversion values were converted into t_{trans} [h], describing the hydrolysis time when transition took place. The high hydrolysis rate at reaction start was designated 'maximum hydrolysis rate' (r_{max}) [g/L/h], while 'intermediate hydrolysis rate' (r_{med}) [g/L/h] and 'limiting hydrolysis rate' (r_{lim}) [g/L/h] refer to the hydrolysis rates at C_{trans} and $C_{50\%}$, respectively.

Protein concentration adsorbed to insoluble substrate, P_{ads}, was defined by the difference between total added protein and measured protein in the supernatant after incubation. Adsorbed protein concentrations at reaction start (0 h), after short (5 h) intermediate (12 h), long (24 h) and extended reaction times (48 h) were designated $P_{ads\_0\ h}$ [g/L], $P_{ads\_5\ h}$ [g/L], $P_{ads\_12\ h}$ [g/L], $P_{ads\_24\ h}$ [g/L] and $P_{ads\_48\ h}$ [g/L]. The specific hydrolysis rate $r_{\_specific}$ was calculated from Eq. (4):

$$r_{\_specific}\ [\mathrm{h}^{-1}] \equiv \frac{r\ [\mathrm{g/L/h}]}{P_{ads}\ [\mathrm{g/L}]} \quad (4)$$

The specific initial hydrolysis rate ($r_{in\_specific}$) [h^{-1}] was obtained by relating r_{max} to $P_{ads\_0\ h}$. Relating r_{med} to P_{ads} at C_{trans} or r_{lim} to P_{ads} at $C_{50\%}$ gave rise to specific intermediate ($r_{med\_specific}$) [h^{-1}] and specific limiting ($r_{lim\_specific}$) [h^{-1}] hydrolysis rates.

To correlate pretreatment parameters, substrate composition or certain characteristics of the substrate (e.g. size) to hydrolysis

Effect of pretreatment severity in continuous steam explosion on enzymatic conversion of wheat straw: Evidence from kinetic analysis of hydrolysis time courses.

descriptors and protein adsorption parameters, regression analysis was performed using the SigmaPlot Version 10.0 program. For detecting a correlation, a number of possible fits were tested. These included linear and hyperbolic fits, exponential decay or rise to maximum, exponential growth and sigmoidal decay. Fits with a determination coefficient of at least 5.0 and a dependency $\geqslant 0.6$ and <1 were considered to be significant.

We carefully considered how experimental error and error propagation affected the determination of the described parameters. Data shown in the figures are mean values of six independent determinations and error bars show the SD. The relative error was typically below 10%. Note: each hydrolysis rate was obtained from fit of an experimental time course consisting of reducing-sugar data from six independent determinations. Therefore no standard deviation is shown. Determination of $r_{\_specific}$ was based on the fit, following the same approach concerning standard deviations.

3. Results and discussion

3.1. Influence of pretreatment parameters on substrate characteristics

Wheat straw and other herbaceous residues differ in their composition and chemical structure from wood biomass. Herbaceous residues have a lower lignin content characterized by a different monomeric composition, containing guaiacyl, syringyl and *p*-hydroxyphenyl subunits in significant amounts (Buranov and Mazza, 2008). Cellulose in wheat straw is mainly cellulose I allomorph with relatively low crystallinity, while hemicellulose is mostly composed of arabino/glucuronoxylans (Sun et al., 2005). Its monosaccharides are substituted with acetyl and especially phenolic acid groups which are implicated to be involved in the crosslinking of hemicellulose and lignin (Buanafina, 2009). Since physicochemical properties and behavior of wheat straw differ from wood biomass, appropriate pretreatments based on its characteristics need to be applied. Thus, an individual analysis is required how structural and compositional changes induced by hydrothermal pretreatment affect the digestibility of wheat straw.

For this study wheat straw was subjected to hydrothermal pretreatment methods, focusing on steam explosion in continuous reactors (SEC). For comparative reasons, wheat straw was pretreated by steam explosion in a batch reactor (SEB) or by acidic autoclaving in a high pressure-autoclave (AA). The pretreatment parameter varied in SEC was the H_2SO_4 loading. Six differently composed substrates (S1–S6) were obtained (Table 1). The raw material contained 36% cellulose (as glucose), 29% hemicellulose (as xylose, arabinose and galactose) and roughly about 14–16% lignin. Pretreatment changed both substrate composition and macroscopic appearance of wheat straw. Hemicellulose solubilization was the main effect of all pretreatment conditions tested. The relative percentage of cellulose and/or lignin increased for some pretreatment conditions and decreased for others, depending on their level of degradation by the chosen method and a subsequent shift in the compositional ratio. Application of increasing acid concentrations in SEC pretreatment resulted in increased removal of hemicellulose, thus reducing the total glycan content. In addition, an increase in acid insoluble lignin from 16.9% to 20.9% was detected. According to Ramos (2003), the formation of extraneous polymeric materials by condensation reactions can cause an apparent increase in the overall recovery yield of lignin, sometimes beyond the theoretical calculation based on the lignin content of the starting material. SEB pretreatment (S1) was performed at a severity comparable to the one used for S2 (SEC with 3.2% acid). It removed less hemicellulose than the continuous system, which was in accordance to the observations of Yang and Wyman (2004). At the same time SEB enhanced the depolymerization of the cellulose fraction and resulted in the lowest lignin content of all tested substrates. Acidic autoclaving (S6) produced a substrate differing considerably from steam-exploded ones. It removed almost the entire hemicellulose fraction of the raw material, resulting in the lowest DM content of all substrates. However this method was the least efficient pretreatment in terms of lignin solubilization. Ibbett et al. (2011) suggested a thermal activation of lignin degradation reactions with aqueous acidic conditions being less efficient. This was in accordance to the high lignin content (36%) of low-temperature AA-pretreated S6.

Pretreated wheat straw varied in particle size, morphology and color. Pretreatment caused a degradation of straw particles into smaller fragments, with SEB-pretreated wheat straw (S1) exhibiting an average fiber size of 2 mm. SEC without acid (S5) resulted in the largest particles (~6 mm) of all pretreatment conditions, while increasing acid concentrations gradually reduced particle sizes to values below 1 mm. Small particles were also observed for AA-pretreated substrate S6 (<1 mm). Even though no measurements of surface area were performed, it is well known that a reduction of particle size in pretreatment is associated with an increase in specific and accessible surface area (Ravindran and Jaiswal, 2015; Zhao et al., 2012b).

Substrates pretreated by SEC without acid or at low acid concentrations (S4, S5) remained in a fibrous shape, while high acid concentrations (S2, S3) resulted in a granulate-like morphology of wheat straw. SEB-pretreated S1 possessed a fibrous and chunky texture and AA turned the fibrous lignocellulosic material into powder. To monitor morphological changes, steam exploded substrates S1–S5 were analyzed with CLSM. Increasing pretreatment severity caused a separation of cell types and individual fibers, a fragmentation of straw particles and an accumulation of droplet-like structures on the particle surface. These structures most likely represent lignin droplets formed by condensation reactions during pretreatment (Li et al., 2014).

Application of increasing acid concentrations in pretreatment resulted in a darkening of the obtained substrates. S1 and S3 exhibited a mid-brown color, while substrates pretreated at acid concentrations above 3.2% possessed a dark-brown hue. Darkening of straw in the pretreatment process has been related to a breakdown of lignin and extractives or sugars caused by high temperatures and to the relocation of lignin onto the particle surface (Holopainen-Mantila et al., 2013). The color change is also accompanied by a partial defibration or separation of individual fibers and cell types of the wheat straw (Kristensen et al., 2008).

3.2. Time course of hydrolysis

Previously we presented a mathematical model based on a double-rectangular hyperbola (Eq. (1)) to describe the experimental time course of reducing sugar release (Monschein et al., 2013). This model was applied to investigate the influence of hydrothermal pretreatment on enzymatic hydrolysis of wheat straw at a kinetic level. Time course analysis was performed for all investigated substrates to obtain hydrolysis parameters. S1 (SEB-pretreated with 3.3% H_2SO_4) and S5 (SEC-pretreated without acid) were chosen to demonstrate the analytical approach. When the model fit was superimposed on the measured data, an apparently accurate description of the release of reducing sugars was achieved (Fig. 1(A)). Between 0.5 h and 5 h of hydrolysis, the reducing sugar release curve of S1 showed a significantly higher slope than the one of S5. Between 5 h and 12 h both curves ascended almost parallel. In the last 12 h of hydrolysis, the sugar release curve of S1 exhibited a stronger increase. Based on the double-rectangular fit the hydrolysis rate r was calculated, describing the reducing sugar release per h. Fig. 1(B) depicts the bi-phasic decline of r with increasing C. Compared to S1 hydrolysis of S5 resulted in a 1.8-fold

Effect of pretreatment severity in continuous steam explosion on enzymatic conversion of wheat straw: Evidence from kinetic analysis of hydrolysis time courses.

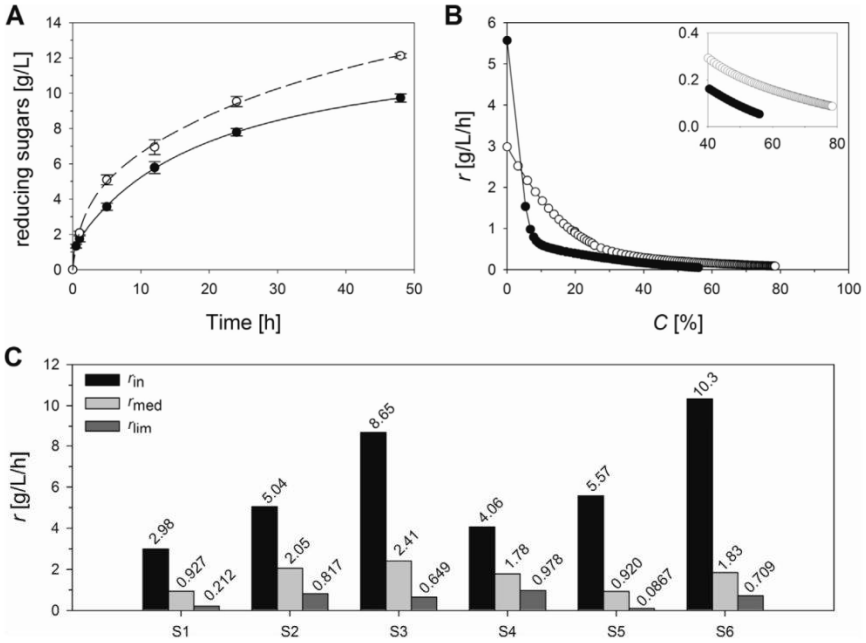

Fig. 1. Enzymatic hydrolysis for hydrothermally pretreated wheat straw and its analysis using hydrolysis rate descriptors. Pretreated wheat straw (2.5% DM) was hydrolyzed for 48 h at 50 °C using 14.4 FPU/g DM ENZ-SC01. (A) Time course of hydrolysis for two substrates pretreated by steam explosion. White circles (○) represent reducing sugar concentrations upon hydrolysis of S1, black circles (●) upon hydrolysis of S5. Solid and dashed lines represent curve fitting according to Eq. (1). (B) Decrease of r with C. Figure inset displays r_{lim} in the last phase of hydrolysis. White circles (○) represent hydrolysis of S1, black circles (●) hydrolysis of S5. Circles were fitted with a third-order polynomial, shown in solid lines. (C) r_{max}, r_{med} and r_{lim} of six hydrothermally pretreated wheat straw substrates (S1–S6).

higher initial hydrolysis rate (r_{max}), descending rapidly until a C value of 7%. For substrate S1, r declined more slowly until a C value of 20%. This transition point was named C_{trans}. From then on the decline in r was significantly slowed down for both substrates, establishing a comparatively steady limiting hydrolysis rate (r_{lim}). In this second phase of hydrolysis, r of S1 was higher and resulted in a C_{max} of 79%, while S5 achieved a C_{max} of 56%.

3.3. Influence of pretreatment on hydrolysis rate descriptors

Based on the discussed analytical approach, differences in the time course of hydrolysis of hydrothermally pretreated substrates were pinned down by determining hydrolysis descriptors. Hydrolysis rate progression was described by the parameters C_{trans}, t_{trans}, r_{max}, r_{med} and r_{lim}. At C_{trans}, there was transition from the fast declining initial rate to the slowly decreasing limiting hydrolysis rate. A higher C_{trans} implies that transition to the slow r_{lim} kinetic regime can be deferred somewhat during the enzymatic reaction, with consequent positive effects on space–time yield (Monschein et al., 2013). Even though the applied pretreatment severity was comparable, SEB-pretreated substrate S1 showed a lower C_{trans}-value (20%) than SEC-pretreated S2 (23%). Among SEC-pretreated substrates, application of increasing acid concentrations was related to higher C_{trans}-values. The highest C_{trans}-value of 26% was observed for SEC-acid-pretreated S3, while S5 showed the lowest one (7%). C_{trans} was converted into t_{trans}, describing the hydrolysis time when transition took place. Substrate S1 showed the highest t_{trans} value of 1.8 h. Although exhibiting high C_{trans}, t_{trans}-values of SEC-acid-pretreated substrates were considerably lower (0.8–1.1 h). The lowest t_{trans}-values were observed for SEC-pretreated S5 (0.4 h) and AA-pretreated S6 (0.2 h).

Due to the almost complete removal of hemicellulose, S6 represented a substrate highly susceptible to enzymatic hydrolysis. In accordance its r_{max} (10 g/L/h) was the highest of all tested substrates, which might be connected to an increased accessibility of the cellulose portion (Fig. 1(C)). Apparently the removal of hemicelluloses was crucial for a high initial hydrolysis rate. The lowest r_{max} (2.9 g/L/h) was observed for SEB-pretreated S1. For SEC-pretreated substrates, r_{max} was between 4.1 g/L/h and 8.7 g/L/h. C_{trans} defined the intermediate hydrolysis rate r_{med}. The highest value of r_{med} (2.4 g/L/h) was achieved for S3, pretreated with 2.3% H_2SO_4. When less acid was used r_{med} decreased gradually. The almost complete removal of hemicellulose was not as beneficial to r_{med} as it was to r_{max}, resulting in an intermediate value of 1.8 g/L/h for S6. Compared to S6 r_{med} of S1 was decreased by 51%. A glycan conversion of 50% was chosen as a reference point for r_{lim}. Compared to r_{max}, r_{lim} was about 10-fold lower. In accordance to the observations made for r_{med}, extensive hemicellulose removal did not ensure high r_{lim}. Hydrolysis of S5 resulted in the lowest r_{lim} (0.1 g/L/h), while low acidic conditions in SEC (S4) increased this value by a factor of 11.

Throughout hydrolysis SEB-pretreated S1 was characterized by low r-values. AA was only able to enhance r_{max}, demonstrating the domineering influence of hemicellulose content on the onset of lignocellulose hydrolysis. High acid concentrations in SEC (S2, S3) ensured high r_{med}, while low acidic conditions had a positive influence on r_{lim}. On the contrary, auto-catalyzed SEC pretreatment resulted in the lowest r_{med} and r_{lim}-values of all substrates.

Effect of pretreatment severity in continuous steam explosion on enzymatic conversion of wheat straw: Evidence from kinetic analysis of hydrolysis time courses.

3.4. Influence of pretreatment on saccharification and substrate conversion

High saccharification within short hydrolysis time is crucial for the industrial exploitation of wheat straw. Even though AA-pretreated S6 showed the highest r_{max}, the achieved saccharification after 5 h was below the $S_{5\ h}$-values of S2, S3 and S4 (Fig. 2 (A)). High concentrations of formic and acetic acid present in S6 could be connected to the rapid slow-down of its hydrolysis rate. Acetic and formic acids are generated during pretreatment by degradation of furfural or acetyl groups (Tomás-Pejó et al., 2011). Both compounds were shown to inhibit the hydrolysis rate of lignocellulose. It can be assumed that high concentrations of carboxylic acids alter the pH value of the reaction mixture, thereby inactivating cellulases (Cantarella et al., 2004; Hodge et al., 2008). Due to the low glycan content the sugar release of S6 did not increase after 12 h of hydrolysis, resulting in the lowest S_{max} of all tested substrates. To achieve a sugar yield comparable to steam exploded substrates, a much higher amount of acid autoclaved material is necessary, thus increasing costs. Therefore hemicellulose removal to such a high extent is not desirable. Despite a comparable pretreatment severity, the SEB-pretreated S1 showed lower S-values than SEC-pretreated S2. This was in accordance to the observations of Zimbardi et al. (1999), who contributed the higher saccharification yield of continuously-pretreated wheat straw to a more effective disruption of the lignocellulosic matrix as compared to the corresponding batch pretreatment. SEC-acid-pretreated substrates exhibited the highest S-values throughout the hydrolysis. In the beginning of reaction S-values increased with the applied acid concentration, but this trend was not observed after 5 h. In the 12 h to 48 h time span the highest saccharification was achieved upon hydrolysis of S4, resulting in a final sugar concentration of 91 mM. For SEC-pretreated substrates low acid concentrations were favorable in terms of achieved saccharification levels. When more acid was used, $S_{12\ h}$, $S_{24\ h}$ and $S_{48\ h}$ gradually decreased. Nevertheless, acidic steam explosion led to higher sugar release values than the autocatalyzed process. Rajan and Carrier (2014) made similar observation for dilute acid-pretreated wheat straw, showing that high acid concentrations in pretreatment inhibited the recovery of reducing sugars. Steam exploded lignins are quite extensively modified during pretreatment through mechanisms involving condensation among (hemi)cellulose-derived by-products and radicals derived from the homolytic cleavage of aryl ether bonds. A part of these condensates are likely to remain within the steam-treated fiber. Lignin condensation leads to a higher degree of hydrophobicity, and the redistribution of modified lignins on the cellulosic fiber has a detrimental effect on substrate accessibility. This would not only limit the substrate available surface area, but also increase the relative amount of nonspecific and/or non-productive binding of the enzymes onto the substrate (Ramos, 2003; Zhao et al., 2012a). For the applied acid concentrations in SEC pretreatment, a balance between hemicellulose removal and recondensation reactions is necessary to ensure high saccharification values.

Based on the saccharification S the conversion C of the total glycan fraction was calculated (Fig. 2(B)). As observed for $S_{5\ h}$, $C_{5\ h}$-values increased with the applied acid concentration in SEC. Due to its exceptionally low glycan content, substrate S6 reached a total conversion of the glycan portion within 12 h of hydrolysis. Although its DM contained ~90% more glycan than S6, hydrolysis of S4 resulted in a $C_{12\ h}$ of 87%. After 24 h the entire hemicellulose and cellulose fraction of this substrate was converted, thus undermining the high hydrolytic efficiency of low acidic SEC. Hydrolysis of S2 or S3, both SEC-pretreated with higher acid concentrations, achieved a conversion of 100% after 48 h of reaction. Substrate S5 contained the highest level of glycan, slightly surpassing the one of S4. Over the entire hydrolysis period, it showed the lowest C-values of all tested substrates, reaching only a C_{max} of 56%.

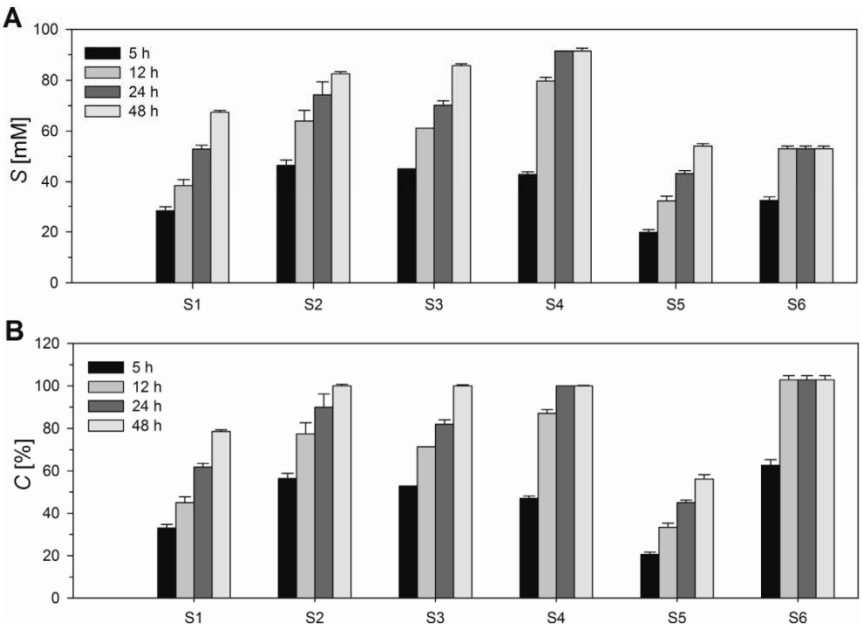

Fig. 2. Comparison of substrate saccharification and conversion. Pretreated wheat straw (2.5% DM) was hydrolyzed for 48 h at 50 °C using 14.4 FPU/g DM ENZ-SC01. (A) $S_{5\ h}$, $S_{12\ h}$, $S_{24\ h}$ and S_{max} of S1–S6. (B) $C_{5\ h}$, $C_{12\ h}$, $C_{24\ h}$ and C_{max} of S1–S6.

Effect of pretreatment severity in continuous steam explosion on enzymatic conversion of wheat straw: Evidence from kinetic analysis of hydrolysis time courses.

Similar to the saccharification values, the digestibility of continuously-pretreated wheat straw was much better than the one of the batch-pretreated sample. A higher efficiency of continuous pretreatment in the disruption of lignocellulose is not the only possible explanation for these results. Since dissolved lignin is quickly removed in a continuous reactor, the increased digestibility could be due to a lower recondensation of lignin droplets on the substrate surface (Yang and Wyman, 2004). In accordance, CLSM showed more droplet-like structures on the surface of SEB-pretreated S1 than on SEC-pretreated S2. Lignin droplets are not only responsible for non-specific protein adsorption. They also block enzymes from moving along cellulose chains, creating traffic jams and negatively affecting enzymatic digestion of cellulose. Inhibition is especially high in the early stages of hydrolysis, but decreases over time. With increasing hydrolysis time droplets are peeled off from the cellulose surface, allowing hydrolysis to continue (Li et al., 2014). This may have been reflected in the conversion values of S1 and S2. $C_{5\ h}$ of S1 was 42% lower than the one of S2, while their $C_{24\ h}$- and C_{max}-values differed only by 31% and 21%, respectively.

By linking C_{trans}, r and C the following correlations were established: as expected an intermediate to high r_{max} combined with a high C_{trans} resulted in increased C_{max}-values (S2, S3, S6). High C_{trans} also compensated the low r_{max}, leading to high conversion levels after 48 h, however requiring that r_{med} was at least 1.8 g/L/h (S4). When low r_{max} was connected with low r_{med}- and r_{lim}-values, $C_{48\ h}$ was reduced despite a relatively high C_{trans} of 20% (S1). Low C_{trans} in combination with small r_{med}- and r_{lim}-values had a major negative impact on hydrolysis yield (S5).

3.5. Influence of pretreatment on protein adsorption

Since volumetric hydrolysis rates usually increase with the amount of adsorbed enzymes, cellulose accessibility is an important factor in the effectiveness of hydrolysis reactions (Zhang and Lynd, 2004). SEC-acid-pretreated S2 and AA-pretreated S6, both characterized by high lignin content, adsorbed initially the highest protein concentration (0.12 g/L) (Fig. 3(A)). Low $P_{ads\_0\ h}$-values were observed for S4 and S5. Throughout hydrolysis S5 adsorbed significantly less protein than any other substrate, which could be explained by its fibrous texture and large particle size, implying small external surface area. Protein adsorption to S4 increased sharply and resulted in an almost 8-fold higher $P_{ads\_5\ h}$-value than S5. With increasing acid concentrations in SEC, the resulting substrates gradually adsorbed more protein within the first 24 h of hydrolysis, corresponding to the increased removal of hemicellulose. Rahikainen et al. (2013) reported an increase in phenolic hydroxyl groups and a decrease in aliphatic hydroxyls in lignin upon steam explosion, resulting in a higher affinity for cellulases. Compared to S4, $P_{ads\_12\ h}$ of S2 was 80% higher, possibly connected to an increased protein adsorption capacity of lignin due to the high acid concentration used in pretreatment. This increased protein adsorption did not result in a higher saccharification, indicating that enzymes adsorbed to S2 were less active than those bound to S4. Acidic autoclaving caused massive hemicellulose solubilization while having almost no effect on the substrates' lignin portion. As a consequence two factors could be responsible for the high P_{ads}-values of substrate S6. Low hemicellulose content increasing cellulose accessibility and/or high lignin content resulting in non-productive enzyme adsorption. Since $S_{5\ h}$- and $S_{12\ h}$-values of S6 are neither especially high nor low, it is difficult to categorize the increase in protein adsorption as productive or non-productive for lignocellulose hydrolysis, making a combined effect of both factors most likely.

For investigating the hydrolytic efficiency of cellulases on a lignocellulosic material, it is crucial to correlate protein adsorption with hydrolysis descriptors. Therefore P_{ads} and r were consolidated in the specific hydrolysis rate $r_{\_specific}$ (Fig. 3(B)). Application of

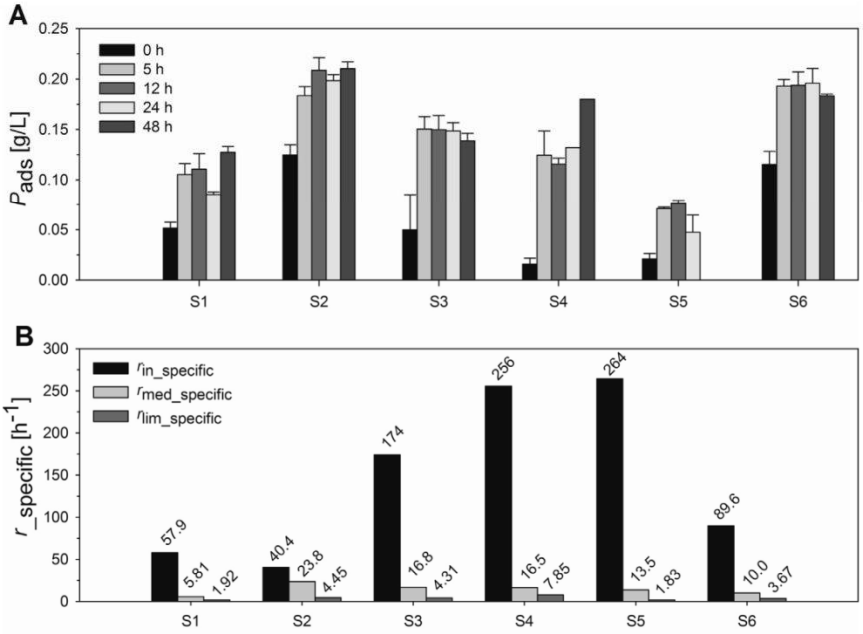

Fig. 3. Influence of pretreatment on protein adsorption parameters and specific hydrolysis rates. Pretreated wheat straw (2.5% DM) was hydrolyzed for 48 h at 50 °C using 14.4 FPU/g DM ENZ-SC01. (A) $P_{ads\_0\ h}$, $P_{ads\_5\ h}$, $P_{ads\_12\ h}$, $P_{ads\_24\ h}$ and $P_{ads\_48\ h}$ of S1–S6. (B) $r_{in\_specific}$, $r_{med\_specific}$ and $r_{lim\_specific}$ of S1–S6.

increasing acid concentrations during SEC resulted in lower $r_{in\_specific}$-values. The highest $r_{in\_specific}$ (263 h^{-1}) of all substrates was observed for S5, the lowest one (40 h^{-1}) for S2. Due to the increased protein adsorption accompanying its exceptionally high r_{max}, S6 showed a reduced $r_{in\_specific}$. Compared to $r_{in\_specific}$, $r_{med\_specific}$-values were 2 to 20-fold lower. Differences in $r_{med\_specific}$ were not as pronounced as the ones observed at hydrolysis start. In contrast to the observations made for $r_{in\_specific}$, $r_{med\_specific}$ increased with the applied acid concentration in SEC. Low $r_{med\_specific}$-values were observed for SEB-pretreated S1 and AA-pretreated S6. In case of S1 this trend was also maintained for $r_{lim\_specific}$, indicating that enzymes adsorbed to this substrate showed reduced activity. S5 exhibited the lowest $r_{lim\_specific}$, while the highest one was detected upon hydrolysis of S4. With exception of S6, $r_{lim\_specific}$-values were directly connected to the achieved saccharification after 24 h or 48 h. Even though exhibiting high P_{ads}, corresponding $r_{\_specific}$-values of S6 were low during the entire hydrolysis process. Similar observations were made for $r_{in\_specific}$ and $r_{lim\_specific}$ of SEC-acid-pretreated substrates. While P_{ads} increased with the applied acid concentration, $r_{\_specific}$ was reduced. Apparently increased enzyme binding to lignocellulose does not necessarily correlate with improved activity per unit bound enzyme. Gao et al. (2013) suggested that low $r_{\_specific}$ could be caused by non-productive binding of enzymes to cellulose I, caused by high fibril surface hydrophobicity. Higher acid concentrations could promote lignin condensation, which increases the degree of hydrophobicity and enhances non-productive enzyme adsorption (Ramos, 2003).

3.6. Correlating pretreatment parameters, substrate characteristics to protein adsorption and hydrolysis descriptors

Pretreatment parameters (acid concentration), hydrolysis descriptors (r, S, C, C_{trans}), protein adsorption parameters (P_{ads}, $r_{\_specific}$), substrate characteristics (particle size) and substrate composition (cellulose and hemicellulose content) were correlated performing a one-dimensional regression analysis. The aim was to detect direct or indirect dependencies, rather than establishing precise mathematical models. Due to the complexity of the hydrolysis process, a propagation of dependencies was observed, resulting in a network of interrelated parameters. The most significant results of the regression analysis are given in Table 2.

The influence of pretreatment parameters on substrate composition has to some extent been discussed in Section 3.1. Application of high acid concentrations in pretreatment reduced both particle size and the substrates' hemicellulose content. These factors increased early-phase protein adsorption ($P_{ads\_0\ h}$, $P_{ads\_5\ h}$) which was also reported by Zhang and Lynd (2004). In accordance, substrates with high $P_{ads\_0\ h}$-values were characterized by increased $P_{ads\_5\ h}$. While low hemicellulose content was the determining factor for increased early-phase protein adsorption, high cellulose content had a positive influence on late-phase protein adsorption ($P_{ads\_48\ h}$) of SEC-pretreated substrates. Reduced hemicellulose content was also beneficial for r_{max}. Apparently hemicellulose removal especially affects the hydrolysis rate at the start of reaction, most likely by enhancing the cellulose accessibility and resulting in a higher level of adsorbed proteins. A direct correlation was detected for P_{ads} and r_{lim}. The application of high acid concentrations in SEC pretreatment enhanced early-phase saccharification values ($S_{5\ h}$). This was connected to a reduction in particle size, a removal of hemicellulose and an increase in $P_{ads\_5\ h}$. High r_{med} was reflected in increased $S_{5\ h}$-values. The same correlation was observed between r_{lim} and S_{max}. P_{ads} always increased strongly at late stages of the hydrolysis without having a beneficial effect on final saccharification or glycan conversion levels. Apparently increased protein adsorption in the late stage of hydrolysis ($P_{ads\_48\ h}$) was mostly non-productive. Glycan conversion C was higher for substrates with small particle sizes showing increased early-phase protein adsorption. As expected, conversion values were higher for substrates low in hemicelluloses. Compared to cellulose, these polymers were more affected by pretreatment thus having a stronger influence on total glycan levels. In accordance to the observations made for saccharification, high r_{med} was reflected in increased $C_{5\ h}$-values, while r_{max} and r_{lim} had a more pronounced effect on C_{max}. Besides r_{max}, r_{med} and r_{lim}, the point of hydrolysis rate transition had a major influence on glycan conversion and saccharification. High C_{trans}-values increased both early- and late-phase saccharification and conversion values, thus undermining the high significance of the transition from high r_{max} to low r_{lim}. C_{trans} itself was affected by particle size and hemicellulose content. Among specific hydrolysis rates, only increased

Table 2
Correlation of pretreatment parameters, substrate composition, protein adsorption and hydrolysis parameters.

	Acid [mg/g]	Size [mm]	Cell. [mM]	Hemic. [mM]	$P_{ads\_0\ h}$ [g/L]	$P_{ads\_5\ h}$ [g/L]	$S_{5\ h}$ [mM]	S_{max} [mM]	$C_{5\ h}$ [%]	C_{max} [%]	r_{lim} [g/L/h]	C_{trans} [%]
Size [mm]	–											–[a]
Cell. [mM]												
Hemic. [mM]	–	+										–[a]
$P_{ads\_0\ h}$ [g/L]	+	–		–		+			+			
$P_{ads\_5\ h}$ [g/L]	+	–		–				+			+	
$P_{ads\_48\ h}$ [g/L]			+[a]								+	
$S_{5\ h}$ [mM]	+[b]	–[a]		–[a]		+						+[b]
S_{max} [mM]							+[a]					+[a]
$C_{5\ h}$ [%]	+[b]	–		–		+	+[a]			+		+[a]
C_{max} [%]		–[a]		–		+	+[a]	+[a]				+[a]
r_{max} [g/L/h]				–						+		
r_{med} [g/L/h]							+		+			+[b]
r_{lim} [g/L/h]				–[a]			+	+[a]	+	+[a]		
$r_{in\_specific}$ [h^{-1}]	–	+[b]		+[b]	–[b]	–[b]						
$r_{med\_specific}$ [h^{-1}]									+[b]			
$r_{lim\_specific}$ [h^{-1}]	–	+						+[a]		+[a]	+	

Abbreviations: Hemic. (Hemicellulose), Cell. (Cellulose).
(+) direct correlation; (–) indirect correlation.
[a] SE.
[b] SEC.

Effect of pretreatment severity in continuous steam explosion on enzymatic conversion of wheat straw: Evidence from kinetic analysis of hydrolysis time courses.

$r_{lim\_specific}$ was connected to high S_{max} and C_{max}. This implicates a major importance of denaturation reactions reducing enzyme activity in the later stages of hydrolysis on achieved sugar release values.

These correlations emphasize the interrelated character of parameters influencing hydrolytic efficiency, especially the large-scale changes induced by hemicellulose removal. For establishing highly efficient and commercially sustainable hydrothermal pretreatment conditions, an integrated approach is necessary that considers increase of cellulose accessibility, loss of glycan and non-productive enzyme adsorption due to modifications of the lignocellulosic material.

4. Conclusion

By applying semi-empirical descriptors on the enzymatic hydrolysis of wheat straw, the effect of hydrothermal pretreatment was analyzed on a kinetic level. Not only r itself, but also its transition from a high initial to a low limiting value was crucial for hydrolytic efficiency. This study demonstrated the beneficial effect of low H_2SO_4 concentrations on the digestibility of continuously steam exploded wheat straw. High acid concentrations increased hemicellulose removal and enhanced the enzyme affinity of lignocellulose, but had no positive effect on saccharification. Apparently high pretreatment severities alter lignocellulose chemistry and structure in a way not advantageous for enzyme activity.

Acknowledgements

The authors wish to thank Dr. Zdenek Petrasek and Manuel Eibinger (Institute of Biotechnology and Biochemical Engineering, Graz University of Technology, Austria) for their support. This study was performed within the COMET K-Project Macro-Fun and the COMET-K2-centre ACIB. Financial support from the Province of Styria is gratefully acknowledged. This work received support from: the Federal Ministry of Economy, Family and Youth (BMWFJ); the Federal Ministry of Traffic, Innovation and Technology (bmvit); the Styrian Business Promotion Agency SFG; the Standortagentur Tirol; and ZIT-Technology Agency of the City of Vienna. Funding was through the COMET-Funding Program managed by the Austrian Research Promotion Agency FFG.

Appendix A. Supplementary data

Photographs and CLSM-pictures of pretreated substrates are shown in Fig. A.1. C_{trans}-values of pretreated substrates are illustrated in Fig. A.2. Examples for the regression analysis correlating pretreatment parameters, substrate composition, protein adsorption and hydrolysis descriptors are given in Fig. A.3. Tables A.1 and A.2 depict the results of the regression analysis involving all 26 parameters.

Supplementary data associated with this article can be found, in the online version, at http://dx.doi.org/10.1016/j.biortech.2015.10.020.

References

Bansal, P., Hall, M., Realff, M.J., Lee, J.H., Bommarius, A.S., 2009. Modeling cellulase kinetics on lignocellulosic substrates. Biotechnol. Adv. 27, 833–848.
Behera, S., Arora, R., Nandhagopal, N., Kumar, S., 2014. Importance of chemical pretreatment for bioconversion of lignocellulosic biomass. Renewable Sustainable Energy Rev. 36, 91–106.
Buanafina, M.M.D., 2009. Feruloylation in grasses: current and future perspectives. Mol. Plant 2, 861–872.
Bubner, P., Dohr, J., Plank, H., Mayrhofer, C., Nidetzky, B., 2012. Cellulases dig deep: in situ observation of the mesoscopic structural dynamics of enzymatic cellulose degradation. J. Biol. Chem. 287, 2759–2765.
Buranov, A.U., Mazza, G., 2008. Lignin in straw of herbaceous crops. Ind. Crops Prod. 28, 237–259.
Cantarella, M., Cantarella, L., Gallifuoco, A., Spera, A., Alfani, F., 2004. Effect of inhibitors released during steam-explosion treatment of poplar wood on subsequent enzymatic hydrolysis and SSF. Biotechnol. Prog. 20, 200–206.
Chen, W.H., Tsai, C.C., Lin, C.F., Tsai, P.Y., Hwang, W.S., 2013. Pilot-scale study on the acid-catalyzed steam explosion of rice straw using a continuous pretreatment system. Bioresour. Technol. 128, 297–304.
Fang, H.X., Deng, J., Zhang, X., 2011. Continuous steam explosion of wheat straw by high pressure mechanical refining system to produce sugars for bioconversion. Bioresources 6, 4468–4480.
Gao, D.H., Chundawat, S.P.S., Sethi, A., Balan, V., Gnanakaran, S., Dale, B.E., 2013. Increased enzyme binding to substrate is not necessary for more efficient cellulose hydrolysis. Proc. Nat. Acad. Sci. U.S.A. 110, 10922–10927.
Hansen, M.A.T., Kristensen, J.B., Felby, C., Jorgensen, H., 2011. Pretreatment and enzymatic hydrolysis of wheat straw (*Triticum aestivum* L.) – the impact of lignin relocation and plant tissues on enzymatic accessibility. Bioresour. Technol. 102, 2804–2811.
Himmel, M.E., Ding, S.Y., Johnson, D.K., Adney, W.S., Nimlos, M.R., Brady, J.W., Foust, T.D., 2007. Biomass recalcitrance: engineering plants and enzymes for biofuels production. Science 315, 804–807.
Hodge, D.B., Karim, M.N., Schell, D.J., McMillan, J.D., 2008. Soluble and insoluble solids contributions to high-solids enzymatic hydrolysis of lignocellulose. Bioresour. Technol. 99, 8940–8948.
Holopainen-Mantila, U., Marjamaa, K., Merali, Z., Kasper, A., de Bot, P., Jaaskelainen, A.S., Waldron, K., Kruus, K., Tamminen, T., 2013. Impact of hydrothermal pretreatment to chemical composition, enzymatic digestibility and spatial distribution of cell wall polymers. Bioresour. Technol. 138, 156–162.
Ibbett, R., Gaddipati, S., Davies, S., Hill, S., Tucker, G., 2011. The mechanisms of hydrothermal deconstruction of lignocellulose: new insights from thermal–analytical and complementary studies. Bioresour. Technol. 102, 9272–9278.
Kristensen, J.B., Thygesen, L.G., Felby, C., Jorgensen, H., Elder, T., 2008. Cell-wall structural changes in wheat straw pretreated for bioethanol production. Biotechnol. Biofuels 1, 5.
Li, H.J., Pu, Y.Q., Kumar, R., Ragauskas, A.J., Wyman, C.E., 2014. Investigation of lignin deposition on cellulose during hydrothermal pretreatment, its effect on cellulose hydrolysis, and underlying mechanisms. Biotechnol. Bioeng. 111, 485–492.
Li, J., Henriksson, G., Gellerstedt, G., 2007. Lignin depolymerization/repolymerization and its critical role for delignification of aspen wood by steam explosion. Bioresour. Technol. 98, 3061–3068.
Meng, X.Z., Ragauskas, A.J., 2014. Recent advances in understanding the role of cellulose accessibility in enzymatic hydrolysis of lignocellulosic substrates. Curr. Opin. Biotechnol. 27, 150–158.
Monschein, M., Reisinger, C., Nidetzky, B., 2014. Dissecting the effect of chemical additives on the enzymatic hydrolysis of pretreated wheat straw. Bioresour. Technol. 169, 713–722.
Monschein, M., Reisinger, C., Nidetzky, B., 2013. Enzymatic hydrolysis of microcrystalline cellulose and pretreated wheat straw: a detailed comparison using convenient kinetic analysis. Bioresour. Technol. 128, 679–687.
Nitsos, C.K., Matis, K.A., Triantafyllidis, K.S., 2013. Optimization of hydrothermal pretreatment of lignocellulosic biomass in the bioethanol production process. ChemSusChem 6, 110–122.
Rahikainen, J.L., Martin-Sampedro, R., Heikkinen, H., Rovio, S., Marjamaa, K., Tamminen, T., Rojas, O.J., Kruus, K., 2013. Inhibitory effect of lignin during cellulose bioconversion: the effect of lignin chemistry on non-productive enzyme adsorption. Bioresour. Technol. 133, 270–278.
Rajan, K., Carrier, D.J., 2014. Effect of dilute acid pretreatment conditions and washing on the production of inhibitors and on recovery of sugars during wheat straw enzymatic hydrolysis. Biomass Bioenergy 62, 222–227.
Ramos, L.P., 2003. The chemistry involved in the steam treatment of lignocellulosic materials. Quim. Nova 26, 863–871.
Ravindran, R., Jaiswal, A.K., 2015. A comprehensive review on pre-treatment strategy for lignocellulosic food industry waste: challenges and opportunities. Bioresour. Technol. http://dx.doi.org/10.1016/j.biortech.2015.07.106 (in press).
Sluiter, J.B., Ruiz, R.O., Scarlata, C.J., Sluiter, A.D., Templeton, D.W., 2010. Compositional analysis of lignocellulosic feedstocks. 1. Review and description of methods. J. Agric. Food Chem. 58, 9043–9053.
Sun, X.F., Sun, R., Fowler, P., Baird, M.S., 2005. Extraction and characterization of original lignin and hemicelluloses from wheat straw. J. Agric. Food Chem. 53, 860–870.
Talebnia, F., Karakashev, D., Angelidaki, I., 2010. Production of bioethanol from wheat straw: an overview on pretreatment, hydrolysis and fermentation. Bioresour. Technol. 101, 4744–4753.
Tomás-Pejó, E., Alvira, P., Ballesteros, M., Negro, M.J., 2011. Pretreatment technologies for lignocellulose-to-bioethanol conversion. In: Pandey, A., Larroche, C., Ricke, S.C., Dussap, C.-G., Gnansounou, E. (Eds.), Biofuels. Academic Press, Amsterdam, pp. 149–176.
Yang, B., Wyman, C.E., 2004. Effect of xylan and lignin removal by batch and flowthrough pretreatment on the enzymatic digestibility of corn stover cellulose. Biotechnol. Bioeng. 86, 88–95.
Zhang, Y.H., Lynd, L.R., 2004. Toward an aggregated understanding of enzymatic hydrolysis of cellulose: noncomplexed cellulase systems. Biotechnol. Bioeng. 88, 797–824.

Effect of pretreatment severity in continuous steam explosion on enzymatic conversion of wheat straw: Evidence from kinetic analysis of hydrolysis time courses.

Zhao, X., Zhang, L., Liu, D., 2012a. Biomass recalcitrance. Part II: fundamentals of different pre-treatments to increase the enzymatic digestibility of lignocellulose. Biofuels Bioprod. Biorefin. 6, 561–579.
Zhao, X.B., Zhang, L.H., Liu, D.H., 2012b. Biomass recalcitrance. Part I: the chemical compositions and physical structures affecting the enzymatic hydrolysis of lignocellulose. Biofuels Bioprod. Biorefin. 6, 465–482.
Zhu, L., O'Dwyer, J.P., Chang, V.S., Granda, C.B., Holtzapple, M.T., 2008. Structural features affecting biomass enzymatic digestibility. Bioresour. Technol. 99, 3817–3828.
Zimbardi, F., Viggiano, D., Nanna, F., Demichele, M., Cuna, D., Cardinale, G., 1999. Steam explosion of straw in batch and continuous systems. Appl. Biochem. Biotechnol. 77–9, 117–125.

SUPPORTING INFORMATION

Effect of pretreatment severity in continuous steam explosion on enzymatic conversion of wheat straw: evidence from kinetic analysis of hydrolysis time courses

Mareike Monschein[a], Bernd Nidetzky[a,b,*]

[a] Austrian Centre of Industrial Biotechnology (ACIB) GmbH, Petersgasse 14, 8010 Graz, Austria
[b] Institute of Biotechnology and Biochemical Engineering, Graz University of Technology, Petersgasse 12/I, 8010 Graz, Austria
*Corresponding author. phone number: +43 316 873-8400
fax: +43 316 873-8434
e-mail address: bernd.nidetzky@tugraz.at (B. Nidetzky)

Figure Captions

Figure A.1: Pretreated wheat straw substrates. Panel Ⅰ: Photographs of pretreated wheat straw substrates. (A) S1. (B) S2. (C) S3. (D) S4. (E) S5. (F) S6. Panel Ⅱ: Exemplary auto-fluorescence images of pretreated wheat straw acquired by confocal laser scanning microscopy. All images are normalized using an ImageJ 1.47v plugin. (A) S1. (B) S2. (C) S3. (D) S4. (E) S5.

Figure A.2: Transition point of hydrolysis rates in terms of achieved conversion. Pretreated wheat straw (2.5% DM) was hydrolyzed for 48 h at 50 °C using 14.4 FPU/g DM ENZ-SC01. C_{trans} [%] of substrates S1-S6.

Figure A.3: Correlation of pretreatment parameters, substrate composition, protein adsorption and hydrolysis parameters of hydrothermally pretreated wheat straw substrates. Pretreated wheat straw (2.5% DM) was hydrolyzed for 48 h at 50 °C using 14.4 FPU/g DM ENZ-SC01. Black dots (•) represent different substrates. Dots were fitted with a linear equation. (A) Dependence of $C_{5\ h}$ on $P_{ads\_5\ h}$. (B) Dependence of t_{trans} on cellulose concentration in substrates. (C) Dependence of $r_{in\_specific}$ on acid concentrations used in pretreatment. (D) Dependence of $C_{24\ h}$ on r_{lim} of steam exploded substrates.

Supporting Figures

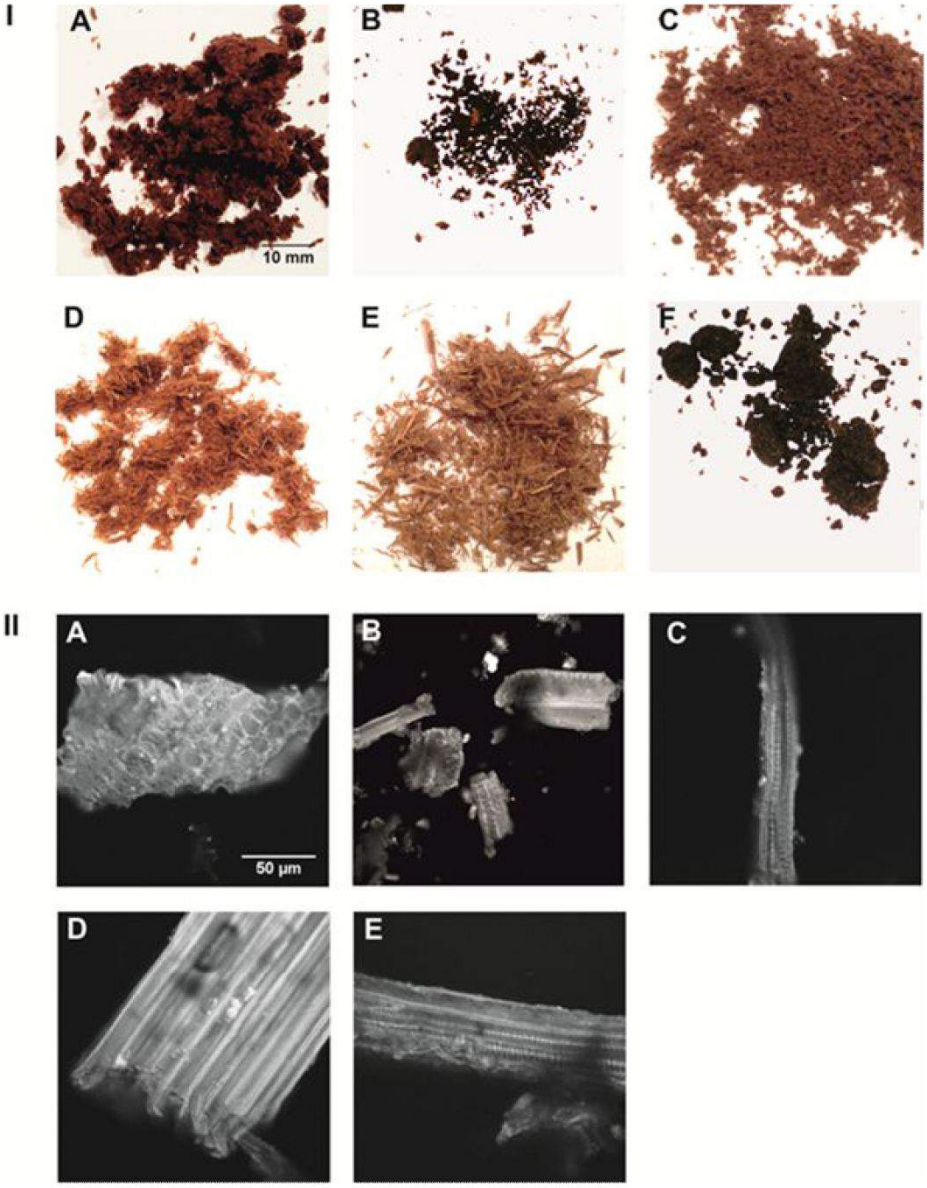

Figure A.1

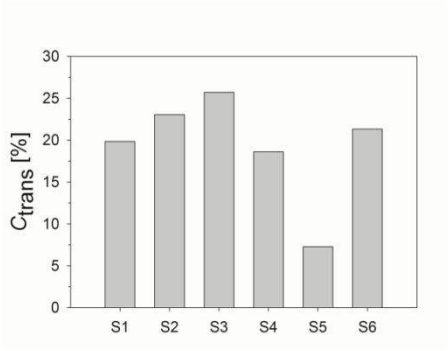

Figure A.2

4

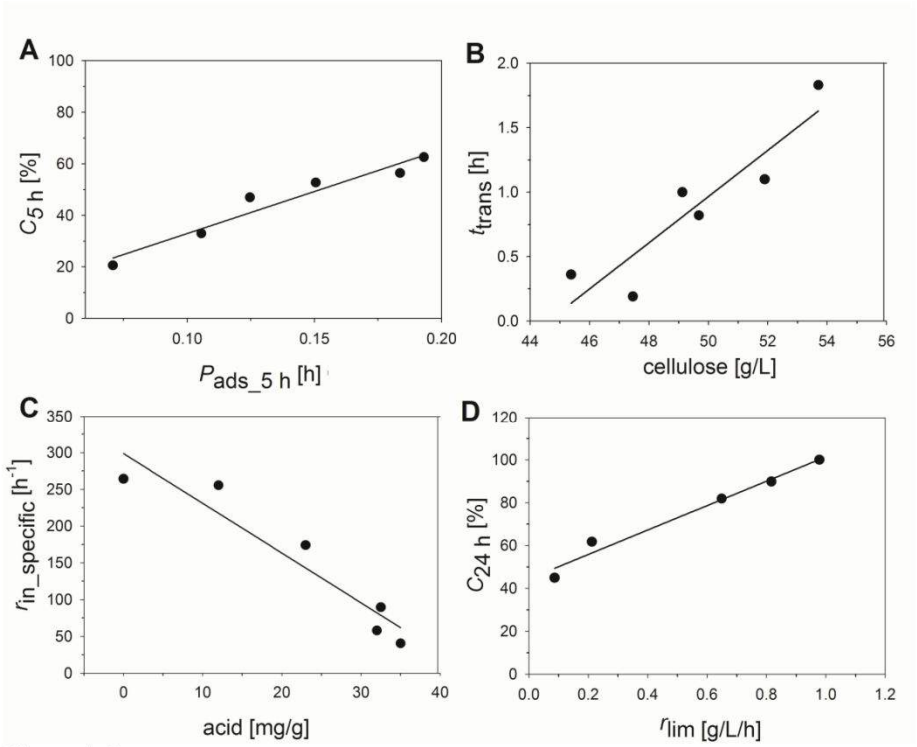
A
$C_{5\ h}$ [%]
$P_{ads\_5\ h}$ [h]
B
t_{trans} [h]
cellulose [g/L]
C
$r_{in\_specific}$ [h^{-1}]
acid [mg/g]
D
$C_{24\ h}$ [%]
r_{lim} [g/L/h]

Figure A.3

5

Supporting Tables

Table A.1: Correlation of pretreatment parameters, substrate composition, protein adsorption and hydrolysis parameters, part Ⅰ.

	Acid [mg/g]	Size [mm]	Cell. [mM]	Hemic. [mM]	Gly. [mM]	$P_{ads\_0\,h}$ [g/L]	$P_{ads\_5\,h}$ [g/L]	$P_{ads\_12\,h}$ [g/L]	$P_{ads\_24\,h}$ [g/L]	$r_{in\_specific}$ [g/L/h]
Size [mm]	—									
Hemic. [mM]	—	+								
Glyc. [mM]	—	+		+						
$P_{ads\_0\,h}$ [g/L]	+	—		—	—					
$P_{ads\_5\,h}$ [g/L]	+	—		—	—	+				
$P_{ads\_12\,h}$ [g/L]	+	—		—	—	+	+			
$P_{ads\_24\,h}$ [g/L]	+	—		—	—	+	+	+		
$P_{ads\_48\,h}$ [g/L]			+[a]							
C_{trans} [%]		—[a]		—[a]					+[a]	
$S_{5\,h}$ [mM]	+[b]	—[a]		—[a]	—[b]		+	+[b]	+[a]	
$S_{12\,h}$ [mM]		—[a]		—[a]			+[a]	+[a]	+[a]	
$S_{24\,h}$ [mM]		—[a]		—[a]			+[a]	+[a]	+[a]	
$C_{5\,h}$ [%]	+[b]	—		—	—	+	+	+	+	
$C_{12\,h}$ [%]		—[a]		—	—		+[a]	+[a]	+	
$C_{24\,h}$ [%]		—[a]		—	—		+	+[a]	+	
C_{max} [%]		—[a]		—	—		+	+	+	
r_{max} [g/L/h]				—	—					
$r_{in\_specific}$ [h^{-1}]	—	+[b]		+[b]	+[a]	—[b]	—[b]	—[b]	—[b]	
$r_{med\_specific}$[h^{-1}]	+[b]	—[b]		—[b]	—[b]	—	+[b]	+[b]	+[b]	+[b]
$r_{lim\_specific}$[h^{-1}]	—	+								+

Abbreviations: Hemic. (Hemicellulose), Cell. (Cellulose), Glyc. (Glycan).
(+)...direct correlation; (—)...indirect correlation.
[a]...SE; [b]...SEC.

Table A.2: Correlation of pretreatment parameters, substrate composition, protein adsorption and hydrolysis parameters, part II.

	$P_{ads\_0\,h}$ [g/L]	$P_{ads\_5\,h}$ [g/L]	$P_{ads\_12\,h}$ [g/L]	$P_{ads\_24\,h}$ [g/L]	r_{max} [g/L/h]	r_{med} [g/L/h]	r_{lim} [g/L/h]	t_{trans} [h]	C_{trans} [%]	$r_{in\_specific}$ [h^{-1}]
Size [mm]									—[a]	
Glyc. [mM]					—					
Cell. [mM]								+		
Hemic. [mM]					—		—[a]		—[a]	
$P_{ads\_0\,h}$ [g/L]										
$P_{ads\_5\,h}$ [g/L]	+						+			
$P_{ads\_12\,h}$ [g/L]	+	+					+			
$P_{ads\_24\,h}$ [g/L]	+	+	+				+		+[a]	
$P_{ads\_48\,h}$ [g/L]							+			
$S_{5\,h}$ [mM]		+	+[b]	+[a]		+	+[a]	+[b]	+[b]	
$S_{12\,h}$ [mM]		+[a]	+[a]	+[a]			+	+[b]		
$S_{24\,h}$ [mM]		+[a]	+[a]	+[a]			+	+[b]		
S_{max} [mM]							+[a]		+[a]	
$C_{5\,h}$ [%]	+	+	+	+		+	+[a]		+[a]	
$C_{12\,h}$ [%]		+[a]	+[a]	+			+			
$C_{24\,h}$ [%]		+	+[a]	+	+		+[a]	+[b]		
C_{max} [%]		+	+	+	+		+[a]	+[b]	+[a]	
r_{lim} [g/L/h]								+[b]		
C_{trans} [%]						+[b]		+[b]		
$r_{in\_specific}$ [h^{-1}]	—[b]	—[b]	—[b]	—[b]						
$r_{med\_specific}$ [h^{-1}]	—	+[b]	+[b]	+[b]						+[b]
$r_{lim\_specific}$ [h^{-1}]							+	+[b]		+

Abbreviations: Hemic. (Hemicellulose), Cell. (Cellulose), Glyc. (Glycan).
(+)...direct correlation; (—)...indirect correlation.
[a]...SE; [b]...SEC.

Identification of a lignacious residue binding protein from *Phanerochaete chrysosporium* boosting early-phase enzymatic hydrolysis of pretreated lignocellulose

Note:

Identification of a lignacious residue binding protein from *Phanerochaete chrysosporium* boosting early-phase enzymatic hydrolysis of pretreated lignocellulose

Mareike Monschein [a], Alexandra Schwarz [a], CLARIANT author(s) [b], Tibor Czabany [c], Barbara Darnhofer[d], Ruth Birner-Gruenberger [d] and Bernd Nidetzky [c,*]

[a] Austrian Center of Industrial Biotechnology (ACIB) GmbH, Petersgasse 14, 8010 Graz, Austria.
[b] CLARIANT Produkte (Deutschland) GmbH, Group Biotechnology, Staffelseestraße 6, 81477 Munich, Germany.
[c] Institute of Biotechnology and Biochemical Engineering, Graz University of Technology, Petersgasse 12/I, 8010 Graz, Austria.
[d] Institute of Pathology, Medical University of Graz, Auenbruggerplatz 25, 8036 Graz, Austria.
*Corresponding author. phone number: +43 316 873-8400
fax: +43 316 873-8434
e-mail address: bernd.nidetzky@tugraz.at (B. Nidetzky)

Identification of a lignacious residue binding protein from *Phanerochaete chrysosporium* boosting early-phase enzymatic hydrolysis of pretreated lignocellulose.

Abstract

In this study a novel lignacious residue binding protein, *Pc*Lrbp, was isolated from the white-rot fungus *Phanerochaete chrysosporium. Pc*Lrbp has a molecular mass of 29 kDa and contains the uncharacterized domain DUF3455, while showing no sequence similarity to known accessory proteins involved in lignocellulose degradation. Multiple sequence alignment and phylogenetic analysis indicated the existence of related hypothetical proteins in a wide range of lignin-degrading fungi. *Pichia pastoris*-expressed *rPc*Lrbp showed synergism with cellulases in early phase-hydrolysis of pretreated wheat straw. Pre-incubation of *rPc*Lrbp with pretreated wheat straw was able to boost the initial hydrolysis rate by 64%. Neither (hemi)celluloytic activity nor adsorption to pure microcrystalline cellulose was detected. Compared to cellulases, *rPc*Lrbp showed a 2.7-fold enhanced adsorption to lignacious hydrolysis residue, pointing towards a specific adsorption of the protein to the lignin fraction of biomass. The reported results open up the possibility for a previously unknown family of accessory proteins prevalent in lignin-degrading fungi.

Keywords: accessory proteins, enzymatic hydrolysis, ligno-cellulosics, lignin binding, *Phanerochaete chrysosporium*

1. Introduction

Lignocellulosic biomass represents an abundant, renewable and cheap source of fermentable sugars, thus having great potential for the industrial production of biofuels, chemicals or polymers (Singhvi et al., 2014). However, the efficient, rapid and complete enzymatic hydrolysis of lignocellulosics using low protein loadings has proven to be one of the major technical and economical bottlenecks in the bioconversion process (Arantes and Saddler, 2010). Several factors have been accounted for sugar release at low space-time yields. The highly crystalline, complex structure of cellulose associated with lignin and hemicelluloses gives biomass a high degree of recalcitrance and makes its depolymerisation a difficult task (Singhvi et al., 2014). Cellulase performance is impaired by enzyme denaturation, degradation, irreversible enzyme adsorption, jamming or end-product inhibition (Eibinger et al., 2014a; Mansfield et al., 1999; Zhao et al., 2012). The need to improve the economic viability of lignocellulose hydrolysis entailed a wide array of scientific approaches tackling these obstacles: Supplementation of the hydrolysis reaction with surfactants and chemical additives (Monschein et al., 2014), optimization of pretreatment technologies for increasing substrate accessibility (Nitsos et al., 2013), recycling of cellulases to reduce enzyme cost (Gomes et al., 2015), protein engineering (Trudeau et al., 2014) or customized optimization of cellulase mixtures (Banerjee et al., 2010).

An emerging strategy for enhancing enzymatic hydrolysis is the screening of microorganisms for new uncharacterized protein families that can aid in the deconstruction of biomass and may be the source for future advances in new biofuel products (Harris et al., 2014). Synergistic or so-called accessory proteins increase cellulase activity without causing significant cellulose hydrolysis themselves. Amorphogenesis inducing proteins disrupt or loosen inaccessible regions by non-hydrolytic mechanisms. They increase cellulose surface area, making it more accessible to the cellulase enzyme complex (Arantes and Saddler, 2010). Various examples for these non-hydrolytic proteins have been detected in fungi and bacteria. Lytic polysaccharide monooxygenases (e.g. GH61B of *Trichoderma reesei*) in the auxiliary activity family 9 represent copper-dependent fungal

enzymes. They catalyze oxidative cleavage of cellulose chains, especially in highly crystalline and recalcitrant regions (Eibinger et al., 2014b; Harris et al., 2014). Non-enzymatic proteins involved in amorphogenesis include low molecular peptides (e.g. short fiber generating factor of *Trichoderma pseudokoningii*; Gt factor of *Gloeophyllum trabeum*), expansins or expansin-like proteins (e.g. swollenin of *T. reesei*). Expansin and expansin-like proteins can enhance cellulase activity, presumably through disruption of hydrogen bonds, resulting in reduced cellulose crystallinity and increased cellulase accessibility (Ekwe et al., 2013; Harris et al., 2014; Wang and Gao, 2003; Wang et al., 2003). In addition, carbohydrate binding modules (CBMs) promote non-hydrolytic disruption of crystalline cellulose by weakening and splitting the hydrogen bonds (Arantes and Saddler, 2010). Besides amorphogenesis inducing proteins and peptides, hemicellulases (e.g. xylanases) and ligninases (e.g. lignin peroxidases, manganese peroxidases, versatile peroxidases, laccases) can also be regarded as accessory proteins. They clear access to cellulose for the main enzymes, thus enhancing digestibility and resulting in faster cellulose hydrolysis (Hu et al., 2011; Margeot et al., 2009; Pollegioni et al., 2015). Addition of small amounts of these proteins could contribute to the development of cheaper and more effective enzyme mixtures (Kim et al., 2014).

Exploration of fungal biodiversity through their secretome could facilitate the identification of up to now unknown accessory proteins. In the present study we focused on the secretome of *Phanerochaete chrysosporium*, screening for proteins able to enhance the performance of the cellulolytic system of *T. reesei* in the hydrolysis of thermo-acidically pretreated wheat straw. This approach led to the identification of a novel lignacious residue binding protein, *Pc*Lrbp, containing the up to now uncharacterized domain DUF3455. This research presents first evidence for a boosting effect of *Pc*Lrbp on reducing sugar release in the initial phase of hydrolysis, presumably by interacting with the lignin component of substrates. Since *Pc*Lrbp is only related to hypothetical proteins without any known function, our results point towards a novel family of non-hydrolytic accessory proteins prevalent among white rot fungi.

2. Materials and methods

2.1. Chemicals and enzymes

Roti-Quant and Roti-Nanoquant reagents were from Carl Roth (Karlsruhe, Germany). Glucose (HK) assay reagent, nitrophenyl glycosides and alkali lignin were from Sigma-Aldrich (St. Louis, MO, USA). All other chemicals were reagent grade and obtained from Carl Roth, Sigma-Aldrich or Megazyme (Wicklow, Ireland).

ENZ-SC01 cellulase-mixture with a protein concentration of 17 g/L and 27 FPU/mL was kindly provided by CLARIANT (Munich, Germany). It contained the entire enzyme system of *T. reesei* with 2.9 U/mg β-glucosidase, 1.9×10^{-2} U/mg β-mannosidase, 2.9×10^{-1} U/mg α-arabinofuranosidase, 3.6×10^{-2} U/mg β-galactosidase , 2.9×10^{-1} U/mg β-xylosidase and 2.1×10^{-1} U/mg cellulase (as exo- and endoglucanase) activities. Glucose oxidase (GOX) from *Aspergillus niger* (Type II, ≥15,000 U/g solid, without added oxygen) was obtained from Sigma-Aldrich.

2.2. (Ligno)cellulosic substrates

Collection of wheat straw, pre-treatment and feed stock analysis was performed by CLARIANT (Munich, Germany). Wheat straw was collected from areas near Munich and grinded to an average particle size of approximately 6 mm. The raw material was pretreated by acidic steam explosion in continuous reactors, steam explosion in batch reactors or acidic hydrothermal pretreatment in high-pressure autoclaves. Wheat straw substrate 2 (WS2) was obtained by supplementation of WS1 with 20% alkali lignin. Hydrolysis residue (HR) was obtained by exhaustive enzymatic hydrolysis of WS1. Avicel PH-101, pure microcrystalline cellulose with a particle size of ~50 µm, was purchased from Sigma-Aldrich. It contained more than 97% cellulose and less than 0.16% water-soluble materials (Yang et al., 2006). Applied pretreatment parameters and composition of the individual substrates are depicted in Table 1.

2.3 Organisms

Phanerochaete chrysosporium SCM21 and *Pichia pastoris* CBS7435 were from CLARIANT.

2.4. Culture media

Potato dextrose agar (PDA) was from Carl Roth. Liquid *Phanerochaete* medium contained 0.1% carboxymethyl cellulose sodium salt, 0.1% glucomannan, 0.1% arabinan, 0.1% xylan, 0.5% lactose×H_2O, 0.5% D-(+)-raffinose*5 H_2O, 2.5% yeast extract, 2.5% KH_2PO_4, 0.6% $CaCl_2$*2 H_2O, 0.3% $MgSO_4$*7 H_2O, 3.75% $(NH_4)_2SO_4$, 0.5% $FeSO_4$*7 H_2O, 0.16% $MnSO_4$*H_2O, 0.14% $ZnSO_4$*7 H_2O, 0.02% $CoCl_2$*6 H_2O, 1.5% ethylenediaminetetraacetic acid and 0.1% Tween 80 (poly(oxyethylene)$_{20}$ sorbitan monooleate). The pH value was adjusted to 6.0. YPD contained 2% peptone, 1% yeast extract, 2% glucose and 1.5% agar. BMD1 medium contained 2% glucose, 1.34% yeast nitrogen base, 4×10^{-5}% biotin and 200 mM potassium phosphate buffer (pH 6.0). BMM medium was composed of 1.34% yeast nitrogen base, 4×10^{-5}% biotin, 200 mM potassium phosphate buffer (pH 6.0) and 1% methanol.

2.5. Cultivation of P. chrysosporium SCM21

P. chrysosporium SCM21 was revitalized on PDA plates by incubation for 6 d at 30 °C. A 1 cm^2 agar slice was used to inoculate 100 mL medium in 300 mL wide-neck shake flasks. Incubation took place at 30 °C and 20 rpm in a rotary shaker for 315 h. Cells were harvested by a 30 min centrifugation at 11300×*g* and 4 °C in a Sorvall Evolution RC Superspeed centrifuge (Thermo Fisher Scientific) with a SLC 3000 fixed angle rotor. The supernatant was concentrated using a Centramate 500S CrossFlow (Pall Corporations, Port Washington, NY, USA) with a10 kDa-cutoff membrane. A buffer exchange to 10 mM potassium phosphate buffer (pH 7.0) was performed by ultrafiltration in Vivaspin 20 tubes (10 kDa cut-off) (Sartorius, Goettingen, Germany).

2.6. Fractionation of P. chrysosporium SCM21 secretome

2.6.1. Hydrophobic interaction chromatography (HIC)

The concentrated supernatant of *P. chrysosporium* SCM21 was brought to 25% saturated ammonium sulfate. After removal of precipitated protein, the supernatant was applied to a phenyl sepharose fast flow column (HiPrep Phenyl HP 16/10, GE-Healthcare) equilibrated with 10 mM potassium phosphate buffer (pH 7.0) containing 30% glycerol. Chromatography was performed

using a BioLogic DuoFlow chromatography system (Bio-Rad, Hercules, CA, USA). Elution was performed by applying a linear gradient from 25 – 0% saturated ammonium sulfate at a flow rate of 8.5 mL/min.

2.6.2. Mixed-mode chromatography (MM)

The HIC-pool showing the highest activity in the complementation assay (section 2.9) was rebuffered to 5 mM potassium phosphate (pH 7.0) by ultrafiltration. The concentrate was loaded on a 15 mL column packed with high-resolution hydroxyapatite (Sigma-Aldrich). Chromatography was performed in a BioLogic DuoFlow system. A linear gradient from 5 – 500 mM potassium phosphate (pH 7.0) was used for elution at a flow rate of 1.5 mL/min.

2.6.3. Anion exchange chromatography (AIEX)

The MM-pool showing the highest activity in the complementation assay was rebuffered to 10 mM potassium phosphate (pH 7.0) by ultrafiltration. The sample was loaded on a Mono Q 5/50 GL column (GE healthcare) equilibrated with 10 mM potassium phosphate buffer, pH 7.0. Protein elution was performed using a linear gradient from 0 – 1 M NaCl in 10 mM potassium phosphate buffer (pH 7.0) at a flow rate of 1 mL/min.

2.7. Determination of protein concentration

Protein concentrations were measured using the Roti-Quant assay according to manufacturers' instructions, calibrated against bovine serum albumin (BSA). Absorbance values were recorded with a Beckman Coulter DU800 spectrophotometer (Beckman Coulter GmbH, Krefeld, Germany). Protein concentration in adsorption assays was measured using the Roti-Nanoquant assay according to the manufacturers' instructions, calibrated against BSA. Absorbance values were recorded with a FLUOstar Omega plate reader (BMG Labtech GmbH, Ortenberg, Germany). For CD spectra analysis, the concentration of purified *rPc*Lrbp was determined by UV measurements in a Nanodrop 1000 spectrometer (Thermo Fisher Scientific, Waltham, MA, USA). The molar extinction coefficient (ε= 82640 $M^{-1}\times cm^{-1}$) of *rPc*Lrbp was calculated from the amino acid sequence using the Expasy Protparam web server (Gasteiger et al., 2005).

2.8. Electrophoresis

SDS-PAGE was done according to Zhao et al. (2007) using pre-cast NuPAGE 4-12% w/v Bis-Tris 1.0 mm midi protein gels (Thermo Fisher Scientific) in 1x Tris-glycine buffer. PageRuler Prestained Protein Ladder (Thermo Fisher Scientific) and RPN 5800 (GE Healthcare, Little Chalfont, UK) were used as molecular mass markers. Gels were run in the vertical XCell SureLock Mini-Cell electrophoresis system (Thermo Fisher Scientific) at 150 V for about 2 h. Silver staining was carried out as described by Chevallet et al. (2006).

2.9. Screening for cellulase-complementing activities

All experiments were done in duplicates. Wheat straw WS1 was suspended in 50 mM sodium acetate buffer (pH 5.0), resulting in a final substrate concentration of 25 g dry matter (DM)/L and transferred to Eppendorf tubes. Ten FPU/g DM ENZ-SC01 were added and supplemented with 10% *P. chrysosporium* SCM21 protein (0.25 g/L). Reference reactions contained only ENZ-SC01. Samples were incubated at 50 °C and 550 rpm for 72 h in an Eppendorf Thermomixer comfort (Eppendorf AG, Hamburg, Germany). At certain times samples were taken and heated to 95 °C for 7 min. Samples were briefly centrifuged (9300×*g*, 30 s) and the cleared supernatant was used for sugar analysis.

2.10. Sugar analysis

The liberated reducing sugar concentration was measured using a 3,5-dinitrosalicylic (DNS) acid based assay calibrated against glucose (Xiao et al., 2004). Forty µL of 50 mM sodium acetate buffer (pH 4.8), 20 µL of sample and 120 µL of DNS reagent were pipetted into a 96-well PCR-plate (Bio-Rad) and sealed with an aluminium seal (VWR International, Radnor, PA, USA). Samples were incubated at 95 °C for 5 min in a thermo-cycler, transferred into 96-well flat-bottom microtiter plates (Greiner Bio-One International, Frickenhausen, Germany) and diluted in distilled water. Measurements were done in duplicates. Absorbance values were recorded at 540 nm in a FLUOstar Omega plate reader.

Glucose concentration was determined using a commercial hexokinase glucose-6-phosphate dehydrogenase assay (Sigma-Aldrich). Measurements were done in duplicates against a substrate blank incubated with H_2O instead of reagent solution. Absorbance values were recorded at 340 nm in a FLUOstar Omega plate reader. For both assays, the sugar concentration at the start of hydrolysis was considered as background resulting from substrate impurities. The blank was subtracted from the measured values.

2.11. Protein identification

Protein identification by mass spectrometry was performed at the Core Facility Mass Spectrometry at the Center for Medical Research, Medical University of Graz. Fifteen µg of supernatant protein were deglycosylated with PNGase F (Roche, Mannheim, Germany) according to the manufacturers' protocol. SDS-page with 4 µg deglycosylated protein solution was performed, followed by silver staining. Bands were excised and tryptically digested (Shevchenko et al. 1996). Resulting peptides were dissolved in 30% acetonitrile containing 0.1% trifluoroacetic acid (TFA). For MALDI-TOF/TOF measurement on a Bruker Ultraflextreme instrument (Billerica, Mass., USA) 1 µl of each in gel digest was spotted onto an 800 µm Bruker MTP Anchorchip. The sample was left to dry before adding 1 µl of 0.7 mg/mL α-cyano-4-hydroxycinnamic acid as matrix in 0.1% TFA, 1 mM $NH_4H_2PO_4$ and 90% acetonitrile (dried droplet method). Full MS spectra were obtained in positive reflectron mode after external calibration using an appropriate peptide standard in the mass/charge range from 700 to 4000. MS/MS of the 20 most intense peaks were triggered. Peaks were assigned using the SNAP algorithm. MS/MS data were searched with Mascot 2.2 (MatrixScience, London, UK) using the following database and settings: The whole genome sequence of *Phanerochaete chrysosporium* (Bioproject PRJNA135) was used as a template for Augustus gene prediction (Stanke et al. 2006). The resulting protein database (10717 sequences, 5178388 residues) was used to search the MS/MS data. The detailed search settings were: no enzyme; fixed modification: carbamidomethylation at cysteine, deamidation of asparagine; precursor mass tolerance 50 ppm; product mass tolerance +/- 0.7 Da. A peptide ion score cut off of 20 and a minimum of two distinct

peptides were chosen as identification criteria. The identified predicted protein sequences were searched for homologues with BLAST software applying the blastp algorithm (Altschul et al., 2005) in the non-redundant protein sequences (nr) database at the National Centre of Biotechnology Information (NCBI) website (http://www.ncbi.nlm.nih.gov/Blast.cgi).

2.12. Sequence analysis of PcLrbp

Secretion signal prediction was performed using the SignalP 4.1 web server (Petersen et al., 2011). The amino acid sequence was investigated for the presence of motifs employing Motif Scan at the MyHits database (http://myhits.isb-sib.ch/). A BLASTp search of the NCBInr database was performed to analyze protein sequence similarity.

Multiple sequence alignments were done with Clustal Omega (Sievers et al., 2011) and the corresponding figure was generated with ESPript (Robert and Gouet, 2014). Phylogenetic tree construction was performed using the Phylogeny.fr web server (Dereeper et al., 2008). A customized approach was chosen combining programs with highest accuracy, stringency and robustness for tree construction: T-Coffee (alignment), Gblocks (alignment curation), MrBayes (tree construction) and TreeDYN (visualization). For physico-chemical characterization of *Pc*Lrbp, the Expasy Protparam web server was used.

2.13. Cloning of lrbp

The *P. chrysosporium* gene *lrbp* was cloned into the MCS of the *E. coli/P. pastoris* shuttle vector pPiccolic, downstream of an *AOX 1* promoter and upstream of a hexahistidine-tag. The native secretion signal was replaced by the *S. cerevisiae* α-mating factor pre-pro signal sequence. The construct was designated pLRBP and transformed into *P. pastoris* CBS7435. Zeocin resistance was used as a selection marker for successful transformation. Cloning and transformation were done by CLARIANT.

2.14. Heterologous expression of rPcLrbp

P. pastoris CBS7435 [pLRBP] was grown at 30 °C for 72 h on YPD plates. Fifty mL of BDM1 medium in 300 mL wide-neck-baffled shake flasks were inoculated with a single colony and

incubated in a rotary shaker at 100 rpm and 30 °C for 24 h. The pre-culture was used to inoculate 100 mL BMM medium in 1000 mL wide-neck-baffled shake flasks, reaching an initial OD_{600} of 0.2. Incubation took place at 28 °C and 100 rpm in a rotary shaker. After 36 h protein expression was induced by addition of 1% methanol. Induction was repeated every 12 h for the next 120 h. Evaporated medium was replaced every second day. The culture was centrifuged twice at 44000×*g* at 4 °C for 30 min in a Sorvall Evolution RC Superspeed centrifuge and the supernatant was collected. After filtration through 0.2 µm Minisart polyamide filters (Sartorius), the supernatant was concentrated and rebuffered to 10 mM potassium phosphate, pH 7.0, by ultrafiltration in Vivaspin 20 columns. *P. pastoris* [pLRBP]-supernatant (*P. p.* [pLRBP]-SN) was used for complementation assays, protein adsorption assays and purification of *rPc*Lrbp.

2.15. Purification of rPcLrbp

Two different strategies were applied for the purification of *rPc*Lrbp:

2.15.1. Affinity chromatography (His-Tag)

P. p. [pLRBP]-SN was dialyzed against 50 mM potassium phosphate buffer containing 50 mM NaCl (pH 7.4) at 4 °C and concentrated by ultrafiltration. The concentrate was loaded on a HisTrap FF column (GE healthcare) equilibrated with 50 mM potassium phosphate buffer containing 50 mM NaCl (pH 7.4). Chromatography was performed in an ÄKTAprime plus chromatography system (GE healthcare) at 4 °C. A linear gradient from 0 – 500 mM imidazole at a flow rate of 4 mL/min was used for protein elution. Protein purity was confirmed by SDS-Page and silver staining. Protein fractions were pooled, concentrated and rebuffered to 10 mM potassium phosphate buffer containing 50 mM NaCl (pH 7.0) by ultrafiltration.

2.15.2. Anion exchange chromatography (AIEX)

Dialysis of *P. p.* [pLRBP]-SN against 20 mM Tris-HCl buffer (pH 7.5) was performed at 4 °C. The supernatant was concentrated by ultrafiltration and loaded onto a HiTrap Q FF column (GE healthcare) equilibrated with 20 mM Tris-HCl buffer (pH 7.5). Chromatography was performed in an ÄKTAprime plus chromatography system at 4 °C. Protein elution was performed using a linear

gradient from 0 – 1M NaCl (pH 7.5) at a flow rate of 4 mL/min. Protein purity was confirmed by SDS-Page and silver staining. Fractions were pooled, concentrated and rebuffered to 20 mM Tris-HCl (pH 7.5) by ultrafiltration.

2.16. Complementation assay for rPcLrbp

Complementation assays were done in triplicates and performed in Eppendorf tubes in a total reaction volume of 1.8 mL. Tested substrates (Avicel, WS1, WS2, WS3) were suspended in 50 mM sodium acetate buffer (pH 5.0) to a concentration of 25 g DM/L. Substrate suspensions were supplemented with 14.4 FPU/g DM ENZ-SC01 and varying concentrations of *rPc*Lrbp-containing protein preparations. Control reactions contained only ENZ-SC01. Eppendorf tubes were incubated at 50 °C and 1000 rpm for up to 48 h in an Eppendorf Thermomixer comfort. Sampling was performed as stated above. At certain times samples were taken and heated to 95 °C for 7 min. Samples were briefly centrifuged (30 s at 9300×*g*) and the cleared supernatant was used for sugar analysis.

For pre-incubation experiments, a suspension of WS1 (25 g DM/L) in 50 mM sodium acetate buffer (pH 5.0) was supplemented with varying concentrations of AIEX-purified *rPc*Lrbp. Samples were pre-incubated at room temperature and 20 rpm for 10 min in a Stuart SB3 tube rotator (Bibby Scientific Limited, Staffordshire, UK). After addition of 14.4 FPU/g DM ENZ-SC01, reaction batches were incubated at 50 °C and 1000 rpm for 48 h in an Eppendorf Thermomixer comfort. Reference reactions were not pre-incubated and contained only ENZ-SC01. Sampling was performed as described above.

2.17. Protein adsorption assay

Adsorption experiments were carried out as triplicates and performed in Eppendorf tubes (1.8 mL reaction volume) or screw-capped glass vessels (4 mL reaction volume). Substrates were suspended in 50 mM sodium acetate buffer (pH 5.0) to a concentration of 25 g DM/L and supplemented with 100 mg/L protein. Control reactions were supplemented with the same concentration of GOX or ENZ-SC01. Blank reactions contained buffer and protein but no substrate. Eppendorf tubes were

incubated at 25 °C and 1000 rpm for 3 h in an Eppendorf Thermomixer comfort. Screw-capped glass vessels were incubated at room temperature and 20 rpm for 3 h in a Stuart SB3 tube rotator. Samples were taken after 0, 0.16, 1 and 3 h of incubation. Samples were briefly centrifuged (9300×*g*, 30 s) and 100 µL of the supernatant was retained for protein determination.

2.18. Circular Dichroism (CD) spectroscopy

Purified *rPc*Lrbp was diluted in 10 mM potassium phosphate buffer (pH 7.0) containing 50 mM NaCl to a concentration of 0.3 g/L and transferred to a 0.2 mm quartz cuvette. A JASCO J-715 spectropolarimeter (JASCO Analytical Instruments, Easton, MD, USA) was used to obtain circular dichroism spectra from 185 to 250 nm at room temperature and at a scanning speed of 100 nm/min. Spectra were an average of three measurements with the buffer spectrum subtracted from the protein spectra. The percentage of α-helices, β-sheets, turns and random coil was determined using the CDSSTR program (Sreerama and Woody, 2000) applying 3 different reference sets (set 4, set 7 and SP175) on the online server DichroWeb (Whitmore and Wallace, 2008). The structural content was averaged.

2.19. Curve fitting and calculations

Non-linear curve fitting using the SigmaPlot Version 10.0 program (Systat Software Inc., San Jose, CA, USA) and calculations were performed according to Monschein et al. (2013). Experimental hydrolysis time courses were fitted with equation (1),

$$y = \frac{ax}{b+x} + \frac{cx}{d+x} \quad (1)$$

where x is time [h] and y is the reducing sugar concentration [g/L]. Based on parameter estimates of equation (1), y was calculated for every 10 min within the first 3 h of hydrolysis, later for every 30 min. The volumetric hydrolysis rate r [g/L/h] was calculated using equation (2) from the y change within the 10- or 30-min time span.

$$r = \frac{\Delta y}{\Delta x} \quad (2)$$

The high hydrolysis rate at reaction start, calculated from the change in reducing sugar concentrations within the first 10 min of hydrolysis, was designated 'maximum hydrolysis rate' (r_{max}) [g/L/h]. The maximum hydrolysis rate in the presence of *Phanerochaete* protein was related to the values of control reactions containing only ENZ-SC01, depicted as increase in r_{max} [%].

The parameter C [%] described the conversion of the glycan portion in (ligno)cellulosic substrates.

$$C[\%] \equiv \frac{reducing\,sugars\,[M]}{glycan[M] \times 100\%} \qquad (3)$$

The glycan concentration was the sum of anhydrohexoses and anhydropentoses present. Plots of C versus r were usually biphasic with high r values at low C and low r values at high C. These dependencies were fitted with a third-order polynomial. Tangents were constructed to the resulting curve and their point of intersection marked C_{trans} [%], the transition between phases of high and low hydrolysis rate.

$C_{10\,min}$ [%], $C_{1\,h}$ [%], $C_{8\,h}$ [%] $C_{24\,h}$ [%] and $C_{48\,h}$ [%] determined the conversion after brief (10 min), short (1 h), intermediate (8 h), extended (24 h) and exhaustive (48 h) hydrolysis time. C in the presence of *Phanerochaete* protein was related to the values of control reactions containing only ENZ-SC01, depicted as increase in C [%].

Protein concentration adsorbed to insoluble substrate, P_{ads}, was defined by the difference between total added protein and protein measured in the supernatant after incubation. A blank for non-specific protein adsorption to reaction vessels was subtracted from the obtained values. The protein adsorption in the 0 – 3 h time span was described by $P_{ads\_0\,h}$ [g/L], $P_{ads\_10\,min}$ [g/L], $P_{ads\_1\,h}$ [g/L] and $P_{ads\_3\,h}$ [g/L]. We carefully considered how experimental error and error propagation affected the determination of the described parameters. Data shown in the figures are mean values of 3 to 6 independent determinations and error bares show the SD. Note that r was derived by fitting an experimental time course containing reducing sugar values of at least 3 independent determinations. Therefore no SD is shown.

3. Results and discussion

3.1. Screening of Phanerochaete chrysosporium SCM21 secretome for accessory proteins.

White-rot fungi possess the unique capability to degrade all major components of wood efficiently. Therefore extensive efforts have been made to characterize their extracellular enzyme system (Bouws et al., 2008). *P. chrysosporium* is the most intensively studied white-rot fungus and served as a model organism for lignin degradation (Moredo et al., 2003). Its genome was the first one of white-rot fungus to be sequenced, revealing a broad array of secreted hydrolytic and oxidative enzymes presumably conferring to its ability to degrade lignocellulose (Martinez et al., 2004). However, genomic analysis of sequences harboring a secretion signal revealed a large number of hypothetical proteins with no known function or protein domain (Ohm et al., 2014). It is reasonable to believe that some of these proteins might be involved in the hydrolysis of lignocellulosics and that further studies will lead to the identification of novel enzymes with industrial application potential in lignocellulose degradation technologies.

In this study the secretome of *P. chryososporium* SCM21 was screened for the presence of proteins complementing the cellulase system of *T. reesei* (ENZ-SC01) in the hydrolysis of pretreated wheat straw. A step-wise approach was chosen to trace potential accessory proteins. *P. chrysosporium SCM21* was grown in a synthetic, cellulose-containing medium and the obtained supernatant (*P. c.* SCM21-SN) was subjected to 3 consecutive purifications steps. Before being applied to the next step, resulting fractions were pooled and tested for an enhancement of ENZ-SC01-catalyzed hydrolysis of WS1. Thereby the protein composition was minimized to a level suitable for protein identification by mass spectrometry. The effect of *P. c.* SCM21-SN and the best complementing fractions on the enzymatic hydrolysis of WS1 in relation to ENZ-SC01 alone is shown in Fig. 1A. Supplementation of the hydrolysis reaction with 10% *P. c.* SCM21-SN protein enhanced the 8 h conversion of the entire glycan fraction by 17% and the one of cellulose by 6%. After hydrophobic interaction chromatography (HIC), these values dropped to 6 and 1%, respectively. This might be associated with removal of *Phanerochaete* cellulases, hemicellulases and ligninases. As expected,

consecutive purification steps led to protein fractions with higher activity. Mixed mode chromatography (MM) of HIC-pool 4 resulted in a pool enhancing $C_{8\,h}$ by 7% (total glycan) and 3% (cellulose), respectively. MM-pool 2 was applied to anion-exchange chromatography (AIEX). The obtained AIEX-pool 3 increased $C_{8\,h}$ of total glycan by 27% and the one of cellulose by 20%.

3.2. Peptide sequence determination and protein identification

The HIC-pool 4/MM-pool 2/AIEX-pool 3 protein preparation was tryptically digested and separated on a 1D SDS gel (Fig. 1B). Five of these lanes were excised and subjected to MALDI-TOF/TOF analysis. According to the MS/MS spectra 13 peptide mass data were obtained. Generated peptide sequence information was compared to the '*Phanerochaete chrysosporium* Augustus gene prediction from whole genome sequence' database by the MASCOT search engine. The lowest MASCOT protein score was 110 points, being well above the minimum (83 points) to reliably confirm known proteins. This approach resulted in the identification of 4 proteins. To predict their function, a BLASTp search of the NCBInr database was performed. Identified proteins contained a putative chitin-synthase, a α/β hydrolase, a glyoxylate reductase/ FAD-binding domain containing protein and *Pc*Lrbp (Table 2). *Pc*Lrbp showed only homology to hypothetical proteins. Due to its abundance in the corresponding fraction, *Pc*Lrbp was chosen for further analysis.

3.3. Domain structure and phylogenetic analysis

The *lrbp* gene encoded a protein of 261 amino acids as shown in Fig. 2. Analysis using SignalP 4.1 revealed a 19 amino acid long N-terminal secretion signal. According to Motif Scan the protein contains one glycosylation site, eight myrostylation sites and eight phosphorylation sites, but no metal binding motif. Sequence analysis by BLASTp revealed the presence of a 188 amino acid long domain of unknown function, DUF3455 (PF11937), spanning from residues 58 to 255. Domains of unknown function are a large set of families within the PFAM database that do not include any protein of known function (Bateman et al., 2010). According to PFAM, the DUF 3455 family contains 842 sequences found in 504 species, mostly fungi, with a typical length between 174 to 251 amino acids (Finn et al., 2014). With more than 50 members in the Fungal Secretome

KnowledgeBase, DUF3455 is listed among highly encoded secreted protein families in fungi, but remains to date functionally uncharacterized (Lum and Min, 2011).

A physico-chemical analysis using Expasy Protparam gave a theoretical isoelectric point (pI) value of 4.99 and a molecular mass of 28542 Da. The estimated half live was determined to be more than 20 h, the aliphatic index 73.72, the instability index 30.53 and the grand average of hydropathicity (GRAVY) -0.115. These results classify *Pc*Lrbp as a stable, hydrophilic compound. A BLASTp searching NCBInr database was performed using *Pc*Lrbp as a query with the 10 best protein hits representing solely hypothetical proteins of *Phanerochaete carnosa* and *Phlebiopsis gigantea*. *P*cLrbp exhibited 55% identity to the hypothetical protein PHACADRAFT_264923 of *P. carnosa* HHB-10118-sp. A multiple sequence alignment of *Pc*Lrbp with the best hits of 9 different fungal species (*P. carnosa*, *P. gigantea*, *Stereum hirsutum*, *Plicaturopsis crispa*, *Punctularia strigosozonata*, *Pleurotus ostreatus, G. trabeum*, *Lentinula edodes*, *Ceriporiopsis subvermispora*) is shown in Fig. 3. These proteins are between 225 and 270 amino acids in length. Residues 30C, 63P, 71G, 74NYTC, 82T, 87G, 94D, 96SC, 114W, 118P, 139G, 174P, 157P, 160DEF, 178A, 191P, 200W, 2015G, 2018A, 223R, 228GG and 236C were conserved in all proteins and embedded in sequence stretches showing high chemical similarity. The longest similar sequence segments were located at residues 70 to 98, 137 to 150, 156 to 163 and 198 to 204. The glycosylation site of *Pc*Lrbp was present in the conserved NYTC motif at position 74. Two phosphorylation sites were associated with regions showing chemical similarity; they were located at positions 122 and 204. Based on the BLASTp results, the best protein hits of 15 different fungal species were selected to construct a phylogenetic tree of *Pc*Lrbp via the phylogeny.fr web server (Fig. 4). Proteins of *P. chrysosporium*, *P. carnosa* and *P. gigantea* shared a common clade. The second clade was divided in 5 subgroups compromised of *Jaapia argillacea*, *Hypholoma sublateritium, P. strigosozonata* (subgroup A); *Piloderma croceum*, *Agaricus bisporus*, *P. ostreatus* (subgroup B); *P. crispa*, *S. hirsutum*, *Hydnomerulius pinastri*, *G. trabeum* (subgroup C); *Gymopus luxurians*, *L. edodes* (subgroup D) and *C. subvermispora* (subgroup E). All of these organisms are basidiomycetes. The

majority has been classified as white-rot fungi, with exception of *P. croceum* (ectomycorrhizal fungus), *A. bisporus* (litter- and straw decomposing fungus), *G. trabeum* and *H. pinastri* (brown-rot fungi). The rotting type of *J. argillacea* is to date still disputed (Blanchette, 1991; Kohler et al., 2015; Rytioja et al., 2014; Van der Nest et al., 2014). In a common simplification white-rot fungi are regarded as efficient degraders of lignin, while brown-rot fungi only modify the aromatic polymer, mainly by demethoxylation (Rytioja et al., 2014). However, the white rot/ brown rot dichotomy of wood rotting fungi is debated. It relies on the presence of high-oxidation potential class II peroxidases while other proteins are also known to contribute to the degradation of lignin (Riley et al., 2014). Even though these 15 fungal species belong to 8 different orders and have been assigned to different rotting-types, all of them share the ability to degrade lignin. This is indicated by the presence of peroxidases, laccases or lignin-degrading low molecular weight peptides (Bonnen et al., 1994; Chen et al., 2001; Floudas et al., 2015; Riley et al., 2014; Wang et al., 2006). The large majority of proteins in the phylogenetic tree are categorized as hypothetical proteins with no assigned activity. The only exceptions are a malate dehydrogenase of *G. trabeum* and a putative malate dehydrogenase of *L. edodes*. Literature research showed no experimental evidence for the assigned function of these proteins, making a malate dehydrogenase activity of *Pc*Lrbp unlikely. These results indicate a wide distribution of up to now uncharacterized *Pc*Lrbp-related proteins among lignin-degrading basidiomycetes.

3.4. Expression and purification of rPcLrbp

The gene *lrbp* was cloned into the MCS of an *E. coli*/*P. pastoris* shuttle vector downstream of an *AOX1* promoter. *rPc*Lrbp equipped with an N-terminal α-mating factor pre-pro secretion signal and a C-terminal HisTag was expressed in *P. pastoris* CBS7435. The culture supernatant (*P. p.* [pLRBP]-SN), showing high levels of *rPc*Lrbp on a coomassie stained SDS-gel, was used for further analysis and protein purification. *rPc*Lrbp was purified from *P. p*. [pLRBP]-SN by affinity- or anion exchange chromatography. Both methods resulted in pure *rPc*Lrbp preparations as confirmed by SDS-page and silver staining (Fig. 5).

3.5. Secondary structure of rPcLrbp

HisTag- and AIEX-purified *rPc*Lrbp were subjected to CD spectroscopy to determine the secondary structure content of the protein. The obtained spectra are shown in Fig. 6. A slightly different structural composition of AIEX- and HisTag-purified proteins was observed. AIEX-purified *rPc*Lrbp was composed of 14% α-helices, 33% β-strands, 19% turns and 34% unordered regions. HisTag-purified *rPc*Lrbp showed a higher content of β-strands (40%), less α-helices (11%) and unordered regions (30%).

3.6. Characterization of the activity of rPcLrbp.

3.6.1. Adsorption of rPcLrbp to (ligno)cellulosic substrates

(Ligno)cellulose is an insoluble substrate, making the adsorption of involved enzymes to the surface of substrate particles a prerequisite for hydrolysis (Zhang and Lynd, 2004). To gain information on its function in enzymatic hydrolysis, the ability of *rPc*Lrbp to adsorb to different (ligno)cellulosic substrates was tested. ENZ-SC01 and GOX and were used as positive and negative controls, respectively. This enabled a differentiation between non-specific and specific adsorption to the tested substrates. Protein adsorption to the glass surface area of the reaction vessels was taken into account by performing blank reactions without substrate. In an initial screening, the adsorption of *rPc*Lrbp containing *P. p.* [pLRBP]-SN to 3 different pretreated wheat straw substrates was monitored for 3 h (Fig. 7). GOX showed almost no adsorption to acidic-autoclave pretreated WS1 (Fig. 7A). Values between 26 mg/L ($P_{ads\_0\ h}$) and 38 mg/L ($P_{ads\_3\ h}$) were observed for the adsorption of ENZ-SC01. While increasing over time, adsorption of *P. p.* [pLRBP]-SN was much slower. Only after 1 h of incubation, a significant protein adsorption of 17 mg/L was detected. *P. p.* [pLRBP]-SN protein reached ~50% of the $P_{ads\_1\ h}$ and $P_{ads\_3\ h}$ values of ENZ-SC01. Acidic-autoclave pretreated WS3 contained more lignin (36%) than WS1. Lignin is known to act as a competitive cellulase adsorbent, reducing the amount of enzymes available for efficient cellulose hydrolysis (Zhang and Lynd, 2004). P_{ads} values of ENZ-SC01 were not significantly influenced by the increased lignin content of WS,3 while the adsorption of GOX and *P. p.* [pLRBP]-SN was

enhanced (Fig. 7B). Adsorption of GOX reached a maximum after 10 min (23 mg/L) and decreased at longer incubation times. P_{ads} values of *P. p.* [pLRBP]-SN increased during the first hour of incubation, reaching a $P_{ads\_1\ h}$ value of 29 mg/L. Even though a small desorption was observed after 3 h, both $P_{ads\_1\ h}$ and $P_{ads\_3\ h}$ values exceeded the ones of GOX. Steam exploded WS4 contained less lignin, but more hemicellulose than acidic-autoclave pretreated substrates. Compared to WS1 and WS3, it adsorbed less ENZ-SC01, probably caused by reduced cellulose and lignin levels in the reaction mixture (Fig. 7C). In accordance to the observations made for WS3, the highest P_{ads} of GOX was detected at the 10-min time point. This indicated a quick non-specific adsorption of GOX, followed by a slower desorption. In contrast, P_{ads} of *P. p.* [pLRBP]-SN increased over the entire incubation period. Only after 3 h of incubation, the level of *P. p.* [pLRBP]-SN adsorption exceeded P_{ads} of GOX. Compared to ENZ-SC01, $P_{ads\_3\ h}$ of *P. p.* [pLRBP]-SN was 34% lower. Apparently adsorption of *P. p.* [pLRBP]-SN to lignocellulosic substrates surpasses the levels of non-specific binding, while showing less affinity than cellulases.

To confirm these results, adsorption assays were repeated with purified *rPc*Lrbp. Assays performed with HisTag-purified *rPc*Lrbp did not yield reliable results (data not shown), which might have been caused by an interference of residual imidazole with Roti-Nanoquant. Thus, adsorption experiments were performed with AIEX-purified *rPc*Lrbp. To ensure a more homogenous distribution of the substrate within the batch, the set-up was changed to incubation in a tube rotator enabling end-over-end mixing. In this set-up adsorption of ENZ-SC01 to WS1 was slightly enhanced, resulting in a $P_{ads\_3\ h}$ of 41 mg/L (Fig. 8A). For GOX, non-specific adsorption reached values ≤ 10 mg/L. *P. p.* [pLRBP]-SN was used for comparative reasons. In relation to *P. p.* [pLRBP]-SN, $P_{ads\_10\ min}$ of pure *rPc*Lrbp was almost 12-fold higher. This indicated an accelerated initial adsorption of the purified protein. After 3 h of incubation P_{ads} of *rPc*Lrbp reached a maximum of 21 mg/L, representing an increase of 57% compared to *P. p.* [pLRBP]-SN. Nevertheless, $P_{ads\_3\ h}$ of *rPc*Lrbp was 53% lower than $P_{ads\_3\ h}$ of ENZ-SC01. To specify if cellulose or lignin was responsible for the adsorption of *rPc*Lrbp to lignocellulosic biomass, assays were

performed with Avicel and lignacious hydrolysis residue (HR). Avicel adsorbed significantly less ENZ-SC01 than WS1, reaching a $P_{ads\_3\ h}$ value of 25 mg/L (Fig. 8B). No adsorption of GOX was detected. Only a minor percentage of the added *P. p.* [pLRBP]-SN was able to adsorb to Avicel with a $P_{ads\_0\ h}$ of 7.5 mg/L representing the highest value. For purified *rPc*Lrbp, values were even lower and afflicted with a high standard deviation. Apparently *rPc*Lrbp was not able to adsorb to pure microcrystalline cellulose. HR was obtained by exhaustive enzymatic hydrolysis of WS1. Even though no feed stock analysis exists for this substrate, it can be assumed that it consists mostly of lignin with a minor percentage of residual cellulose or hemicellulose. For ENZ-SC01, a slight increase of P_{ads} was observed within the first hour of incubation. Between 1 h and 3 h, P_{ads} remained constant at 16 mg/L (Fig. 8C). Due to the degradation of cellulose and hemicellulose, adsorption of ENZ-SC01 might be mostly non-productive binding to lignin. Of all substrates tested, HR adsorbed the highest concentration of *P. p.* [pLRBP]-SN. Adsorption increased continuously over time, surpassing the level of ENZ-SC01 beyond reaction start. $P_{ads\_3\ h}$ of *P. p.* [pLRBP]-SN was 76% higher than the one of ENZ-SC01. Purified *rPc*Lrbp showed even higher adsorption values. As observed for *P. p.* [pLRBP]-SN, its P_{ads} increased during the entire incubation period. Compared to ENZ-SC01, $P_{ads\_3\ h}$ of *rPc*Lrbp was 2.7-fold higher, reflecting an enhanced binding capacity of this protein for HR. These results point towards a specific binding of *rPc*Lrbp to lignacious hydrolysis residue, supported by increased P_{ads}-values of *P. p.* [pLRBP]-SN on highly lignacious WS3 (Fig. 7B).

Lignin is a relatively hydrophobic and aromatic heteropolymer, possessing a heterogeneous structure. Basic units (guaiacyl, syringyl and *p*-hydroxyphenyl propanol) are linked by C-C and aryl-ether linkages (Horn et al., 2012). Up to now most research on lignin binding has focused on non-productive adsorption of cellulases (Gao et al., 2014; Guo et al., 2014). It has been suggested that carbohydrate binding modules (CBMs) and their hydrophobic aromatic amino acid residues facilitate non-productive cellulase binding to lignin in a pH-dependent manner (Rahikainen et al., 2013). Specific adsorption to lignin has been experimentally confirmed for laccases and lignin

peroxidases (Johjima et al., 1999; Saarinen et al., 2009; Shleev et al., 2006).Nevertheless, knowledge about the involved binding mechanism is still limited. Research is hampered by the branched three-dimensional structure of lignin lacking stereo regularity and the use of lignin model substrates in most studies. Chen et al. (2011) determined the specific binding modes of laccase, lignin peroxidase and manganese peroxidase to lignin in molecular docking and molecular dynamics simulations. Lignin was either located close to the surface of a binding pocket (laccaase) or buried within (lignin peroxidase, manganese peroxidase). Results indicated hydrophobic contacts to be the most common ones in the enzyme-lignin complex. Work of Bianchetti et al. (2013) showed that the CBM of *Streptomyces* sp. SACTE_2871 dioxygenase represents a lignin binding module, localizing the catalytic domain to lignin surfaces. Residues surrounding a conserved buried Y form a binding pocket highly complementary to the shape of coniferyl alcohol. Other possible interaction mechanisms between enzymes and lignin involve solvent-exposed aromatic residues. *Pc*Lrbp harbors several conserved aromatic (75Y, 114W, 161F, 200W) and hydrophobic (30C, 77C, 97C, 114W, 161F, 200W, 236C) amino acid residues. To date we can only speculate if some of these residues are located on the surface of *Pc*Lrbp or form a binding pocket. Due to the lack of DUF3455 containing homologous protein structures in the RSCB protein data bank (http://www.rcsb.org), the position of these residues in *rPc*Lrbp needs to be elucidated by crystallization. Further experiments are required to verify the specific adsorption of *rPc*Lrbp to lignin and if so, determine the involved mechanism.

3.6.2 Influence of rPcLrbp on the enzymatic hydrolysis of lignocellulosic substrates.

P. p. [pLRBP]-SN, containing secreted *rPc*Lrbp in excess, was used to test the effect of the recombinant protein on lignocellulose hydrolysis. Previously we presented a mathematical model based on a double-rectangular hyperbola (equation 1) to describe the experimental time course of reducing sugar release (Monschein et al., 2013). This model was applied to investigate the influence of *rPc*Lrbp on the enzymatic hydrolysis of wheat straw at a kinetic level (Fig. 9). When 6 mg/L *P. p.* [pLRBP]-SN were added, an enhancement of reducing sugar release from WS1 in early phase

hydrolysis was observed (Fig. 9A). This effect was maintained for the first 4 h of hydrolysis, before sugar release values of *P. p.* [pLRBP]-SN supplemented reactions dropped below those of the control. Even though the enhancing effect was less pronounced than the one on reducing sugar release, addition of *P. p.* [pLRBP]-SN was also beneficial to glucose liberation (Fig. 9B). The hydrolysis rate *r*, describing the reducing sugar release per h, was calculated based on a double-rectangular fit of the hydrolysis time course. Fig. 4C depicts the decline of *r* with increasing conversion *C* during the first 1.5 h of reaction. This represents a detail of the typical bi-phasic decrease of *r* during hydrolysis (Monschein et al., 2013). Supplementation of *P. p.* [pLRBP]-SN resulted in a 19% higher initial hydrolysis rate (r_{max}) compared to the control. The hydrolysis rate of supplemented reactions surpassed the one of ENZ-SC01 alone, until a *C* value of ~21% was reached. Application of *P. p.* [pLRBP]-SN resulted also in a small delay of C_{trans}, representing the transition from the fast declining initial hydrolysis rate to the more slowly declining limiting hydrolysis rate. A higher C_{trans} implies that transition from a high initial to a steady low hydrolysis rate can be deferred somewhat during the enzymatic reaction, with consequent positive effects on space-time yield (Monschein et al., 2013). While the control exhibited a C_{trans} of 13%, this value was shifted to 16% upon supplementation of *P. p.* [pLRBP]-SN.

To determine if a concentration dependent effect exists, the enzymatic hydrolysis of WS1 was supplemented with 0.3 – 27 mg/L *P. p.* [pLRBP]-SN (Fig. 10A). Compared to ENZ-SC01 alone, all supplemented reactions showed an increase in r_{max}. Even very low concentrations of *P. p.* [pLRBP]-SN were effective in enhancing r_{max} with 0.3 mg/L resulting in a 7% increase in relation to the control. This value was raised to 28% when higher concentrations of *P. p.* [pLRBP]-SN were used.

To gain insights into substrate composition influencing the activity of *rPc*Lrbp, the susceptibility of different (ligno)cellulosic substrates to the *P. p.* [pLRBP]-SN-associated effect was compared (Fig. 10B). Addition of 27 mg/L *P. p.* [pLRBP]-SN increased r_{max} of all tested substrates. Its effect on Avicel was rather small, resulting only in an enhancement of r_{max} by 7.5%. As discussed before, r_{max} of WS1 was increased by 28%. WS2 was obtained by supplementation of WS1 with lignin

alkali to a total lignin content of 46%. Due to the equal DM content applied in the reaction set-up, samples of WS2 contained less (hemi)cellulose than WS1. *rPc*Lrbp was less efficient in accelerating early phase hydrolysis of WS2, resulting in a 10% increase of r_{max}. This could be explained by trapping of *rPc*Lrbp by supplemented lignin particles, resulting in less protein available for action on the lignocellulosic substrate *per se*. With a 41% higher r_{max}, the most pronounced effect of *P. p.* [pLRBP]-SN supplementation was observed on WS3. WS3 was characterized by the highest innate lignin content of the tested substrates. Apparently the effect of *rPc*Lrbp is linked to the presence of lignin.

To verify its cellulase enhancing activity, hydrolysis experiments were performed in the presence of purified *rPc*Lrbp (Fig. 11). The enzymatic hydrolysis of WS1 was supplemented with 6 – 110 mg/L HisTag-purified *rPc*Lrbp. As expected, pure *rPc*Lrp resulted in a higher increase in r_{max} than *P. p.* [pLRBP]-SN, being related to the lower content of *rPc*Lrbp in the supernatant preparation (Fig. 11A). Between 6 and 55 mg/L protein, the effect on r_{max} increased with the applied protein concentration. At 55 mg/L the *rPc*Lrbp-associated effect reached a maximum with an enhancement of r_{max} by 64%. The effect on r_{max} was less pronounced at higher concentrations of *rPc*Lrbp with 82 and 110 mg/L increasing r_{max} by 36 and 28%, respectively. Presence of *rPc*Lrbp was also reflected in $C_{1\ h}$ values, showing a concentration-dependent effect (Fig. 11B). While the lowest tested concentration of *rPc*Lrbp increased $C_{1\ h}$ by 13%, addition of 110 mg/L resulted in an enhancement of 17%. The increasing effect of *rPc*Lrbp on $C_{1\ h}$ was much weaker than the one on r_{max}, supporting the hypothesis that *rPc*Lrbp accelerates the onset of hydrolysis.

To clarify if increased adsorption of *rPc*Lrbp had a positive influence on its hydrolysis-enhancing effect, pre-incubation experiments were performed (Fig. 11C, Fig. 11D). AIEX-purified *rPc*Lrbp was pre-incubated with WS1 at room temperature and 20 rpm for 10 min in a tube rotator before initiating enzymatic hydrolysis with addition of ENZ-SC01. The pre-incubation step was able to enhance the effect of low protein concentrations on r_{max} (Fig. 10A). While simultaneous addition of 6 mg/L *rPc*Lrbp and ENZ-SC01 increased r_{max} by 33%, this value was raised to 52% by pre-

incubation. In contrast to observations made upon addition of *rPc*Lrbp at hydrolysis start, higher protein concentrations resulted in a smaller increase of r_{max}. Application of 14 mg/L *rPc*Lrbp enhanced r_{max} by 42%, but dropped to 16% when the protein concentration was doubled. This indicated that higher amounts of adsorbed *rPc*Lrbp impair the activity of the protein. A similar effect has been observed for processive cellulases. High adsorption levels of cellulases create traffic jams on cellulose stalling the enzymatic hydrolysis (Igarashi et al., 2011). However, this effect was reversed after 1 h of hydrolysis. Increasing concentrations of *rPc*Lrbp resulted in higher $C_{1\ h}$, $C_{24\ h}$ and $C_{48\ h}$ values (Fig. 10D). For 6 and 14 mg/L *rPc*Lrbp the enhancing effect decreased in the 1h- to 48 h-time span. While $C_{1\ h}$ was increased by 12% and 15%, $C_{48\ h}$ was only enhanced by 2% and 6%, respectively. Different results were obtained at 27 mg/L *rPc*Lrbp, showing a higher increase in $C_{24\ h}$ (33%) than in $C_{1\ h}$ (17%) compared to the control. After 48 h of hydrolysis the increase in C dropped to 11%.

3.6.3. Test of rPcLrbp for hydrolytic activities.

P. p. [pLRBP]-SN was tested for activity against chromogenic nitrophenyl glycoside substrates and hydrolytic activity on (ligno)cellulosic substrates. However, these assays gave no positive result. A potential β-glucosidase activity was dismissed after repeating the assay with purified protein, allegedly being caused by minor impurities of an intracellular *P. pastoris* protein (data not shown). Therefore we were able to exclude *rPc*Lrbp from being a cellulase, β-glucosidase, β-galactosidase, α-arabinofuranosidase, β-mannosidase or β-xylosidase.

Taken together these results show a boosting effect of *rPc*Lrbp on early phase hydrolysis of lignocellulosic substrates by a non-hydrolytic activity. Even though the mechanism of action of *rPc*Lrbp needs to be elucidated, several possible explanations exist for a lignin-coupled effect of accessory proteins. Some lytic polysaccharide monooxygenases rely on the presence of lignin, which functions as a natural electron donor for their oxidative activity (Kim et al., 2014). These enzymes act in a metal-dependent manner, but to date no metal-binding motif was detected in *Pc*Lrbp. Protein adsorption to lignin could also reduce non-productive adsorption of cellulases,

increasing the amount of enzymes present for efficient cellulose hydrolysis, thus increasing cellulose conversion. However, the effect of such non-catalytic proteins like BSA increases with the adsorbed protein amount and is prevalent during long-term hydrolysis between 24 and 48 h (Kumar and Wyman, 2009). This is in contrast to the observations made for *rPc*Lrbp. Therefore we exclude an activity of *rPc*Lrp as a blocking agent for non-specific enzyme adsorption to lignin. The third possibility would be a modification of lignin chemistry or a disruption of its structure by *rPc*Lrbp, increasing the accessibility of cellulose. Further studies are needed to gain insight on how *rPc*Lrbp accelerates the onset of hydrolysis.

4. Conclusion

This study reports the isolation of the novel lignacious residue binding protein *Pc*Lrbp from *P. chrysosporium* followed by recombinant expression in *P. pastoris*. The non-hydrolytic protein exhibited synergism with cellulases in early-phase hydrolysis of pretreated wheat straw, boosting the initial hydrolysis rate by up to 64%. Our results indicate a specific adsorption of *rPc*Lrbp to the lignin fraction of biomass. *Pc*Lrbp showed no sequence similarity to other known accessory proteins, but related hypothetical proteins were widely distributed among basidiomycetes. These results open up the possibility for a new family of accessory proteins involved in lignocellulose hydrolysis, prevalent among lignin-degrading fungi.

Supplementary information

Elution profiles of the fractionation of *P. c.* SCM21-SN are shown in Fig. A.1. The screen of *P. p* [pLRBP]-SN for a hydrolytic activity on (ligno)cellulosic substrates is depicted in Fig. A.2. Specific activity of *P. p.* [pLRBP]-SN against chromogenic nitrophenyl glycoside substrates is shown in Fig. A.3. Fig. A.4 presents a predicted protein structure model of *Pc*Lrbp. See Table A.1 for an enzymatic characterization of *P. c.* SCM21-SN. Table A.2. provides information on the pools obtained by fractionation of *P. c* SCM21-SN supernatant used for protein identification.

Acknowledgements

The authors wish to thank Dr. Georg Schirrmacher (CLARIANT, Munich) for many useful discussions and comments. Support of Margaretha Schiller and Manuel Reisinger (Institute of Biotechnology and Biochemical Engineering, Graz University of Technology) is gratefully acknowledged. This study was performed within the COMET K-Project Macro-Fun and the COMET-K2-centre ACIB. Financial support from the Province of Styria is gratefully acknowledged. This work received support from: CLARIANT; the Federal Ministry of Economy, Family and Youth (BMWFJ); the Federal Ministry of Traffic, Innovation and Technology (bmvit); the Styrian Business Promotion Agency SFG; the Standortagentur Tirol; and ZIT-Technology Agency of the City of Vienna. Funding was through the COMET-Funding Program managed by the Austrian Research Promotion Agency FFG.

References

1. Altschul, S.F., Wootton, J.C., Gertz, E.M., Agarwala, R., Morgulis, A., Schaffer, A.A., Yu, Y.K., 2005. Protein database searches using compositionally adjusted substitution matrices. FEBS J. 272, 5101-5109.
2. Arantes, V., Saddler, J.N., 2010. Access to cellulose limits the efficiency of enzymatic hydrolysis: the role of amorphogenesis. Biotechnol. Biofuels 3, art. no. 1.
3. Banerjee, G., Car, S., Scott-Craig, J.S., Borrusch, M.S., Walton, J.D., 2010. Rapid optimization of enzyme mixtures for deconstruction of diverse pretreatment/biomass feedstock combinations. Biotechnol. Biofuels 3, art. no. 22.
4. Bateman, A., Coggill, P., Finn, R.D., 2010. DUFs: families in search of function. Acta Crystallogr. Sect. F Struct. Biol. Crystall. Comm. 66, 1148-1152.
5. Bianchetti, C.M., Harmann, C.H., Takasuka, T.E., Hura, G.L., Dyer, K., Fox, B.G., 2013. Fusion of dioxygenase and lignin-binding domains in a novel decreted enzyme from cellulolytic *Streptomyces* sp SirexAA-E. J. Biol. Chem. 288, 18574-18587.

6. Blanchette, R.A., 1991. Delignification by wood-decay fungi. Annu. Rev. Phytopathol. 29, 381-398.
7. Bonnen, A.M., Anton, L.H., Orth, A.B., 1994. Lignin-degrading enzymes of the commercial button mushroom, *Agaricus bisporus*. Appl. Environ. Microbiol. 60, 960-965.
8. Bouws, H., Wattenberg, A., Zorn, H., 2008. Fungal secretomes - nature's toolbox for white biotechnology. Appl. Microbiol. Biotechnol. 80, 381-388.
9. Chen, D.M., Taylor, A.F.S., Burke, R.M., Cairney, J.W.G., 2001. Identification of genes for lignin peroxidases and manganese peroxidases in ectomycorrhizal fungi. New Phytol. 152, 151-158.
10. Chen, M., Zeng, G.M., Tan, Z.Y., Jiang, M., Li, H., Liu, L.F., Zhu, Y., Yu, Z., Wei, Z., Liu, Y.Y., Xie, G.X., 2011. Understanding lignin-degrading reactions of ligninolytic enzymes: binding affinity and interactional profile. PLoS ONE 6. art. no. e25647.
11. Chevallet, M., Luche, S., Rabilloud, T., 2006. Silver staining of proteins in polyacrylamide gels. Nat. Protoc. 1, 1852-1858.
12. Dereeper, A., Guignon, V., Blanc, G., Audic, S., Buffet, S., Chevenet, F., Dufayard, J.F., Guindon, S., Lefort, V., Lescot, M., Claverie, J.M., Gascuel, O., 2008. Phylogeny.fr: robust phylogenetic analysis for the non-specialist. Nucleic Acids Res. 36, W465-469.
13. Eibinger, M., Bubner, P., Ganner, T., Plank, H., Nidetzky, B., 2014a. Surface structural dynamics of enzymatic cellulose degradation, revealed by combined kinetic and atomic force microscopy studies. FEBS J. 281, 275-920.
14. Eibinger, M., Ganner, T., Bubner, P., Rosker, S., Kracher, D., Haltrich, D., Ludwig, R., Plank, H., Nidetzky, B., 2014b. Cellulose surface degradation by a lytic polysaccharide monooxygenase and its effect on cellulase hydrolytic efficiency. J. Biol. Chem. 289, 35929-35938.

15. Ekwe, E., Morgenstern, I., Tsang, A., Storms, R., Powlowski, J., 2013. Non-hydrolytic cellulose active proteins: research progress and potential application in biorefineries. Ind. Biotechnol. 9, 123-131.

16. Finn, R.D., Bateman, A., Clements, J., Coggill, P., Eberhardt, R.Y., Eddy, S.R., Heger, A., Hetherington, K., Holm, L., Mistry, J., Sonnhammer, E.L.L., Tate, J., Punta, M., 2014. Pfam: the protein families database. Nucleic Acids Res. 42, D222-230.

17. Floudas, D., Held, B.W., Riley, R., Nagy, L.G., Koehler, G., Ransdell, A.S., Younus, H., Chow, J., Chiniquy, J., Lipzen, A., Tritt, A., Sun, H., Haridas, S., LaButti, K., Ohm, R.A., Kues, U., Blanchette, R.A., Grigoriev, I.V., Minto, R.E., Hibbett, D.S., 2015. Evolution of novel wood decay mechanisms in *Agaricales* revealed by the genome sequences of *Fistulina hepatica* and *Cylindrobasidium torrendii*. Fungal Genet. Biol. 76, 78-92.

18. Gao, D., Haarmeyer, C., Balan, V., Whitehead, T.A., Dale, B.E., Chundawat, S.P., 2014. Lignin triggers irreversible cellulase loss during pretreated lignocellulosic biomass saccharification. Biotechnol. Biofuels 7, art. no. 175.

19. Gasteiger, E., Hoogland, C., Gattiker, A., Duvaud, S., Wilkins, M.R., Appel, R.D., Bairoch, A., 2005. Protein identification and analysis tools on the ExPASy Server. in: Walker, J.M. (Ed.), The proteomics protocols handbook. Humana Press, New York City, NY, USA, pp. 571-607

20. Gomes, D., Rodrigues, A.C., Domingues, L., Gama, M., 2015. Cellulase recycling in biorefineries - is it possible? Appl. Microbiol. Biotechnol. 99, 4131-4143.

21. Guo, F., Shi, W., Sun, W., Li, X., Wang, F., Zhao, J., Qu, Y., 2014. Differences in the adsorption of enzymes onto lignins from diverse types of lignocellulosic biomass and the underlying mechanism. Biotechnol. Biofuels 7, art. no. 38.

22. Harris, P.V., Xu, F., Kreel, N.E., Kang, C., Fukuyama, S., 2014. New enzyme insights drive advances in commercial ethanol production. Curr. Opin. Chem. Biol. 19, 162-170.

23. Horn, S.J., Vaaje-Kolstad, G., Westereng, B., Eijsink, V.G.H., 2012. Novel enzymes for the degradation of cellulose. Biotechnol. Biofuels 5, art. no. 45.

24. Hu, J.G., Arantes, V., Saddler, J.N., 2011. The enhancement of enzymatic hydrolysis of lignocellulosic substrates by the addition of accessory enzymes such as xylanase: is it an additive or synergistic effect? Biotechnol. Biofuels 4., art. no. 36.

25. Igarashi, K., Uchihashi, T., Koivula, A., Wada, M., Kimura, S., Okamoto, T., Penttila, M., Ando, T., Samejima, M., 2011. Traffic jams reduce hydrolytic efficiency of cellulase on cellulose surface. Science 333, 1279-1282.

26. Johjima, T., Itoh, N., Kabuto, M., Tokimura, F., Nakagawa, T., Wariishi, H., Tanaka, H., 1999. Direct interaction of lignin and lignin peroxidase from Phanerochaete chrysosporium. Proc. Natl. Acad. Sci. U.S.A. 96, 1989-1994.

27. Kim, I.J., Lee, H.J., Choi, I.G., Kim, K.H., 2014. Synergistic proteins for the enhanced enzymatic hydrolysis of cellulose by cellulase. Appl. Microbiol. Biotechnol. 98, 8469-8480.

28. Kohler, A., Kuo, A., Nagy, L.G., Morin, E., Barry, K.W., Buscot, F., Canback, B., Choi, C., Cichocki, N., Clum, A., Colpaert, J., Copeland, A., Costa, M.D., Dore, J., Floudas, D., Gay, G., Girlanda, M., Henrissat, B., Herrmann, S., Hess, J., Hogberg, N., Johansson, T., Khouja, H.R., LaButti, K., Lahrmann, U., Levasseur, A., Lindquist, E.A., Lipzen, A., Marmeisse, R., Martino, E., Murat, C., Ngan, C.Y., Nehls, U., Plett, J.M., Pringle, A., Ohm, R.A., Perotto, S., Peter, M., Riley, R., Rineau, F., Ruytinx, J., Salamov, A., Shah, F., Sun, H., Tarkka, M., Tritt, A., Veneault-Fourrey, C., Zuccaro, A., Tunlid, A., Grigoriev, I.V., Hibbett, D.S., Martin, F., Co, M.G.I., 2015. Convergent losses of decay mechanisms and rapid turnover of symbiosis genes in mycorrhizal mutualists. Nat. Genet. 47, 410-415.

29. Kumar, R., Wyman, C.E., 2009. Effect of additives on the digestibility of corn stover solids following pretreatment by leading technologies. Biotechnol. Bioeng. 102, 1544-1557.

30. Lum, G., Min, X.J., 2011. FunSecKB: the Fungal Secretome KnowledgeBase. Database, art. no bar001.

31. Mansfield, S.D., Mooney, C., Saddler, J.N., 1999. Substrate and enzyme characteristics that limit cellulose hydrolysis. Biotechnol. Prog. 15, 804-816.

32. Margeot, A., Hahn-Hagerdal, B., Edlund, M., Slade, R., Monot, F., 2009. New improvements for lignocellulosic ethanol. Curr. Opin. Biotechnol. 20, 372-380.

33. Martinez, D., Larrondo, L.F., Putnam, N., Gelpke, M.D.S., Huang, K., Chapman, J., Helfenbein, K.G., Ramaiya, P., Detter, J.C., Larimer, F., Coutinho, P.M., Henrissat, B., Berka, R., Cullen, D., Rokhsar, D., 2004. Genome sequence of the lignocellulose degrading fungus *Phanerochaete chrysosporium* strain RP78. Nat. Biotechnol. 22, 695-700.

34. Monschein, M., Reisinger, C., Nidetzky, B., 2014. Dissecting the effect of chemical additives on the enzymatic hydrolysis of pretreated wheat straw. Bioresour. Technol. 169, 713-722.

35. Monschein, M., Reisinger, C., Nidetzky, B., 2013. Enzymatic hydrolysis of microcrystalline cellulose and pretreated wheat straw: a detailed comparison using convenient kinetic analysis. Bioresour. Technol. 128, 679-687.

36. Moredo, N., Lorenzo, M., Dominguez, A., Moldes, D., Cameselle, C., Sanroman, A., 2003. Enhanced ligninolytic enzyme production and degrading capability of *Phanerochaete chrysosporium* and *Trametes versicolor*. World J. Microb. Biot. 19, 665-669.

37. Nitsos, C.K., Matis, K.A., Triantafyllidis, K.S., 2013. Optimization of hydrothermal pretreatment of lignocellulosic biomass in the bioethanol production process. Chemsuschem. 6, 110-122.

38. Ohm, R.A., Riley, R., Salamov, A., Min, B., Choi, I.G., Grigoriev, I.V., 2014. Genomics of wood-degrading fungi. Fungal Genet. Biol. 72, 82-90.

39. Petersen, T.N., Brunak, S., von Heijne, G., Nielsen, H., 2011. SignalP 4.0: discriminating signal peptides from transmembrane regions. Nature Methods 8, 785-786.

40. Pollegioni, L., Tonin, F., Rosini, E., 2015. Lignin-degrading enzymes. FEBS J. 282, 1190-1213.

41. Rahikainen, J.L., Evans, J.D., Mikander, S., Kalliola, A., Puranen, T., Tamminen, T., Marjamaa, K., Kruus, K., 2013. Cellulase-lignin interactions-the role of carbohydrate-binding module and pH in non-productive binding. Enzyme Microb. Technol. 53, 315-321.

42. Riley, R., Salamov, A.A., Brown, D.W., Nagy, L.G., Floudas, D., Held, B.W., Levasseur, A., Lombard, V., Morin, E., Otillar, R., Lindquist, E.A., Sun, H., LaButti, K.M., Schmutz, J., Jabbour, D., Luo, H., Baker, S.E., Pisabarro, A.G., Walton, J.D., Blanchette, R.A., Henrissat, B., Martin, F., Cullen, D., Hibbett, D.S., Grigoriev, I.V., 2014. Extensive sampling of basidiomycete genomes demonstrates inadequacy of the white-rot/brown-rot paradigm for wood decay fungi. Proc. Natl. Acad. Sci. U.S.A. 111, 9923-9928.

43. Robert, X., Gouet, P., 2014. Deciphering key features in protein structures with the new ENDscript server. Nucleic Acids Res. 42, W320-324.

44. Rytioja, J., Hilden, K., Yuzon, J., Hatakka, A., de Vries, R.P., Makela, M.R., 2014. Plant-polysaccharide-degrading enzymes from basidiomycetes. Microbiol. Mol. Biol. Rev. 78, 614-649.

45. Saarinen, T., Orelma, H., Gronqvist, S., Andberg, M., Holappa, S., Laine, J., 2009. Adsorption of different laccases on cellulose and lignin surfaces. Bioresources 4, 94-110.

46. Shleev, S., Persson, P., Shumakovich, G., Mazhugo, Y., Yaropolov, A., Ruzgas, T., Gorton, L., 2006. Interaction of fungal laccases and laccase-mediator systems with lignin. Enzyme Microb. Technol. 39, 841-847.

47. Sievers, F., Wilm, A., Dineen, D., Gibson, T.J., Karplus, K., Li, W.Z., Lopez, R., McWilliam, H., Remmert, M., Soding, J., Thompson, J.D., Higgins, D.G., 2011. Fast, scalable generation of high-quality protein multiple sequence alignments using Clustal Omega. Mol. Syst. Biol. 7, art. no. 539.

48. Singhvi, M.S., Chaudhari, S., Gokhale, D.V., 2014. Lignocellulose processing: a current challenge. Rsc Adv. 4, 8271-8277.

49. Sreerama, N., Woody, R.W., 2000. Estimation of protein secondary structure from circular dichroism spectra: comparison of CONTIN, SELCON, and CDSSTR methods with an expanded reference set. Anal. Biochem. 287, 252-260.

50. Trudeau, D.L., Lee, T.M., Arnold, F.H., 2014. Engineered thermostable fungal cellulases exhibit efficient synergistic cellulose hydrolysis at elevated temperatures. Biotechnol. Bioeng. 111, 2390-2397.

51. Van der Nest, M.A., Olson, A., Lind, M., Velez, H., Dalman, K., Durling, M.B., Karlsson, M., Stenlid, J., 2014. Distribution and evolution of *het* gene homologs in the basidiomycota. Fungal Genet. Biol. 64, 45-57.

52. Wang, W., Gao, P.J., 2003. Function and mechanism of a low-molecular-weight peptide produced by *Gloeophyllum trabeum* in biodegradation of cellulose. J. Biotechnol. 101, 119-130.

53. Wang, W., Huang, F., Mei Lu, X., Ji Gao, P., 2006. Lignin degradation by a novel peptide, Gt factor, from brown rot fungus *Gloeophyllum trabeum*. Biotechnol. J. 1, 447-453.

54. Wang, W., Liu, J., Chen, G.J., Zhang, Y.S., Gao, P.J., 2003. Function of a low molecular weight peptide from *Trichoderma pseudokoningii* S38 during cellulose biodegradation. Curr. Microbiol. 46, 371-379.

55. Whitmore, L., Wallace, B.A., 2008. Protein secondary structure analyses from circular dichroism spectroscopy: methods and reference databases. Biopolymers 89, 392-400.

56. Xiao, Z., Storms, R., Tsang, A., 2004. Microplate-based filter paper assay to measure total cellulase activity. Biotechnol. Bioeng. 88, 832-837.

57. Yang, B., Willies, D.M., Wyman, C.E., 2006. Changes in the enzymatic hydrolysis rate of avicel cellulose with conversion. Biotechnol. Bioeng. 94, 1122-1128.

58. Zhang, Y.H., Lynd, L.R., 2004. Toward an aggregated understanding of enzymatic hydrolysis of cellulose: noncomplexed cellulase systems. Biotechnol. Bioeng. 88, 797-824.

59. Zhao, X.B., Zhang, L.H., Liu, D.H., 2012. Biomass recalcitrance. Part I: the chemical compositions and physical structures affecting the enzymatic hydrolysis of lignocellulose. Biofuel. Bioprod. Bior., 6, 465-482.

60. Zhao, Z., Aliwarga, Y., Willcox, M.D., 2007. Intrinsic protein fluorescence interferes with detection of tear glycoproteins in SDS-polyacrylamide gels using extrinsic fluorescent dyes. J. Biomol. Tech. 18, 331-335.

Figure Captions

Figure 1: Screening of *P. chrysosporium* SCM21 secretome for accessory proteins.

(A) Supplementation of ENZ-SC01 with fractions of the *P. chrysosporium* SCM21 secretome. WS1 [25 g DM/L] was hydrolyzed for 48 h at 50 °C and 550 rpm using 14.4 FPU/g DM ENZ-SC01 supplemented with 10% *P. chrysosporium* SCM21 protein (*P. c.* SCM21-SN; HIC-pool 4; HIC-pool 4/MM-pool 2; HIC-pool 4/MM-pool 2/AIEX-pool 3). Increase in $C_{8\ h}$ [%] in relation to ENZ-SC01 alone. Black bars represent reducing sugars, grey bars glucose. (B) Separation of *P. chrysosporium* SCM21 protein fractions by 1D SDS-Page. Proteins were separated on a 4-12% Bis-Tris gel and silver stained. Lane 1: RPN 5800 standard; lane 2: HIC-Pool 4/MM-pool 2/AIEX-pool 2; lane 3: HIC-pool 4/MM-pool 2/AIEX-pool 3; lane 4: HIC-pool 4/MM-pool 2/AIEX-pool 2 digested with PNGase F; lane 5: HIC-pool 4/MM-pool 2/AIEX-pool 3 digested with PNGase F. Arrow indicates position of *Pc*Lrbp.

Figure 2: Amino acid sequence of *Pc*Lrbp.

N-terminal secretion signal is shown in yellow, predicted conserved domain DUF3455 in red. Stars (*) indicate phosphorylation sites, dots (●) gycosylation sites.

Figure 3: Multiple amino acid sequence alignment of *Pc*Lrbp with 9 fungal proteins.

Selection was based on BLASTp searches of the NCBInr database. Strictly conserved regions are shown in red blocks, similar residues in yellow blocks. Grey boxes indicate chemical similarity across a group of residues. Alignments were performed with Clustal Omega and the figure was generated with ESPript 3 (http://espript.ibcp.fr). References: *Pc*Lrbp of *Phanerochaete chrysosporium* SCM21 (>gi|46851341|gb|AADS01000591.1|); hypothetical protein PHACADRAFT_264923 of *Phanerochaete carnosa* HHB-10118-sp. (>gi|599402937|ref|XP_007401487.1|); hypothetical protein PHLGIDRAFT_182502 of *Phlebiopsis gigantea* 11061_1 CR5-6 (>gi|754371965|gb|KIP04689.1|); hypothetical protein

STEHIDRAFT_167031 of *Stereum hirsutum* FP-91666 SS1 (>gi|597909468|ref|XP_007302033.1|); hypothetical protein PLICRDRAFT_48366 of *Plicaturopsis crispa* FD-325 SS-3 (>gi|749771076|gb|KII95406.1|); hypothetical protein PUNSTDRAFT_44769 of *Punctularia strigosozonata* HHB-11173 SS5 (>gi|599110192|ref|XP_007384139.1|); hypothetical protein PLEOSDRAFT_1075615 of *Pleurotus ostreatus* PC15 (>gi|646307443|gb|KDQ28587.1|); malate dehydrogenase of *Gloeophyllum trabeum* ATCC 11539 (>gi|630360299|ref|XP_007869424.1|); putative malate dehydrogenase of *Lentinula edodes* (>gi|242389916|dbj|BAH80448.1|); hypothetical protein CERSUDRAFT_124747 of *Ceriporiopsis subvermispora* B (>gi|449544462|gb|EMD35435.1|).

Figure 4: Phylogenetic analysis of *Pc*Lrbp.

Phylogenetic relation of *Pc*Lrbp with proteins of 15 different fungal species. Analyzed proteins were chosen based on results of pBLAST searches of the NCBInr database. Branch lengths represent the amount of genetic change between a node and its descendant. Scale bar represents 0.2 substitutions per site. References: *Pc*Lrbp of *Phanerochaete chrysosporium* SCM21 (>gi|46851341|gb|AADS01000591.1|); hypothetical protein PHACADRAFT_264923 of *Phanerochaete carnosa* HHB-10118-sp. (>gi|599402937|ref|XP_007401487.1|); hypothetical protein PHLGIDRAFT_182502 of *Phlebiopsis gigantea* 11061_1 CR5-6 (>gi|754371965|gb|KIP04689.1|); hypothetical protein STEHIDRAFT_167031 of *Stereum hirsutum* FP-91666 SS1 (>gi|597909468|ref|XP_007302033.1|); hypothetical protein PLICRDRAFT_48366 of *Plicaturopsis crispa* FD-325 SS-3 (>gi|749771076|gb|KII95406.1|); hypothetical protein PUNSTDRAFT_44769 of *Punctularia strigosozonata* HHB-11173 SS5 (>gi|599110192|ref|XP_007384139.1|); hypothetical protein PLEOSDRAFT_1075615 of *Pleurotus ostreatus* PC15 (>gi|646307443|gb|KDQ28587.1|); malate dehydrogenase of *Gloeophyllum trabeum* ATCC 11539 (>gi|630360299|ref|XP_007869424.1|); putative malate dehydrogenase of *Lentinula edodes* (>gi|242389916|dbj|BAH80448.1|); hypothetical protein CERSUDRAFT_124747 of

Ceriporiopsis subvermispora B (>gi|449544462|gb|EMD35435.1|); hypothetical protein PILCRDRAFT_816656 of *Piloderma croceum* F 1598 (>gi|751737836|gb|KIM86121.1|); hypothetical protein AGABI1DRAFT_130486 of *Agaricus bisporus* var. *burnettii* JB137-S8 (>gi|597990315|ref|XP_007332041.1|); hypothetical protein GYMLUDRAFT_68480 of *Gymnopus luxurians* FD-317 M1 (>gi|751026930|gb|KIK68624.1|); hypothetical protein HYPSUDRAFT_1010005 of *Hypholoma sublateritium* FD-334 SS-4 (>gi|763720088|gb|KJA17572.1|); hypothetical protein JAAARDRAFT_69216 of *Jaapia argillacea* MUCL 33604] (>gi|646394383|gb|KDQ58797.1|); hypothetical protein HYDPIDRAFT_31172 of *Hydnomerulius pinastri* MD-312 (>gi|749893775|gb|KIJ61564.1|).

Figure 5: Purification of *rPc*Lrbp.

(A) SDS-PAGE of HisTag-purified protein fractions of *P. p*. [pLRBP]-SN. Proteins were separated on a 4-12% Bis-Tris gel and silver stained. Lane 1-14: fractions of HisTag-purification; lane 12: PageRuler Prestained Protein Ladder. Arrow indicates position of *rPc*Lrbp. (B) SDS-PAGE of AIEX-purified protein fractions of *P. p.* [pLRBP]-SN. Lane 1: PageRuler Prestained Protein Ladder; lane 2: *P. p.* [pLRBP]-SN; lane 3-10: fractions of AIEX-purification; lane 11: PageRuler prestained protein ladder. Arrow indicates position of *rPc*Lrbp.

Figure 6: CD-Spectra of purified *rPc*Lrbp.

*rPc*Lrbp (0.3 g/L) in 10 mM potassium phosphate buffer containing 50 mM NaCl (pH 7.0) was used for measurements. CD spectra were obtained from 185 to 250 nm at room temperature and a scanning speed of 100 nm/min. Spectra are an average of three measurements with the buffer spectrum subtracted from the protein spectra. Black curves represent AIEX-purified *rPc*Lrbp, red curves HisTag- purified *rPc*Lrbp. (A) Molar ellipticity [deg × cm^2 × $dmol^{-1}$] depending on wavelength [nm]. (B) High tension (HT) voltage [V] depending on wavelength [nm].

Figure 7: Adsorption of *P. p.* [pLRBP]-SN proteins to pretreated wheat straw substrates.

P. p. [pLRBP]-SN [100 mg/L protein] was incubated with suspensions of different substrates (25 g DM/L) in 50 mM sodium acetate buffer, pH 5.0. Samples were incubated at 25 °C and 1000 rpm for 3 h in an Eppendorf Thermomixer. GOX and ENZ-SC01 were used as negative and positive controls. (A) WS1. (B) WS3. (C) WS4.

Figure 8: Adsorption of purified *rPc*Lrbp to cellulose, lignocellulose or lignin substrates.

P. p. [pLRBP]-SN proteins and AIEX-purified *rPc*Lrbp [100 mg/L] were incubated with different substrates (25 g DM/L) in 50 mM sodium acetate buffer, pH 5.0. Incubation took place at room temperature and 20 rpm for 3 h in a tube rotator. GOX and ENZ-SC01 were used as negative and positive controls. (A) Avicel. (B) WS1. (C) HR.

Figure 9: Enzymatic hydrolysis of thermo-acidically pretreated wheat straw upon supplementation of *P. p.* [pLRBP]-SN proteins.

WS1 (25 g DM/L) was hydrolyzed for 12 h at 50 °C using 14.4 FPU/g DM ENZ-SC01. Figures depict hydrolysis within the first 1.5 h. (A) Time course of hydrolysis based on reducing sugar release. Black circles (•) represent hydrolysis of WS1 with ENZ-SC01. White circles (○) describe hydrolysis of WS1 with ENZ-SC01 supplemented with 6 mg/L *P. p.* [pLRBP]-SN. Solid and dashed lines represent curve fitting according to equation (1). (B) Time course of hydrolysis based on glucose release. Black circles (•) represent hydrolysis of WS1 with ENZ-SC01. White circles (○) describe hydrolysis of WS1 with ENZ-SC01 supplemented with 6 mg/L *P. p.* [pLRBP]-SN. Solid and dashed lines represent curve fitting according to equation (1). (C) Decrease of r with C. Black circles (•) describe hydrolysis of WS1 with ENZ-SC01, white circles (○) hydrolysis upon supplementation of 6 mg/L *P. p.* [pLRBP]-SN. Circles were fitted with a third-order polynomial, shown in solid lines.

Figure 10: Effect of *P. p* [pLRBP]-SN on r_{max}.

Substrates (25 g/L DM) were hydrolyzed for 24 h at 50 °C using 14.4 FPU/g DM ENZ-SC01. (A) Increase of r_{max} [%] in the hydrolysis of WS1 upon addition of various concentrations of *P. p.* [pLRBP]-SN. Depicted values are in relation to ENZ-SC01 alone. (B) Increase of r_{max} [%] in the hydrolysis of different substrates upon supplementation of 27 mg/L *P. p*. [pLRBP]-SN. Depicted values are in relation to ENZ-SC01.

Figure 11: Effect of purified *rPc*Lrbp on the enzymatic hydrolysis of thermo-acidically pretreated wheat straw.

(A, B) WS1 (25 g DM/L) was hydrolyzed for 1 h at 50 °C using 14.4 FPU/g DM ENZ-SC01, supplemented with various concentrations of HisTag-purified *rPc*Lrbp. (A) Increase of r_{max} [%] in relation to ENZ-SC01 alone. (B) Increase of $C_{1\ h}$ [%] in relation to ENZ-SC01 alone. (C, D) WS1 (25 g DM/L) was supplemented with different concentrations of AIEX-purified *rPc*Lrbp and pre-incubated at room temperature and 20 rpm for 10 min in a tube rotator. Hydrolysis was performed with 14.4 FPU/g DM ENZ-SC01 at 50 °C and 1000 rpm for 48 h. (C) Increase of r_{max} [%] in relation to ENZ-SC01 alone. (D) Increase of $C_{1\ h}$ [%], $C_{24\ h}$ [%] and $C_{48\ h}$ [%] in relation to ENZ-SC01 alone.

Identification of a lignacious residue binding protein from *Phanerochaete chrysosporium* boosting early-phase enzymatic hydrolysis of pretreated lignocellulose.

Figures and tables

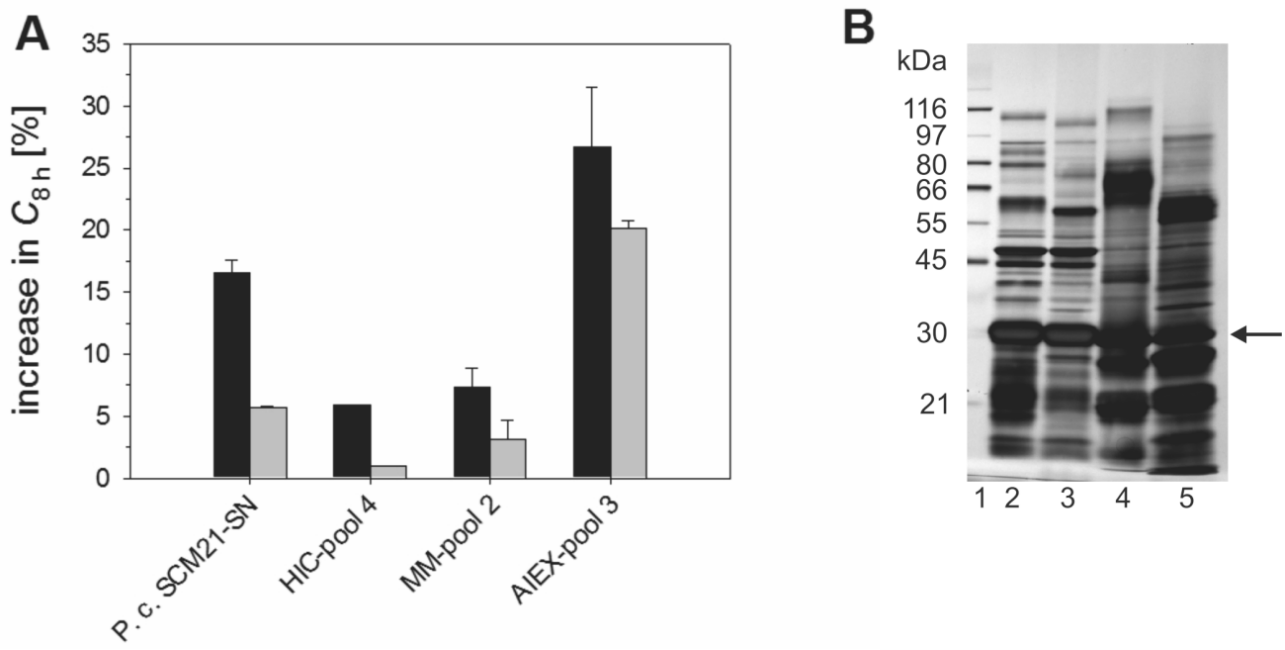

Figure 1

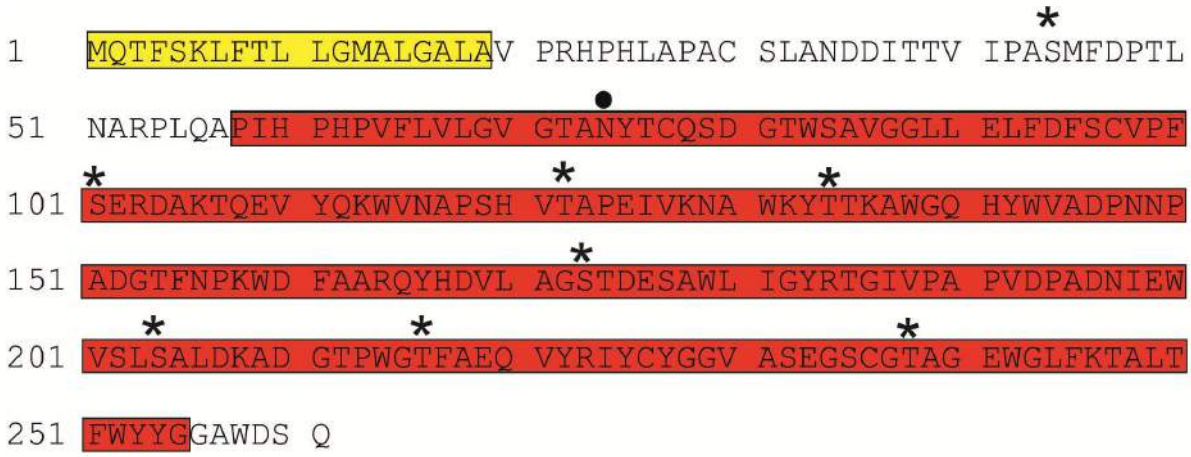
1 MQTFSKLFTL LGMALGALAV PRHPHLAPAC SLANDDITTV IPASMFDPTL
51 NARPLQAPIH PHPVFLVLGV GTANYTCQSD GTWSAVGGLL ELFDFSCVPF
101 SERDAKTQEV YQKWVNAPSH VTAPEIVKNA WKYTTKAWGQ HYWVADPNNP
151 ADGTFNPKWD FAARQYHDVL AGSTDESAWL IGYRTGIVPA PVDPADNIEW
201 VSLSALDKAD GTPWGTFAEQ VYRIYCYGGV ASEGSCGTAG EWGLFKTALT
251 FWYYGGAWDS Q

Figure 2

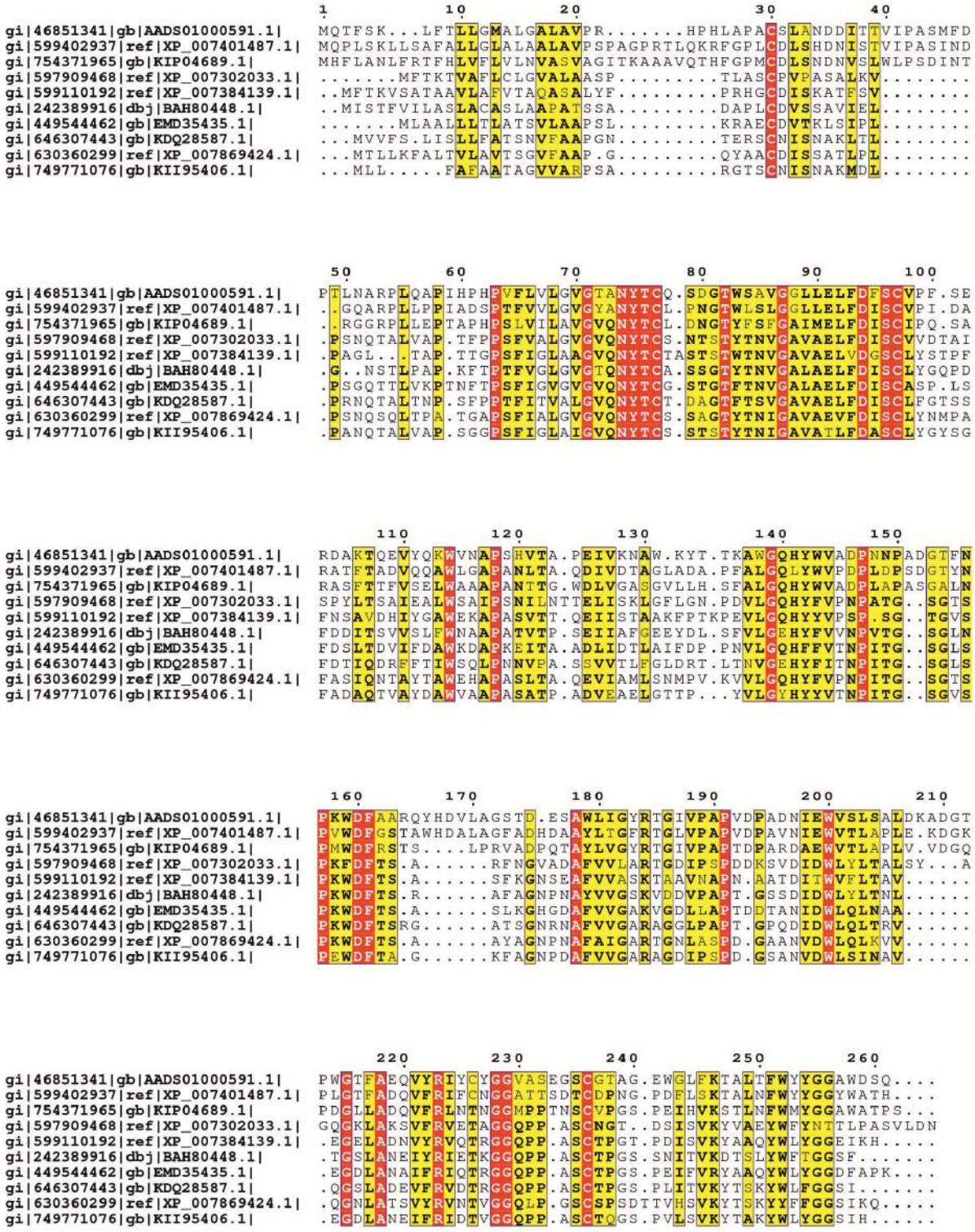
gi|46851341|gb|AADS01000591.1|
gi|599402937|ref|XP_007401487.1|
gi|754371965|gb|KIP04689.1|
gi|597909468|ref|XP_007302033.1|
gi|599110192|ref|XP_007384139.1|
gi|242389916|dbj|BAH80448.1|
gi|449544462|gb|EMD35435.1|
gi|646307443|gb|KDQ28587.1|
gi|630360299|ref|XP_007869424.1|
gi|749771076|gb|KII95406.1|

Figure 3

Identification of a lignacious residue binding protein from *Phanerochaete chrysosporium* boosting early-phase enzymatic hydrolysis of pretreated lignocellulose.

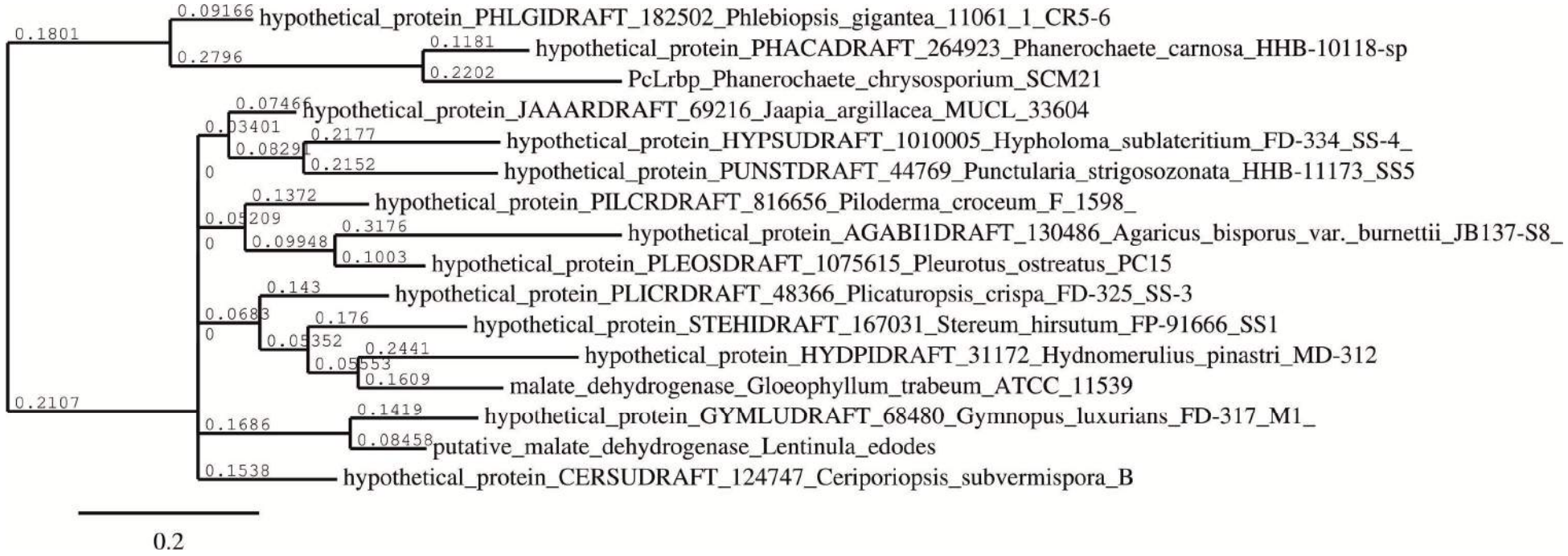

Figure 4

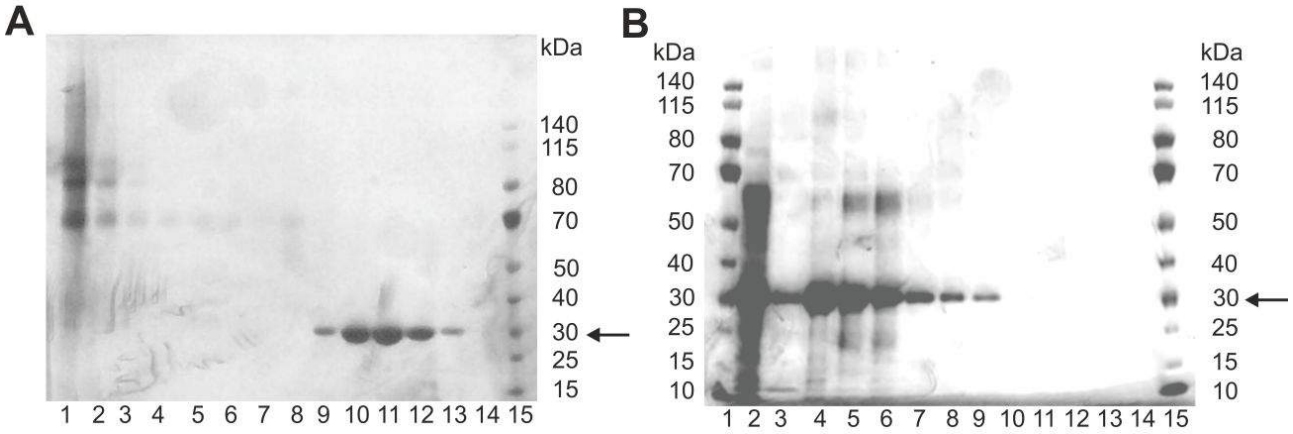
A
kDa
140
115
80
70
50
40
30
25
15
1 2 3 4 5 6 7 8 9 10 11 12 13 14 15
B
kDa
140
115
80
70
50
40
30
25
15
10
1 2 3 4 5 6 7 8 9 10 11 12 13 14 15

Figure 5

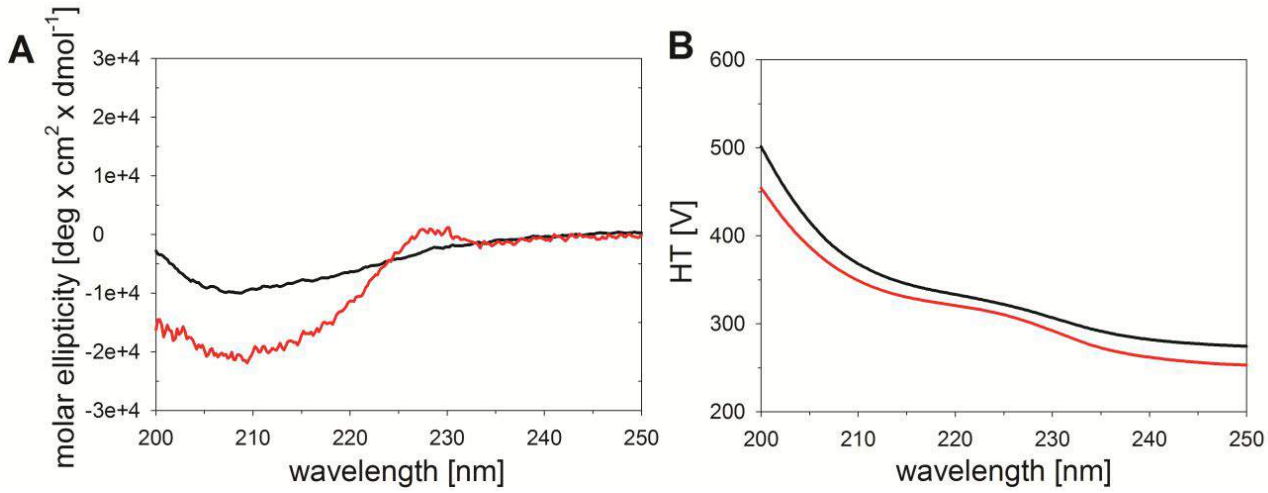
A
molar ellipticity [deg x cm^2 x dmol^{-1}]
3e+4
2e+4
1e+4
0
-1e+4
-2e+4
-3e+4
200
210
220
230
240
250
wavelength [nm]
B
HT [V]
600
500
400
300
200
200
210
220
230
240
250
wavelength [nm]

Figure 6

Identification of a lignacious residue binding protein from *Phanerochaete chrysosporium* boosting early-phase enzymatic hydrolysis of pretreated lignocellulose.

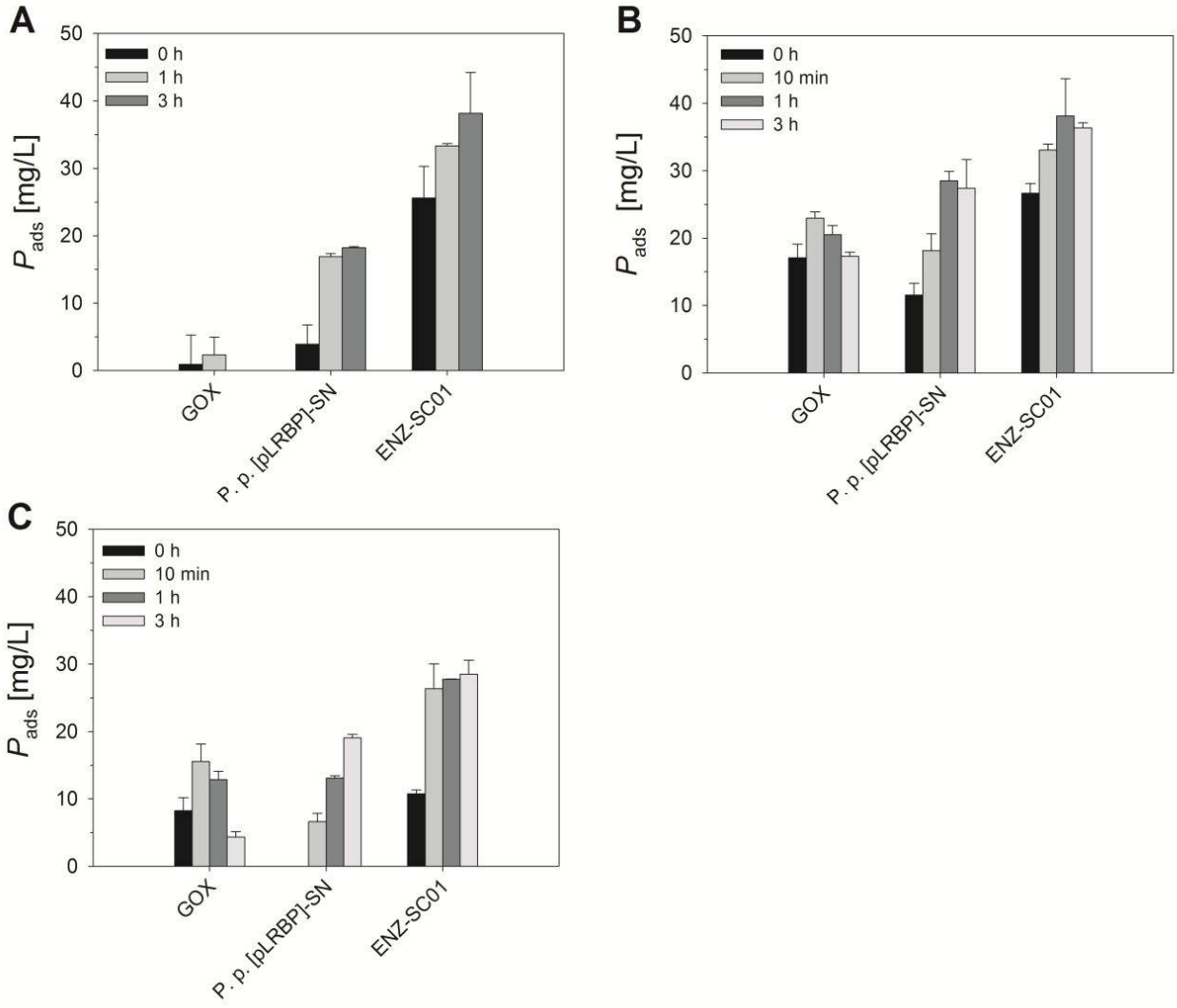

Figure 7

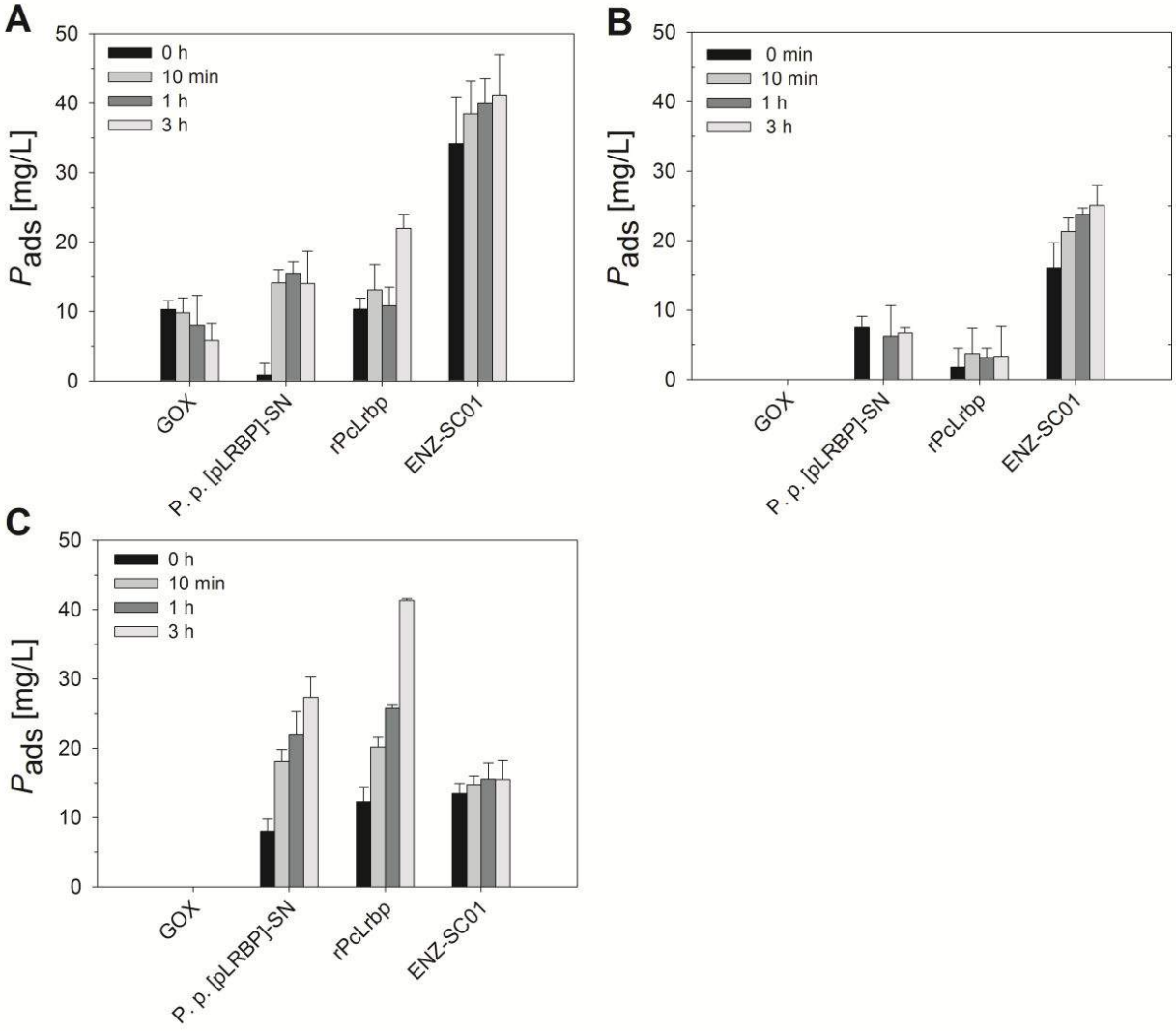
A
B
C
P_{ads} [mg/L]
0 h
10 min
1 h
3 h
0 min
GOX
P. p. [pLRBP]-SN
rPcLrbp
ENZ-SC01
0
10
20
30
40
50

Figure 8

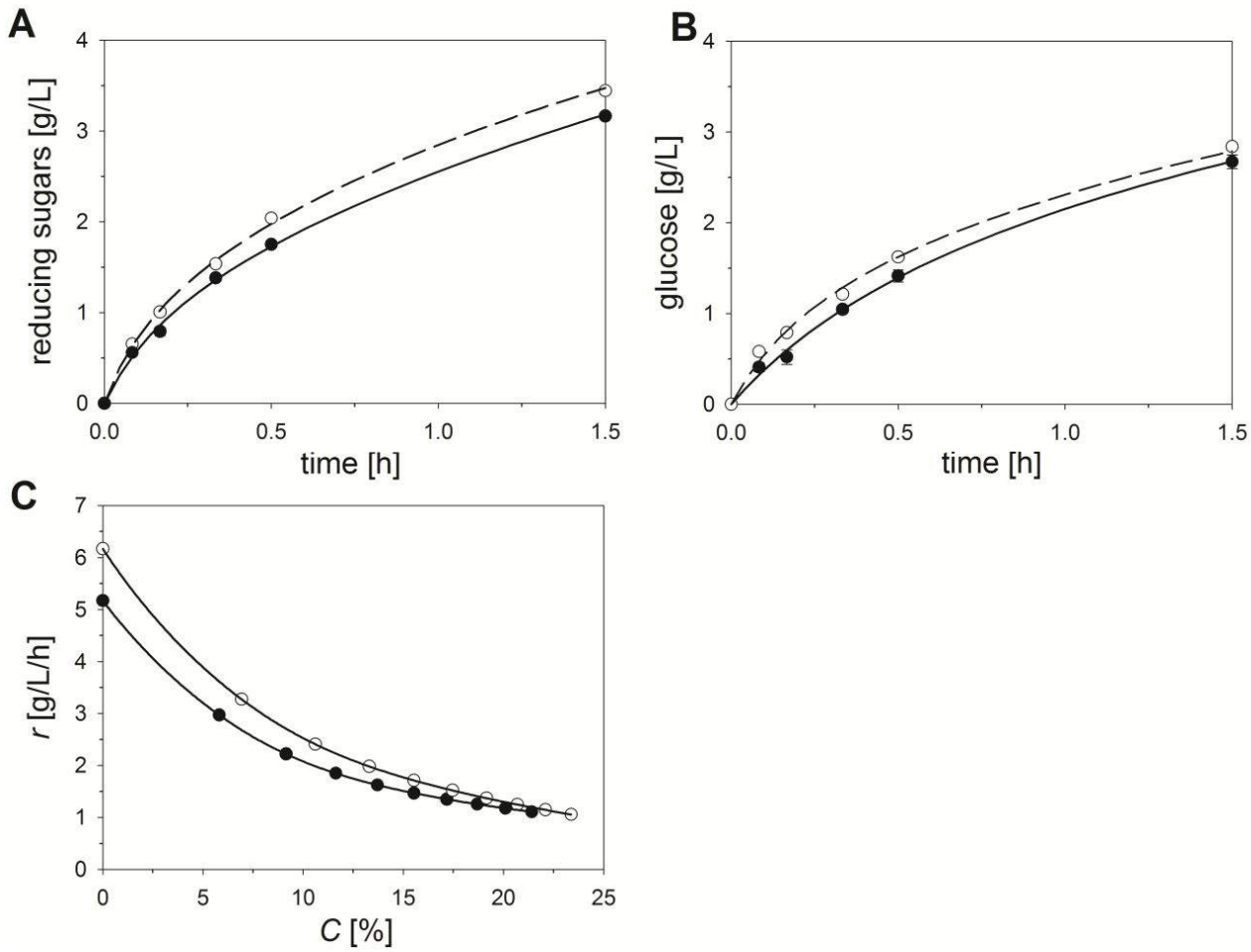

Figure 9

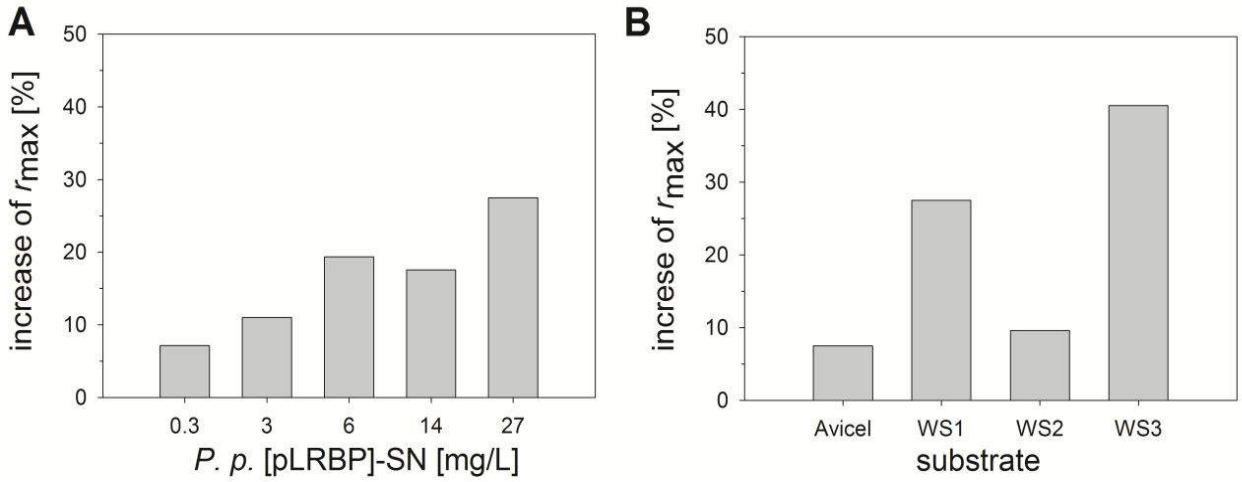
A
increase of r_{max} [%]
50
40
30
20
10
0
0.3
3
6
14
27
P. p. [pLRBP]-SN [mg/L]
B
increse of r_{max} [%]
50
40
30
20
10
0
Avicel
WS1
WS2
WS3
substrate

Figure 10

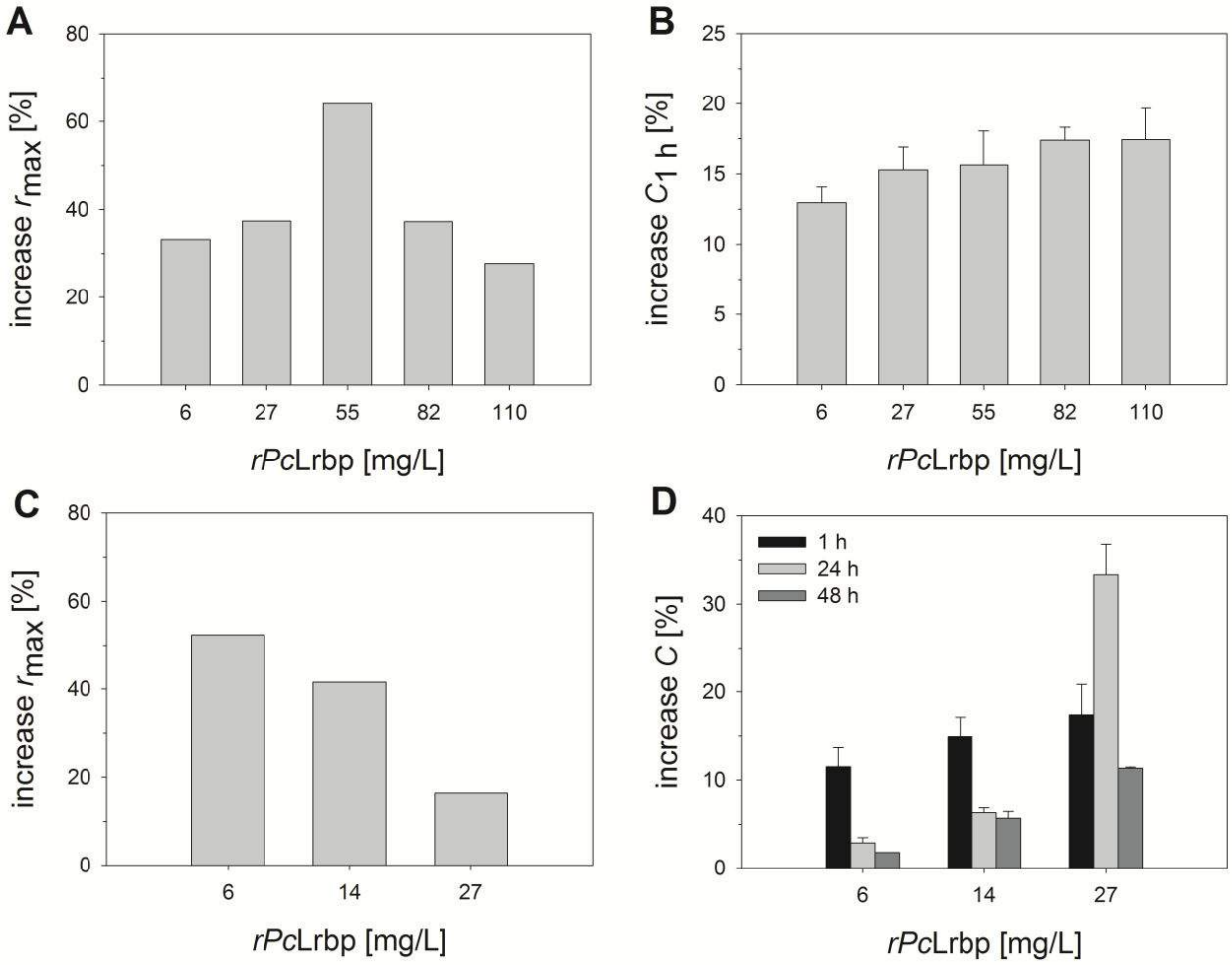
A
increase r_{max} [%]
0
20
40
60
80
6
27
55
82
110
*rPc*Lrbp [mg/L]
B
increase $C_{1\ h}$ [%]
0
5
10
15
20
25
6
27
55
82
110
*rPc*Lrbp [mg/L]
C
increase r_{max} [%]
0
20
40
60
80
6
14
27
*rPc*Lrbp [mg/L]
D
increase C [%]
1 h
24 h
48 h
0
10
20
30
40
6
14
27
*rPc*Lrbp [mg/L]

Figure 11

Table 1: Pretreatment parameters and composition of substrates used. SE: steam explosion; HPA: high-pressure autoclaving; operation mode: c, continuous; b, batch.

	Avicel PH-101	WS1	WS2	WS3	WS4	HR
Pretreatment						
Method	—	HPA_b	HPA_b	HPA_b	SE_c	HPA_b
Acid loading [% of DM]	—	3.3	3.3	3.3	2.3	3.3
Substrate composition						
Glycan [% of DM]		58.1	55.5	36.5	58	n.d.
Cellulose [% of DM]	97	50	47.8	34	35	n.d.
Hemicellulose [% of DM]		8.1	7.7	2.5	23	n.d.
Lignin [% of DM]	—	25.6	45.6	36	16	n.d.
DM [%]	<99.8	20.7	26.2	20.9	38	31

Identification of a lignacious residue binding protein from *Phanerochaete chrysosporium* boosting early-phase enzymatic hydrolysis of pretreated lignocellulose.

Table 2: Results of MALDI-TOF/TOF analysis of *P. chrysosporium* SCM21 HIC-pool 4/MM-pool 2/AIEX-pool 3. Proteins were identified using MASCOT software employing the '*Phanerochaete chrysosporium* Augustus gene prediction from whole genome sequence' database. Conserved domains and functions were predicted by BLASTp searching NCBInr database.

Accession	MW [kDa]	pI	Position	Nr. of peptides	Score	Sequence coverage [%]	Conserved domains	nrBLASTp hits
g178|gi|46851929|gb|AADS01000003.1	98.9	5.0	13279 - 17507	11	599.4	17.3	GDH (cd05301) FAD_binding_4 (pfam01565) BBE (pfam08031)	N-terminal: glyoxylate reductase gi|630177925|ref|XP_007844336.1| C-terminal: FAD-binding domain containing protein gi|597980733|ref|XP_007363327.1
g3546|gi|46851784|gb|AADS01000148.1	56.2	4.3	3179 - 5208	5	389.6	16.8	Abhydrolase_1 (pfam00561) Abhydrolase_4 (pfam08386) MhpC (COG0596)	α/β-hydrolase (gi|595785710|ref|XP_007271398.1|)
g4082|gi|46851765|gb|AADS01000167.1	49.8	4.7	33808 - 36035	2	113.5	4.0	DNase_NucA_NucB (pfam14040)	N-terminal: chitin synthase gi|630209035|ref|XP_007854398.1| C-terminal: hypothetical protein (gi|648157465|gb|KDR71222.1|)
lrbp|gi|46851341|gb|AADS01000591.1|	28.5	4.9	23140 - 24093	5	362.7	22.2	DUF3455 (pfam11937)	hypothetical protein gi|599402937|ref|XP_007401487.1|

SUPPORTING INFORMATION

Identification of a lignacious residue binding protein from *Phanerochaete chrysosporium* boosting early-phase enzymatic hydrolysis of pretreated lignocellulose

Mareike Monschein [a], Alexandra Schwarz [a], CLARIANT author(s) [b], Tibor Czabany [c], Barbara Darnhofer[d], Ruth Birner-Gruenberger [d] and Bernd Nidetzky [c,*]

[a] Austrian Center of Industrial Biotechnology (ACIB) GmbH, Petersgasse 14, 8010 Graz, Austria.
[b] CLARIANT Produkte (Deutschland) GmbH, Group Biotechnology, Staffelseestraße 6, 81477 Munich, Germany.
[c] Institute of Biotechnology and Biochemical Engineering, Graz University of Technology, Petersgasse 12/I, 8010 Graz, Austria.
[d] Institute of Pathology, Medical University of Graz, Auenbruggerplatz 25, 8036 Graz, Austria.
*Corresponding author. phone number: +43 316 873-8400
fax: +43 316 873-8434
e-mail address: bernd.nidetzky@tugraz.at (B. Nidetzky)

Identification of a lignacious residue binding protein from *Phanerochaete chrysosporium* boosting early-phase enzymatic hydrolysis of pretreated lignocellulose.

Supporting material and methods:

Test of rPcLrbp for (hemi)cellulolytic activity on (ligno)cellulosic substrates.

Assays were done in duplicates and performed in Eppendorf tubes (1.8 mL reaction volume).. Tested substrates (Avicel, WS1, WS3) were suspended in 50 mM sodium acetate buffer (pH 5.0) to a concentration of 25 g DM/L and supplemented with 300 mg/L *P. p* [pLRBP]-SN. Control reactions contained 14.4 FPU/g DM ENZ-SC01. Samples were incubated for 24 h at 25 °C without shaking in an Eppendorf Thermomixer. At certain times samples were taken and heated to 95 °C for 7 min. Samples were briefly centrifuged (9300×*g*, 30 s) and the cleared supernatant was used for reducing sugar analysis.

Measurement of enzyme activities

For measurement of arabinosidase, galactosidase, glucosidase, cellobiohydrolase, mannosidase and xylosidase activity, the nitrophenol assay was used. Fifty µL substrate (4-nitrophenyl-α-L-arabinofuranoside, 4-nitrophenyl-β-D-xylopyranoside, 2-nitrophenyl-β-D-galactopyranoside, 4-nitrophenyl-β-D-glucopyranoside, 4-nitrophenyl-β-D-mannopyranoside or 4-nitrophenyl-β-D-cellobioside) were transferred in 96-well flat-bottom microtiter plates and mixed with 50 µL protein sample diluted in 50 mM sodium acetate buffer, pH 5.0. To inhibit β-glucosidase activity, 5 mM D-(+)-gluconic acid δ-lactone were added in 4-nitrophenyl-β-D-cellobioside assays. Incubation was performed at various temperatures (30 °C, 40 °C, 50 °C) for 10 min in an Eppendorf Thermomixer comfort without shaking. After 5 min on ice, reactions were stopped by addition of 100 µL 1M sodium carbonate and the amount of liberated nitrophenol was measured at 405 nm in a FLUOstar Omega plate reader calibrated against 4-nitrophenol and 2-nitrophenol, respectively.

Identification of a lignacious residue binding protein from *Phanerochaete chrysosporium* boosting early-phase enzymatic hydrolysis of pretreated lignocellulose.
Supporting figure captions

Figure A.1: Elution profiles of the fractionation of *P. chrysosporium* SCM21 supernatant.

(A) Fractionation by hydrophobic interaction chromatography (HIC) using a HiPrep Phenyl HP 16/10 column. (B) Fractionation by mixed-mode chromatography (MM) using a high-resolution hydroxyapatite packed column. (C) Fractionation by anion exchange chromatography (AIEX) using a Mono Q 5/50 GL column.

Results and discussion: Obtained pools were subjected to the next fractionation step depending on their ability to enhance the enzymatic hydrolysis of WS1. Accordingly, HIC-pool 4 (fractions 47-60) was applied to mixed mode chromatography (Fig.A.1.B) and MM-pool 2 (fractions 9-13) to anion exchange chromatography (Fig.A.1.C). AIEX-pool 3 (fractions 15-21) was used for protein identification in MALDI-TOF/TOF.

Figure A.2: Test of *P. p.* [pLRBP]-SN for hydrolytic activity on (ligno)cellulosic substrates.

Substrates (25 g DM/L) were supplemented with *P. p* [pLRBP]-SN protein [300 mg/L] and incubated for 24 h at 25 °C in an Eppendorf Thermomixer without shaking. Control reactions were supplemented with 253 mg/L ENZ-SC01. Figures show reducing sugar release [mM] after 10 min, 3 h and 24 h of incubation. (A) WS1. (B) Avicel. (C) WS3.

Results and discussion: No reducing sugars were detected in *P. p* [pLRBP]-SN supplemented samples after 24 h of incubation. Since hemicelluloses and celluloses result in increasing reducing sugar values over time, a (hemi)cellulolytic activity of *rPc*Lrbp was ruled out.

Figure A.3: Test of *P. p.* [pLRBP]-SN for activity against chromogenic nitrophenyl glycoside substrates.

Chromogenic substrates (2-nitrophenyl-α-L-arabinofuranoside, 4-nitrophenyl-β-D-xylopyranoside, 2-nitrophenyl-β-D-galactopyranoside, 4-nitrophenyl-β-D-glucopyranoside, 4-nitrophenyl-β-D-mannopyranoside or 4-nitrophenyl-β-D-cellobioside) were supplemented with *P. p.* [pLRBP]-SN and incubated at various temperatures for 10 min in an Eppendorf Thermomixer comfort without shaking. Specific activities [U/mg] of β-glucosidase, β-galactosidase, β-mannosidase, β-xylosidase, α-arabinofuranosidase and cellulase (as exo- and endoglucanases) were calculated from absorption values at 405 nm.

Results and discussion: With exception of the 4-nitrophenyl-β-D-glucopyranoside substrate, specific activities of *P. p.* [pLRBP]-SN were $\leq 7.5\times10^{-3}$ U/mg. In comparison, the corresponding activities of ENZ-SC01 were between 20 and 300-fold higher. The effect of *rPc*Lrbp on enzymatic hydrolysis was apparently not caused by a α-arabinofuranosidase, β-galactosidase, β-mannosidase or β-xylosidase activity of the protein. This is in accordance with the results presented in Fig. A.1. Highest specific activity (1.8×10^{-2} U/mg) was observed using 4-nitrophenyl-β-D-glucopyranoside. However, a potential β-glucosidase activity of *rPc*Lrbp was dismissed after testing AIEX-purified *rPc*Lrbp (data not shown).

Figure A.4: Protein structure prediction of *Pc*Lrbp.

The model was constructed using the I-TASSER web server, combining *ab initio* and homology modeling (Yang et al., 2015). The figure was created with PyMol (www.pymol.org). Conserved residues (74NYTC; 96SC; 114W; 223RI; 226C; 228GG; 236C) are shown in red and blue color.

Discussion: Visualization of conserved residues in the model structure shows a close proximity of these residues. To date we can only speculate if these amino acids create a specific active site, which is responsible for the functionality of *Pc*Lrbp.

Identification of a lignacious residue binding protein from *Phanerochaete chrysosporium* boosting early-phase enzymatic hydrolysis of pretreated lignocellulose.

Supporting figures

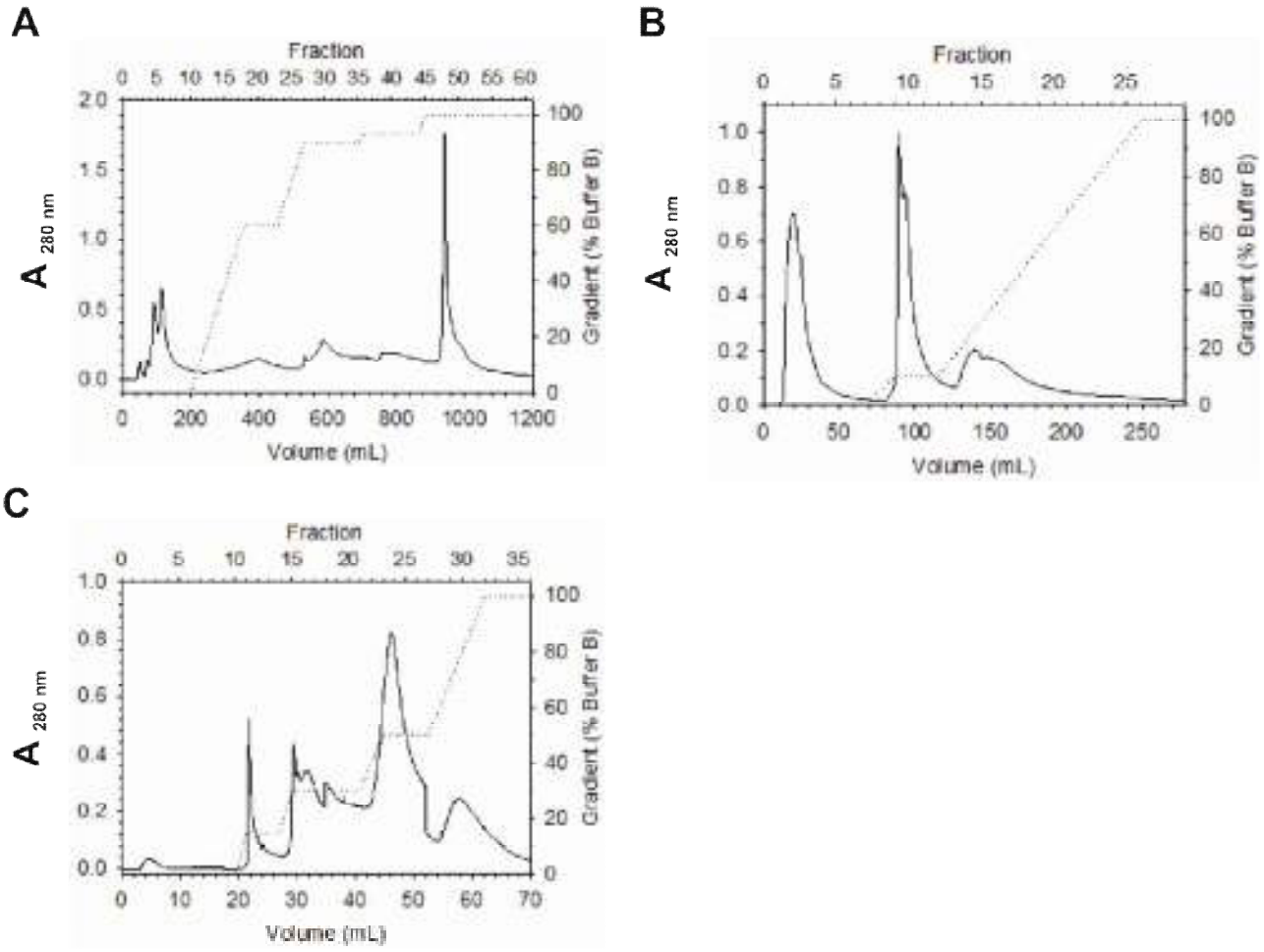

Figure A.1

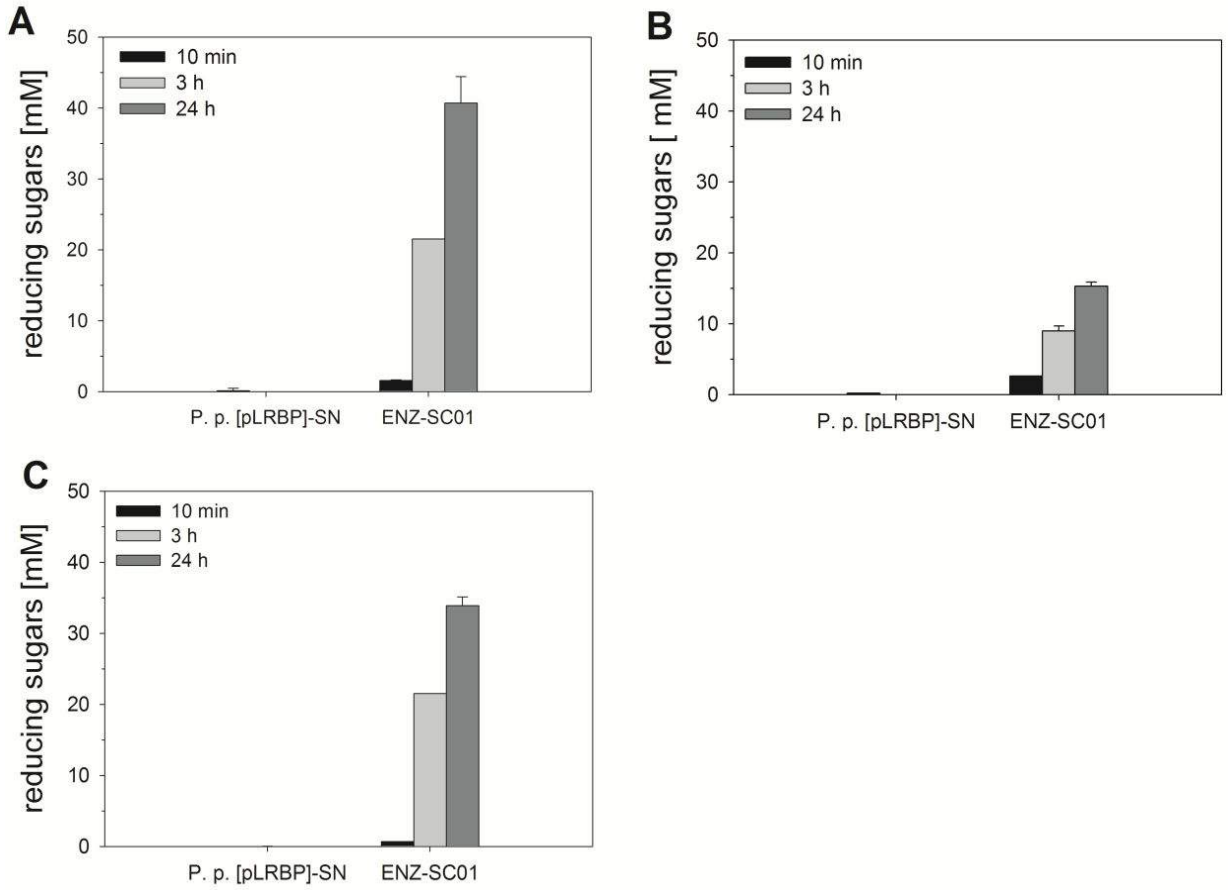
A
B
C
reducing sugars [mM]
reducing sugars [mM]
10 min
3 h
24 h
0
10
20
30
40
50
P. p. [pLRBP]-SN
ENZ-SC01

Figure A.2

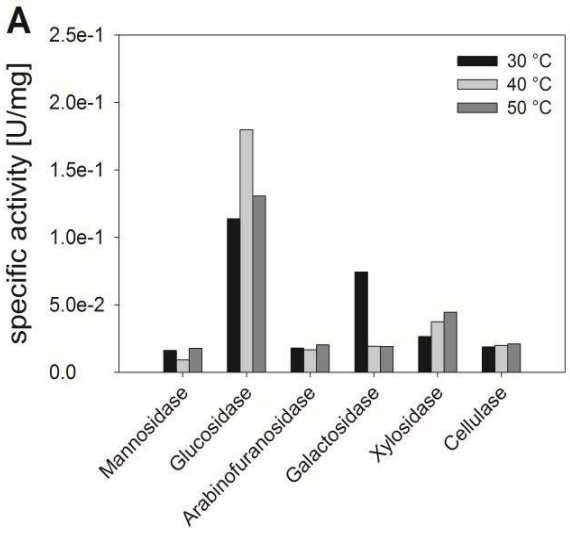
A
specific activity [U/mg]
2.5e-1
2.0e-1
1.5e-1
1.0e-1
5.0e-2
0.0
30 °C
40 °C
50 °C
Mannosidase
Glucosidase
Arabinofuranosidase
Galactosidase
Xylosidase
Cellulase

Figure A.3

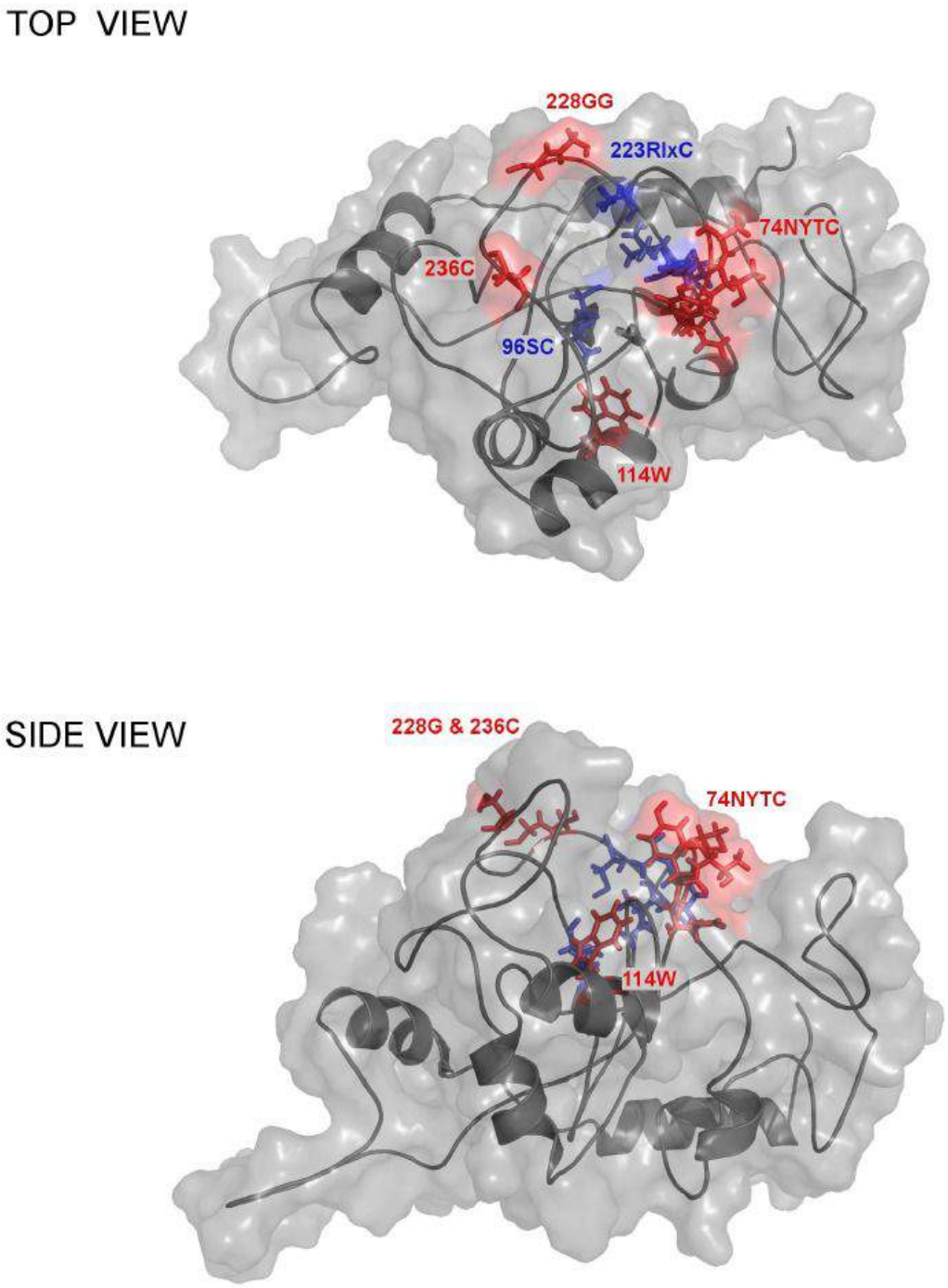
TOP VIEW
228GG
223RIxC
74NYTC
236C
96SC
114W
SIDE VIEW
228G & 236C
74NYTC
114W

Figure A.4

Identification of a lignacious residue binding protein from *Phanerochaete chrysosporium* boosting early-phase enzymatic hydrolysis of pretreated lignocellulose.

Supporting tables

Table A.1: Analysis of *P. chrysosporium* SCM21 supernatant.

Protein concentration [g/L]	6.5×10^{-2}
Total protein after ultrafiltration [g]	3.7×10^{-2}
Activity against nitrophenyl glycosides	
Cellulase[a] [U/mg]	7.8×10^{-1}
β-Glucosidase [U/mg]	1.6×10^{-1}
β-Galactosidase [U/mg]	1.1×10^{-1}
α-Arabinofuranosidase [U/mg]	4.5×10^{-2}
β-Mannosidase [U/mg]	9.4×10^{-3}
β-Xylosidase [U/mg]	1.1×10^{-1}

[a]…as exo- and endoglucanases

Table A.2: Fractionation of *P. chrysosporium* SCM21.

Pool	Fractions	Total protein [mg]
P. c. SCM21-SN	—	360
HIC-Pool 4	47-60	61
MM-Pool 2	9-13	1.88
AIEX-Pool 3	15-21	0.63

Identification of a lignacious residue binding protein from *Phanerochaete chrysosporium* boosting early-phase enzymatic hydrolysis of pretreated lignocellulose.

Supporting reference

1. Yang, J.Y., Yan, R.X., Roy, A., Xu, D., Poisson, J., Zhang, Y., 2015. The I-TASSER Suite: protein structure and function prediction. Nature Methods 12, 7-8.

Scientific record

Publications

Monschein, M., Reisinger, C., Nidetzky, B., 2013. Enzymatic hydrolysis of microcrystalline cellulose and pretreated wheat straw: A detailed comparison using convenient kinetic analysis. Bioresour. Technol. 128, 679-687.

Monschein, M., Reisinger, C., Nidetzky, B., 2014. Dissecting the effect of chemical additives on the enzymatic hydrolysis of pretreated wheat straw. Bioresour. Technol. 169, 713-722.

Monschein, M., Nidetzky, B., 2016. Effect of pretreatment severity in continuous steam explosion on enzymatic conversion of wheat straw: Evidence from kinetic analysis of hydrolysis time courses. *Bioresour. Technol.* 200, 287-296.

Oral presentations

Monschein, M., Nidetzky, B., 2012. Enzymatic hydrolysis of microcrystalline cellulose and pretreated wheat straw: A detailed comparison using practical kinetic analysis. 16th Austrian Carbohydrate Workshop, Vienna, Austria.

Monschein, M., Nidetzky, B., 2012. Comparing enzymatic hydrolysis of microcrystalline cellulose and pretreated wheat straw by applying practical kinetic analysis. Workshop Converting Poly-Saccharides. Graz, Austria.

Poster presentations

Monschein, M., Schwarz, A., Nidetzky, B., 2011. Kinetic analysis of enzymatic saccharification of lignocelluloses. Biotrans 2011, 10th International Symposium on Biocatalysis and Biotransformations, Giardini Naxos, Italy.